PET and SPECT imaging of bone marrow disorders

Agool, Ali

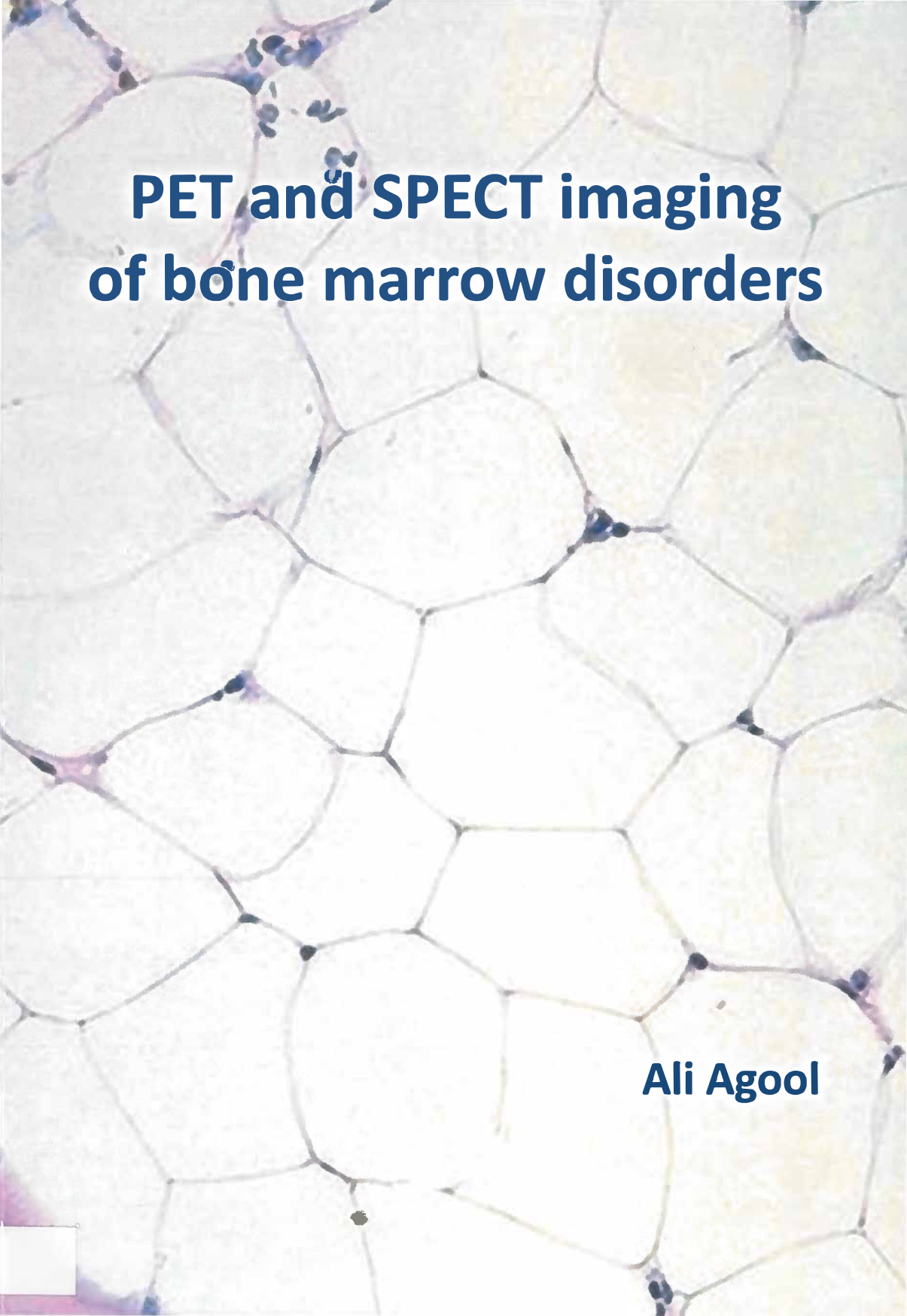

PET and SPECT imaging of bone marrow disorders

Ali Agool

PET and SPECT imaging of bone marrow disorders

Ali Agool

Stellingen bij het proefschrift

PET and SPECT imaging of bone marrow disorders

door Ali Agool

1. ^{18}F-FLT-PET kan gebruikt worden om de proliferatieve activiteit van het beenmerg compartiment aan te tonen en kan van nut zijn om separate hematologische aandoeningen te onderscheiden *(dit proefschrift).*

2. ^{18}F-FLT-PET bevestigt de significant verhoogde proliferatieve activiteit van de CD34+ celfractie na een autologe stamceltransplantatie *(dit proefschrift).*

3. ^{18}F-FLT-PET is een aantrekkelijke niet-invasieve techniek voor het aantonen van extramedullaire hematopoiesis *(dit proefschrift).*

4. Somatostatine receptor scintigrafie is een waardevolle techniek om myeloom activiteit te detecteren, vooral bij hernieuwde ziekteactiviteit *(dit proefschrift).*

5. Analyse van al de somatostatine receptor subtypen op myeloom cellen kan de eerste stap zijn richting radionuclide therapie. *(dit proefschrift).*

6. ^{18}F-FLT-PET lijkt accurater te zijn dan ^{18}F-FDG-PET in de differentiatie tussen tumor versus ontstekingsaktiviteit.
Tae Sup Lee, Nuclear Medicine and Biology, 2009;36:681–686

7. De bijdrage van nucleaire onderzoekingen aan de effectieve volgdosis per persoon per jaar in Nederland is gering ten opzichte van de overige bronnen.
RIVM, Informatiesysteem Medische Stralingstoepassingen, versie 7.0, 3 juni 2010

8. One of the first duties of the physician is to educate the masses not to take medicine
William Osler

9. Als dit universum in zijn miljoenvoudige orde en precisie het resultaat van blind toeval zou zijn, dan is dat net zo geloofwaardig als wanneer een drukkerij explodeert en alle druklettertjes weer op de grond terecht komen in de voltooide en foutloze vorm van het woordenboek.
Albert Einstein

10. Het belangrijkste bij communicatie, is horen wat niet wordt gezegd.
Peter Drucker

11. Ik sliep en droomde dat het leven vreugde was; ik ontwaakte en zag: het leven is plicht; ik werkte en zei: de plicht is vreugde.
Saadi

Publication of this thesis was financially supported by:

Ziekenhuisgroep Twente (ZGT)
De Stichting tot Bevordering der Hematologie te Groningen
Faculty of Medical Sciences, University of Groningen
Siemens Medical Solutions
COVIDIEN NEDERLAND BV
IBA Molecular

Cover picture: www.wikidoc.org/index.php/Bone_marrow_aspiration

Printed by: Proefschriftmaken.nl || Printyourthesis.com
Published by: Uitgeverij BOXPress, Oisterwijk

ISBN: 978-90-8891-236-8

RIJKSUNIVERSITEIT GRONINGEN

PET and SPECT imaging of bone marrow disorders

Proefschrift

ter verkrijging van het doctoraat in de
Medische wetenschappen
aan de Rijksuniversiteit Groningen
op gezag van de
Rector Magnificus, dr. E. Sterken,
in het openbaar te verdedigen op
woensdag 2 maart 2011
om 16:15 uur

Door

Ali Agool
geboren op 14 juli 1967
te Bagdad , Irak

Promotores:	Prof. dr. E. Vellenga Prof. dr. R.A.J.O. Dierckx
Copromotor:	Dr. R.H.J.A. Slart
Beoordelingscommissie:	Prof. dr. P.M. Kluin Prof. dr. P.H. Elsinga Prof. dr. C. van de Wiele

Paranimfen: Klaas Pieter Koopmans
Thi Thanh Ha Tan-Phan

Voor mijn ouders

Contents

Chapter 1	General introduction and scope of this thesis	11
Chapter 2	Radionuclide imaging of bone marrow disorders *(Eur J Nucl Med Mol Imaging. 2011;38:166-78).*	15
Chapter 3	^{18}F-FLT-PET in haematological disorders: A novel technique to analyze the bone marrow compartment. *(J Nucl Med. 2006 Oct;47:1592-8).*	47
Chapter 4	Auto-SCT induces a phenotypic shift from CMP to GMP progenitors, reduces clonogenic potential and enhances in vitro and in vivo cycling activity defined by ^{18}F-FLT-PET scanning. *(Bone Marrow Transplant. In press).*	65
Chapter 5	^{18}F-FLT-PET: a non-invasive diagnostic tool for visualization the bone marrow compartment in patients with aplastic anemia. *(Clin Nucl Med. In press).*	81
Chapter 6	Effect of radiotherapy and chemotherapy on bone marrow Activity: a ^{18}F-FLT-PET study. *(Nucl Med Commun. 2011;32:17-22).*	95
Chapter 7	Extramedullary hematopoiesis imaging with ^{18}F-FLT-PET. *(Eur J Nucl Med Mol Imaging. 2010;37:1620).*	111
Chapter 8	Somatostatin receptor scintigraphy might be useful for detecting skeleton abnormalities in patients with multiple myeloma and plasmacytoma. *(Eur J Nucl Med Mol Imaging. 2010;37:124-30).*	117
Chapter 9	Summary and future perspectives	133
Chapter 10	Nederlandse samenvatting	143
	List of abbreviations	147
	Dankwoord	149
	Curriculum vitae	153

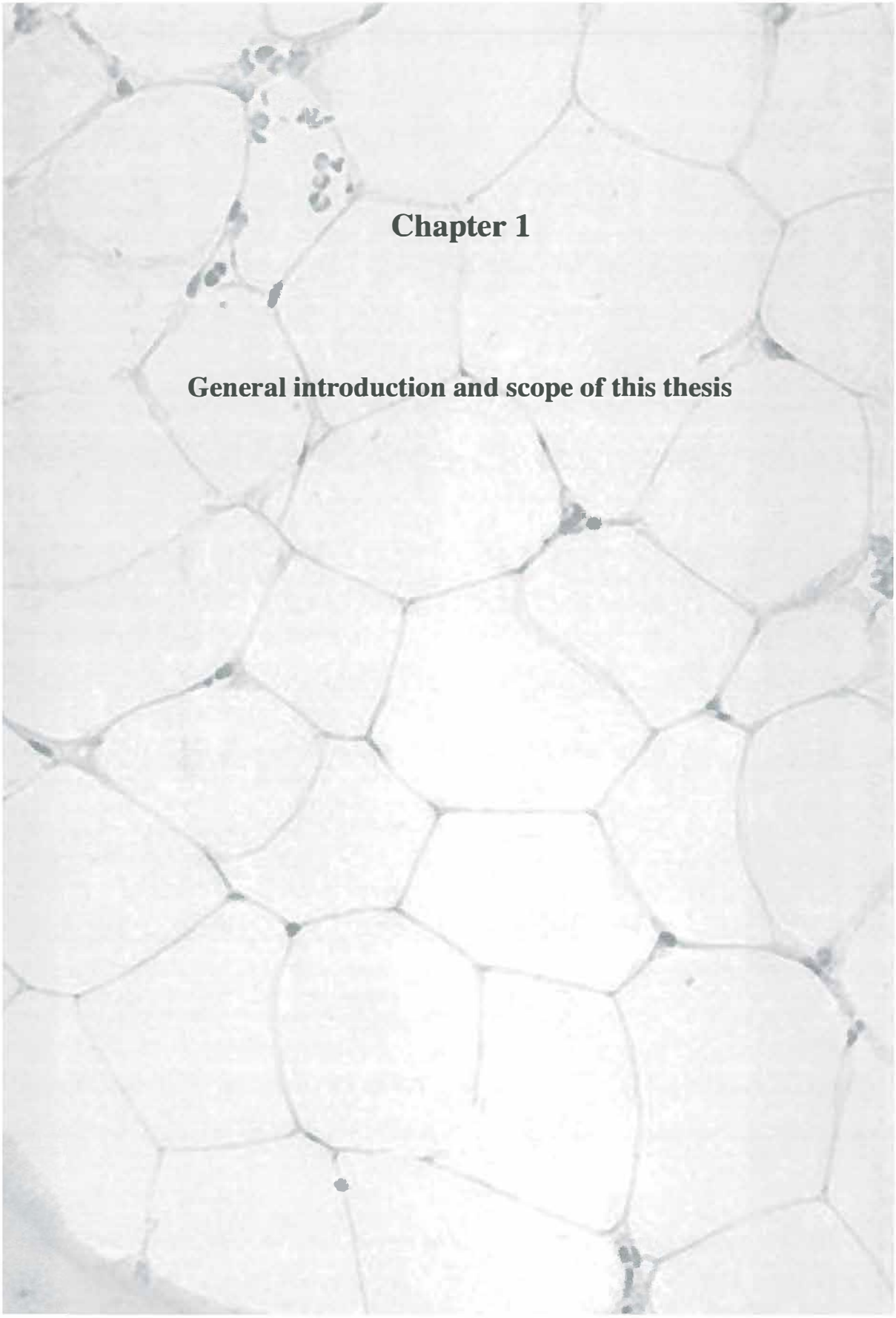

Chapter 1

General introduction and scope of this thesis

General introduction

In the bone marrow different hematopoietic cells are produced that originate from a limited number of hematopoietic stem cells. These cells are not only intrinsically instructed but are also strongly modulated by surrounding cells including osteoblasts, adipocytes and sinus-endothelial cells that together forms the micro-environment. Depending on the type of disease different disorders can be recognized, including myelodysplasia, aplastic anemia and myelofibrosis. Non invasive imaging techniques have been used in the past for visualization of the functional activity of the bone marrow compartment as ^{99m}Tc-nanocolloid, ^{99m}Tc-sulphur colloid, ^{111}Indium-chloride, and radiolabeled white blood cells.
With these techniques the reticulo-endothelial system, the erythroid and the myeloid-compartment can be recognized. The recent development in research and clinical use of PET tracers make it possible to analyze additional properties such as cellular metabolism and proliferative activity by using ^{18}F-FDG and ^{18}F-FLT. ^{18}F-FDG is a glucose analogue that enters the cell and resembles the glucose metabolism in activated cell processes, especially in malignant disorders. ^{18}F-FLT is used to study the proliferative activity, and is also mainly used in malignant disorders. A positive correlation has been found between the FLT uptake and the proliferative activity of normal and malignant tissue. The FLT uptake is more specific compared to ^{18}F-FDG. The aim of this thesis is to evaluate new applications of ^{18}F-FDG and ^{18}F-FLT- PET in patients with various haematological disorders.

Scope of this thesis

In chapter 2 the background of several hematological disorders are discussed. Different bone marrow targets imaged with radionuclides, including PET tracers are described. Current indications for radionuclide bone marrow imaging are listed.
Chapter 3 demonstrates the feasibility of visualisation and quantification of the bone marrow compartment activity with ^{8}F-FLT-PET to distinguish different haematological disorders. The role of ^{18}F-FLT-PET in myelodysplasia, myelofibrosis, and myeloproliferative disorders are studied. The uptake, distribution, and extension of ^{18}F-FLT are compared with a control group.

In chapter 4 the long term effects of autologous stem cell transplantation on the haematopoietic stem cell compartment is investigated. Phenotypical changes in the composition of progenitor subsets are studied and the enhanced in vivo cycling activity is compared to the ^{18}F-FLT PET. The intensity of the uptake, distribution, and extension are investigated and compared with a control group.
In chapter 5 a distinctive overview of the bone marrow compartment in aplastic anemia (AA) is investigated by using ^{18}F-FLT-PET. The ^{18}F-FLT-PET patterns are assessed in two groups of AA patients i.e. patients with active disease and following treatment.
Chapter 6 describes the role of ^{18}F-FLT-PET in patients following radio- and chemotherapy. Two groups of patients are studied Patients with laryngeal carcinoma and patients with metastatic nonseminomatous testicular germ cell tumor treated with radio- and chemotherapy is investigated respectively. The uptake of ^{18}F-FLT in the affected area due to therapy is compared to a control group.

Chapter 7 describes a case report about the role of the ^{18}F-FLT-PET in detecting extramedullary haematopoiesis in a patient with β-thalassemia.
Chapter 8 demonstrates the role of the somatostatin receptor scintigraphy (SRS) as a tool to detect multiple myeloma activity in newly diagnosed and relapsing multiple myeloma patients. Also the effect of therapy on disease activity is monitored by repeating SRS after 3-4 months of treatment.
Chapter 9 provides a summary of the thesis, and the results are discussed as well as potential future prospectives.

Chapter 2

Radionuclide imaging of bone marrow disorders

Ali Agool[1,2], Andor W.J.M. Glaudemans[2], Hendrikus H. Boersma[2], Rudi A.J.O. Dierckx[2,3], Edo Vellenga[4], Riemer H.J.A. Slart[2]

[1]Department of Nuclear Medicine, Medical Center Twente, Hengelo, the Netherlands; [2]Department of Nuclear Medicine and Molecular Imaging, University Medical Center Groningen, Groningen, the Netherlands; [3]Ghent University, Ghent, Belgium; [4]Department of Hematology, University Medical Center Groningen, Groningen, the Netherlands

European Journal of Nuclear Medicine and Molecular Imaging. 2011;38:166-78

Abstract

Non invasive imaging techniques have been used in the past for visualization the functional activity of the bone marrow compartment. Imaging with radiolabeled compounds offers the opportunity to make a distinction between separate bone marrow disorders. These imaging techniques, almost all with the use of radionuclide labeled tracers, such as ^{99m}Tc-nanocolloid, ^{99m}Tc-sulphur colloid, ^{111}Indium-chloride, and radiolabeled white blood cells, are already used in nuclear medicine for several decades. With these techniques three separate compartments can be recognized including the reticulo-endothelial system, the erythroid and the myeloid-compartment. The recent development in research and clinical use of PET tracers make it possible to analyze additional properties such as cellular metabolism, and proliferative activity, by using ^{18}F-FDG and ^{18}F-FLT. These tracers may lead to better quantification and targeting of different cell systems in the bone marrow. In this review imaging of different bone marrow targets with radionuclides, including PET tracers will be discussed in various bone marrow diseases.

Introduction

Bone marrow is a dynamic tissue compartment in the cavity of bones. In adults, hematopoietic cells are produced by the bone marrow cells in the large bones that accounts for 2 to 5% of an adult's weight [1]. In the past, a distinction was made between red marrow which consists of hematopoietic cells and yellow marrow which consists of adipocytes. It is now general accepted that a small fraction of cells, the so-called hematopoietic stem cells (HSCs) reside in specific areas of the bone marrow including the osteoblastic and vascular niche [1]. These HSC have the potential of self-renewal but also to proliferate and differentiate to the different cell lineages including the myeloid, erythroid and megakaryocytic lineage [2]. This process is strongly dependent on surrounding cells of the microenvironment including mesenchymal stem cells that have the capacity to differentiate into osteoblasts, chondrocytes, adipocytes, myocytes, and endothelial cells [1]. During life distinct changes occur in the composition of the bone marrow cavity. At birth, the whole bone marrow cavity contains hematopoietic cells which are gradually replaced by adipose tissue during life. Especially the distal parts of the skeleton are depleted from hematopoietic cells upon ageing. The architecture of the hematopoietic system can be distorted strongly by a number of disorders, including malignancy. Transformation of a hematopoietic stem cell can result in the expansion of the malignant clone and a disruption of the normal hematopoietic system [3]. In acute leukemia the bone marrow contains a population of immature cells that has lost the potential to differentiate. For myeloproliferative disorders however, there is an expansion of a certain hematopoietic lineage that has the persisting potential of differentiation [4]. Exposure to radiation or chemotherapy for both hematological malignancies as well as solid tumors will eliminate many of the rapidly dividing cells of the bone marrow. The degree and extent of this process will determine the severity of the bone marrow aplasia and duration of peripheral pancytopenia. Limited diagnostic procedures are available to determine the extent of bone marrow involvement. It is assumed that the material obtained with a bone marrow aspiration and biopsy from the sternum or the crista iliaca are a reflection of the total bone marrow compartment. Using these methods, its composition and cellular components can be analyzed. In addition, in vitro assays can be used to measure the potential of more primitive progenitors or stem cells [5]. However, bone marrow biopsy has distinct limitations: it is an invasive procedure and only a small proportion of the total bone marrow content is investigated. The latter may cause

sampling errors. A non invasive technique to evaluate the total bone marrow activity in hematological diseases, as well as for the evaluation of hematological effects concerning solid tumors is therefore of invaluable importance.
In this review we will describe the clinical indications of bone marrow imaging as well as the most common bone marrow disorders, including bone marrow transplantation. This is combined with a review of the literature on nuclear medicine techniques that are used in diagnostic protocols for determination of bone marrow disorders. There will be special attention on recent development of Positron Emitting Tomography (PET) techniques to image the bone marrow.

Clinical indications

A list of current indications for radionuclide bone marrow imaging are listed in table 1. Bone marrow aspiration and biopsy are usually the standard techniques for evaluation of the bone marrow function. However, sometimes a discrepancy can be found between histology of the bone marrow and patients' lab and clinical findings. This may be due to a bone marrow sampling error. Non invasive imaging using a specific bone marrow tracer can be helpful to confirm a suspected sampling error and will visualize a specific part of bone marrow functionality.
Many patients suffering from malignancies are treated with chemotherapy and/ or radiotherapy. These therapy modalities commonly cause adverse events on bone marrow activity. Bone marrow imaging may determine the amount of remaining functional bone marrow tissue and shows its biodistribution.
Extramedullary hematopoiesis (EMH) refers to hematopoiesis taking place outside the bone marrow. This is a symptom for several hematologic disorders, including chronic hemolytic anemia and myeloproliferative disorders. EMH is mainly present in liver and spleen, where it contributes to organ enlargement. It may however also occur within other organs or structures [6]. Clinical arguments supporting evaluation of EMH can be 1) to determine the extent of EMH in liver or spleen, 2) to evaluate the presence and contribution of splenic erythropoiesis in patients under consideration for splenectomy, and 3) to evaluate mass lesions outside liver and spleen to differentiate from other processes. Bone marrow imaging is a diagnostic tool for determination and staging of

several hematologic bone marrow disorders. The latter will be further addressed in the next paragraph "Bone marrow disorders".

Detection of bone marrow activity as well as bone metastases is another indication for bone marrow imaging. Solid tumors have the propensity to metastasize to bone and may, therefore, influence the bone marrow compartment. Appropriate radiopharmaceuticals and clinical results are discussed in section "Imaging the bone marrow using radionuclides".

Bone marrow infarctions are common in patients with sickle cell anemia and its variants S-C and S-thalassemia. Thalassemia is an inherited autosomal recessive blood disease. Patients with hemoglobin SC disease inherit a gene for hemoglobin S from one parent, and a gene for hemoglobin C from the other. In fact, more than half of all patients suffering from these pathologies will experience bone marrow infarctions at a particular time point during the course of their disease [7]. Plain X-ray images are usually normal in acute bone marrow infarction; therefore, radionuclide imaging can play an additional role for the detection of acute bone marrow infarctions [8]. Finally, bone marrow imaging techniques may be useful to study the proliferative activity of the hematopoietic compartment following intensive chemotherapy with and without stem cell support. Especially in the setting of autologous stem cell transplantation, determination of the remaining activity of the hematopoietic activity and its susceptibility for chemotherapeutic intervention in the case of relapse may be valuable. Bone marrow imaging may also be indicated to differentiate sepsis from bone marrow, after unclear skeletal and leukocytes scintigraphy findings, however this will be beyond the scope of this review.

Table 1: Indications for bone marrow imaging

1. Evaluation of patients with a discrepancy between bone marrow histology and clinical status
2. Evaluation of the degree of radiotherapy effect on bone marrow
3. Detection of extramedullary hematopoiesis
4. Location of the optimal site for bone marrow biopsy
5. Diagnosing and staging of hematologic bone marrow disorders
6. Detection of bone marrow metastases
7. Diagnosis of bone marrow infarctions
8. Evaluation of bone marrow transplantation

Bone marrow disorders

Myeloproliferative diseases

Myeloproliferative diseases (MPDs) are clonal hematopoietic stem cell disorders characterized by proliferation in the bone marrow of one or more cell lines resulting in an excessive production of cells belonging to the granulocytic, erythroid and megakaryocytic lineage (table 2). Nowadays, a WHO classification is used for making a distinction between the separate disorders [9].

Different molecular markers have been defined such as JAK2 and TET2 mutations that might further be helpful in categorizing the disorders [10]. Most frequently diagnosed are chronic myeloid leukemia, polycythemia vera, chronic idiopathic myelofibrosis, and essential thrombocythemia [11]. These disorders are characterized by the fact that enhanced proliferation of different cell lines is accompanied with a relatively normal maturation, resulting in increased number of granulocytes, red blood cells and/or platelets in the peripheral blood. MPDs are mainly occurring in adult population with higher prevalence in the fifth to seventh decade of life. The MPDs can have a stepwise progression that is leading to bone marrow failure due to myelofibrosis or ineffective hematopoiesis. Furthermore, transformation to acute leukemia may occur.

Frequently, there is a coincidence of symptoms for the specific MDP entities. Leukocytosis, thrombocytosis, excessive megakaryocytic proliferation, myelofibrosis and organomegaly are features that can occur in almost any of the MDP diseases. For example, both polycythemia vera (malignant red blood cell proliferation) and myelofibrosis (MF, proliferation of mainly megakaryocytic elements, associated with deposition of bone marrow connective tissue) can also be associated with increased white blood cells. Polycythemia vera (PV) is usually associated with a mild increase in white blood cell counts. The latter is associated with a regular white blood cell differentiation, whereas myelofibrosis is frequently associated with a mild increase of immature white blood cells. Leukocytosis in PV is associated with an increased risk of thrombosis. However, the primarily treatment is directed towards the control of increased red blood cells [12]. Today there remains a distinct subgroup of elderly patients with polycythaemia vera for whom ^{32}P is the most optimal treatment option, as described in the guideline of the EANM [13]. MF is associated with variable abnormalities in white blood cells, either increased with circulating immature precursors, or decreased in the presence of massive splenomegaly. The number of white blood cells in MF is therefore important for treatment decisions. Recently, a prognostic score index has been defined that may be helpful for adjusting the proper treatment [14]. For example in PV, a survival time longer than 10 years is not uncommon [11]. The recent development of therapy targeting specific molecular defects in MPDs is an exiting field of interest in which nuclear medicine can play a key role.

Table 2: Features of myeloid disorders at diagnosis.

Disease	BM cellularity	Blasts	Maturation	Morpho-logy	Hemato poiesis	Blood counts	Organo-megaly
Myelodys-plastic syndromes	Usually increased, occasionally decreased	Normal or increased (<20%)	Present	Dysplasia	Ineffective	Cytopenia	Uncommon
Myelo-proliferative disorders	Usually increased	Normal or slightly increased (<10%)	Present	Relatively normal	Effective	One or more myeloid cell lines in-creased	Common
Acute myeloid leukemia	Usually increased, occasionally decreased	Increased (>20%)	Varies, frequently minimal	Sometimes associated with dysplasia	Ineffective or effective	Variable	Uncommon

Myelodysplastic syndromes

Myelodysplastic syndromes (MDS) are clonal hematopoietic stem cell diseases characterized by dysplasia and ineffective hematopoiesis in one or more of the major cell lines (table 2). The clinical behavior of MDS can be highly variable and separation in subgroups is based on the bone marrow cytology and cytogenetic findings according to the WHO classification [9,15]. Subgroups that can be distinguished are refractory anemia (with or without ringed sideroblasts), refractory cytopenia with multilineage dysplasia, refractory anemia with excess of blasts, and myelodysplastic syndrome (unclassified or with a chromosome abnormality). MDS occurs predominantly in older adults with a median age of 70 years. Secondary MDS, a result of chemotherapy and/or radiotherapy for other malignant disorders, is an increasing problem and may represent as many as 15% of all MDS diagnosed [16]. Secondary MDS tends to be much more severe than primary MDS. Clinical symptoms are related to cytopenia(s), most frequently anemia, and less commonly neutropenia and/or thrombocytopenia. Organomegaly is infrequently observed. MDS prognosis depends on its morphological subtype and cytogenetic characteristics by which patients can be subdivided in low- and high- risk group. The low-risk group is treated with transfusion, hematopoietic growth factors, immunosuppressive therapy or lenolidamide. The high risk group is treated in general

with therapy regimens, commonly used for patients with acute leukemia including allogeneic stem cell transplantation [17].

Aplastic anemia

Aplastic anemia (AA) is a rare hematological disorder caused by immune-mediated destruction of hematopoietic stem cells in the bone marrow [18]. Hematopoiesis fails, blood cell counts are extremely low (pancytopenia) and the bone marrow appears empty. Massive AA is a life-threatening bone marrow disorder, which is associated – if untreated – with high mortality rates [19]. Almost half of AA-cases occur during the first three decades of life. Often, the etiology remains unclear. AA is associated with exposure to toxins such as benzene, or with the use of certain drugs, such as chloramphenicol, carbamazepine, phenytoin, and quinine. AA is present in up to 2% of patients with acute viral hepatitis. Clinical symptoms are related to the cytopenia(s). Anemia leads to malaise, pallor and related symptoms such as palpitations, thrombocytopenia to an increased risk of hemorrhage, bruising and petechia, and granulocytopenia to an increased risk of infection. AA can be effectively treated by immunosuppressive therapy or allogeneic stem cell transplantation. When initial treatment is started promptly, the five year survival rate is up to 75%. Patients after well-matched bone marrow transplantation, have a long-term survival rate of up to 90% [20].

Hemolytic anemia

Hemolytic anemia (HA) is anemia due to the abnormal breakdown of red blood cells either in the blood vessels (intravascular hemolysis) or extravascular by an overactive, enlarged spleen that traps circulating red blood cells and destroys them. HA can be either acquired or inherited. Acquired HA can be either immune or non-immune mediated. HA represents approximately 5% of all anemia's. Signs of anemia (fatigue, palpitations and later heart failure) are generally present. Jaundice (as a result of bilirubin accumulation which is caused by hemoglobin degradation) can be the first sign. The overall incidence of death is low in cases of HA. However, older patients and patients with cardiovascular impairment are at higher risk compared to the rest of the population. Symptomatic treatment can be given by blood transfusion. In immune mediated HA steroid therapy is

highly effective. Splenectomy can be helpful in extravascular hemolysis, because in this case most red blood cells are removed by the spleen.

Imaging the bone marrow using radionuclides

Based on the target cell system, bone marrow imaging using radionuclides may be divided into three categories: (1) imaging the reticulo-endothelial system (RES), (2) imaging erythroid precursor cells, and (3) imaging the myeloid compartment in the bone marrow. These imaging techniques, almost all using radionuclides for gamma cameras, have been already used in nuclear medicine for many years. The recent development in research and application of PET tracers lead to targeting two other pathways for imaging the bone marrow: (4) the metabolic activity, and (5) the proliferative activity. In general, PET tracers will provide absolute quantification options and a better resolution compared to gamma camera tracers. So the use of PET tracers may be an advantage compared to the use of gamma camera techniques for the evaluation of bone marrow disorders. The five target cell systems and the tracers for imaging the bone marrow will now be discussed.

1. Imaging the reticulo-endothelial system

The reticulo-endothelial system (RES) is part of the immune system and consists of phagocytic cells located in reticular connective tissue, primarily monocytes and macrophages. Major components of this system are the hepatic Kupffer's cells, the phagocytic cells in the spleen and the phagocytic reticulum cells in the bone marrow. The RES can be easily imaged using radiolabeled colloids. Colloids are small particles that remain suspended in an appropriate solvent. After intravenous injection, they are phagocytosed by macrophages and distributed throughout the body in the RES. This property is used for RES targeted bone marrow scintigraphy.

The two most widely used tracers for scintigraphy of the RES are ^{99m}Tc-sulfur colloid and ^{99m}Tc-nanocolloid. ^{99m}Tc-sulfur colloid is widely used in the United States. The size of the particles ranges from 100-1000 nm. After intravenous administration, 5% of the injected activity accumulates in the RES of the bone marrow, about 90% in the liver and 5% in the spleen [21]. Because of the high liver uptake it is difficult to evaluate the bone marrow in the lower thoracic and upper lumbar spine. ^{99m}Tc-nanocolloid is

produced from microaggregated human serum albumin. More than 95% of the particles range below 80 nm. After intravenous injection, ^{99m}Tc-nanocolloid is rapidly cleared from plasma and taken up by the RES. About 15-20% is accumulated in the bone marrow by macrophages, the rest being distributed to the liver (70%) and spleen (10%) [22]. The small size of the nanocolloids causes an increased marrow uptake compared with the larger colloids. There is a small sized fraction of the nanocolloid which is not incorporated by RES and is probably slowly excreted by the kidneys, thereby giving rise to a considerable blood background and urinary tract activity.

Normal bone marrow scintigraphy shows homogeneous activity in the bone marrow of the axial skeleton with uptake in the humeri and femora limited to the proximal one-third. Skull, sternum and ribs may show a variable degree of uptake. The scans are evaluated for homogeneity and intensity of uptake in normally hematopoietic marrow-containing structures, presence and extent of peripheral marrow expansion, central marrow depletion and focal marrow defects. Bone marrow infarctions due to sickle cell anemia can be imaged with ^{99m}Tc-sulphur colloid, since RES activity is lacking in infarcted bone marrow, showing demarcated defects in bone marrow [23]. In the past, bone marrow images were often obtained using nanocolloids. Currently, this method is not in use anymore because of its unfavourable target to background ratio [24].

2. Imaging the erythroid bone marrow ('the red cells')

The erythropoietic part of the bone marrow can be imaged with the PET-tracer ^{52}Fe. Iron is incorporated in the hemoglobin of erythrocytes.

^{52}Fe is a cyclotron-produced positron-emitting isotope with a half-life of 8.2 hours and decays by positron emission (57%) and by electron capture (43%) to the radioactive daughter ^{52m}Mn (table 3). Another iron radioisotope, ^{59}Fe, emits β-rays with a high energy of 1,59 MeV and gamma rays of 1,1 and 1,3 MeV. It has a half-life of 45 days, and therefore imaging of low quality and a high radiation dose. Bone marrow expansion has been demonstrated in patients with chronic HA (not in acute HA), MF and, on rare occasions, with PV [25]. However, the aforementioned disadvantages, the limited availability of the isotope and PET facilities have precluded its widespread use.

The tracer ^{111}Indium-chloride (^{111}In-Cl_3) distributes in the skeletal system partly similar to iron isotopes and partly like nanocolloids [26]. ^{111}In-Cl_3 binds to transferrin in exactly the same manner as iron. The biological behavior of indium and iron is different, because

In^{3+} is not reduced like iron to In^{2+} state, but in many respects they are similar, and marrow $^{111}In\text{-}Cl_3$ uptake likely reflects the distribution of erythropoietic marrow. $^{111}In\text{-}Cl_3$ has been used clinically for bone marrow studies [27,28]. It is a cyclotron-produced isotope with a half-life of 2.8 days emitting gamma rays with energies of 171 (89%) and 245 (94%) keV. It decays by electron capture to the stable ^{111}Cadmium. After intravenous injection, $^{111}In\text{-}Cl_3$ is rapidly coupled to serum transferrin and eliminated from plasma with a half-life of 5 hours. About 30% of the applied tracer is found in the bone marrow, 20% in the liver, 7% in the kidneys, and 1 % in the spleen. The remaining activity is distributed throughout the body fluids without any specific tissue accumulation. $^{111}In\text{-}Cl_3$ is incorporated into erythrocytes only to a minor degree (4% of injected dose) [22]. In patients with normal bone marrow function and iron storage, the distribution of $^{111}In\text{-}Cl_3$ was similar to that of the ^{99m}Tc-labelled colloids (fig. 1) [26].

Patients with MF showed an extension of $^{111}In\text{-}Cl_3$ uptake beyond the central skeleton towards the knees and sometimes ankles and elbows, together with uptake in the spleen. The clinical severity of the disease may be predicted by uptake of indium, particularly the disappearance of a physiologically active bone marrow (fig. 1) [29]. $^{111}In\text{-}Cl_3$ scintigraphy of the bone marrow was reported in patients with AA before therapeutic intervention. In almost all patients a marked reduction in the uptake was seen. Failure of $^{111}In\text{-}Cl_3$ uptake correlated with poor prognosis in patients with AA [30]. Another study was performed in patients with AA in remission for more than 2 years. Bone marrow scintigrams using $^{111}In\text{-}Cl_3$ showed patchy hematopoiesis which appeared to characterize the residual marrow damage in remission of AA [31].

Overall, the results are not very encouraging. Moreover, bone marrow irradiated with 5 Gy failed as expected to accumulate iron but had unimpaired $^{111}In\text{-}Cl_3$ uptake. Together with its nearly negligible incorporation into erythrocytes and the relatively high radiation exposure of the erythroid compartment, this almost completely precludes the use of $^{111}In\text{-}Cl_3$ as a reliable agent for the assessment of erythropoietic bone marrow activity.

Table 3: Overview of different radiopharmaceuticals for imaging of the bone marrow.

Radiopharmaceutical	Physical half life	Effective dose on bone marrow per MBq (mSv)	Cyclotron	Quantification (absolute)	Target
Gammacamera					
^{99m}Tc-sulfur colloid	6 h	0.0019	-	-	RES
^{99m}Tc-nanocolloid	6 h	0.0094	-	-	RES
^{111}Indium-chloride	2.3 d	0.21	-	-	Erythropoietic
^{99m}Tc-WBC	6 h	0.023	-	-	RES
^{111}In-WBC	2.3 d	0.36	-	-	RES
^{99m}Tc-AGAb	6 h	0.0055	-	-	Granulopoietic
PET					
^{52}Fe	8.2 d	6.1	+/-	+	Erythropoietic
^{18}F-FDG	2 h	0.011	+/-	+	Metabolic activity (glucose)
^{18}F-FLT	2 h	0.029	+/-	+	Proliferative activity (DNA)
^{11}C-methionine	20 min	0.00045	+	+	Metabolic activity (amino acid)
^{11}C-acetate	20 min	0.0057	+	+	Metabolic activity (fatty acid)
^{11}C-choline	20 min	0.0019	+	+	Cell proliferation
^{18}F-choline	2 h	0.012	+/-	+	

AGAb antigranulocyte antibodies; WBC; white blood cells; +/-; ^{18}F cyclotron produced, but transportable for local labeling procedures.

3. Imaging the myeloid bone marrow compartment ('the white cells')

^{99m}Tc-HMPAO or ^{111}In-oxinate labeled white blood cells (WBC) are useful bone marrow imaging tracers. As granulocytes may become damaged during the labeling process, they will be trapped in the marrow, so the obtained images presumably represent the distribution of marrow reticuloendothelial cells. Although there is considerable liver activity with this technique, it is significantly less than seen with the colloid agents so the spine is usually minimally obscured. However, the labor-intensive cell labeling procedure and risk of contamination makes this technique only suitable for well-equipped laboratories with qualified personnel. Labelling of WBC may be improved using new derived kits that are safe and easy to use methods, with a high labelling efficiency of WBC without affecting cell vitality and function and with less risk of contamination. An alternative technique to label WBC in-vivo is based on the use of antigranulocyte murine monoclonal antibodies, or Fab' fragments, labelled with ^{99m}Tc. ^{99m}Tc-labelled murine monoclonal antibodies have been developed to target granulocytes in vivo. Immunoscintigraphy using ^{99m}Tc-labelled antigranulocyte antibodies (^{99m}Tc-AGAb) directed against the non-specific cross reacting antigen 95 (NCA-95) has been found to be a suitable modality for bone marrow imaging because of the simplicity of its use and a high target-to-background ratio [32]. NCA-95 is expressed at the cell membrane of circulating granulocytes in blood as well as in matured myeloid cells in the bone marrow [33]. The binding of the AGAb to cells in the bone marrow is very rapid and extensive because of the high concentration of granulocytes, promyelocytes and myelocytes that all express the NCA-95 antigen [34]. Myeloid cells in the bone marrow are in 50-100:1 excess compared with granulocytes in peripheral blood. ^{99m}Tc-AGAb was found to distribute primarily to bone marrow after intravenous injection [35], and a progressive increase in activity in the spleen and the bone marrow is visible [34]. The uptake in the spleen can potentially be used for assessment of extramedullary hematopoiesis [22].

The bone marrow status can be classified in three different ways: (a) estimation of the bone marrow distribution pattern, (b) identification of focal lesions (cold and hot), and (c) calculation of the uptake ratio between the sacroiliac region (corrected for background activity) and the background [36].

The bone marrow appearance on ^{99m}Tc-AGAb scans seemed to be characteristic for the different hematological diseases. In PV, a moderately increased uptake in the spleen is described, probably related to extramedullary hematopoiesis [37]. In MDS, generalized,

small and focal defects in uptake of the bone marrow are described without indication of extramedullary hematopoiesis or peripheral expansion [22].

In patients with MF, diffusely decreased bone marrow activity and prominent splenic uptake was seen. In AA, highly reduced and patchy marrow uptake was observed, but also a diffusely decreased uptake.

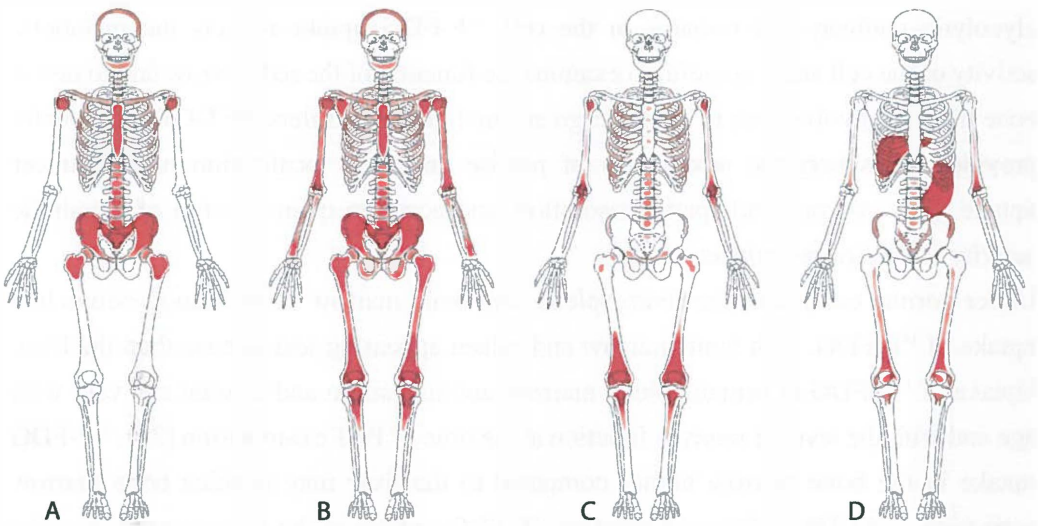

Figure 1: Different patterns of hematopoietic bone marrow imaging. A) Normal pattern of hematopoietic bone marrow activity in the central skeleton and skull; B) Expansion of hematopoietic bone marrow activity more distal in the extremities; C) Reduced hematopoietic bone marrow activity in the central compartment of the skeleton and skull, as seen in aplastic anemia; D) Myelofibrosis with extramedullary erythropoiesis in spleen and liver and reduced hematopoietic bone marrow activity in the central compartment of the skeleton and skull.

4. Imaging of the metabolic activity

The well known PET tracer ^{18}F-Fluorodeoxyglucose (^{18}F-FDG) is widely used in oncologic and infectious diseases. The ^{18}F-FDG uptake is a measure of cell glucose utilization (glycolysis). ^{18}F-FDG is metabolically trapped in the cell after phosphorylation to ^{18}F-FDG-6-phosphate. Unlike glucose, ^{18}F-FDG does not further participate in the glycolytic pathway and remains in the cell. ^{18}F-FDG uptake reflects the metabolic activity of the cell and it is useful to examine the function of the red marrow and to detect bone marrow involvement in both benign and malignant disorders. PET-CT additionally provides the synergistic advantages of precise anatomic localization of radiotracer uptake, high contrast and spatial resolution, and accurate quantification of metabolic activity at sites of radiotracer uptake.

Under normal conditions the liver, spleen, and bone marrow show homogeneous low uptake of ^{18}F-FDG, with bone marrow and spleen appearing less intense than the liver. Uptake of ^{18}F-FDG in hematopoietic marrow, and its pattern and amount can vary with age and with the level of marrow function at the time of PET examination [24]. ^{18}F-FDG uptake in the bone marrow higher compared to the liver may indicate bone marrow activation. [38] This diffuse increase of ^{18}F-FDG uptake in the bone marrow may be caused by the involvement of malignancy or hematopoietic disease but also due to an inflammatory reaction, stimulation by some types of malignancy, as a result of recent chemotherapy, or by the administration of hematopoietic growth factors. To determine efficacy of granulocyte colony-stimulating factor (G-CSF) and granulocyte-macrophage colony-stimulating factor (GM-CSF) on bone marrow glucose metabolism, the specific uptake of ^{18}F-FDG in bone marrow was evaluated. It was shown that a substantial increase in bone marrow ^{18}F-FDG uptake is rapidly induced by CSF treatments and should not be misinterpreted as diffuse bone metastases or bone marrow disease [39]. Therefore, ^{18}F-FDG uptake is a sensitive marker of stimulated hematopoiesis, and both the extension and the intensification of uptake should be taken into account during hematopoietic growth factor (HGF) therapy [40]. ^{18}F-FDG uptake in the bone marrow compartment can be quantified using the standardized uptake value (SUV).

Patients with PV show a diffuse elevated ^{18}F-FDG uptake in the bone marrow, as a result of bone marrow stimulation related to the clonal expansion of multipotent hematopoietic progenitor cells in this disease. When diffuse high marrow uptake of ^{18}F-FDG is seen PV should be considered in the differential diagnosis in the absence of an another etiology

[41,42]. A case report of a patient with MF showed a markedly increased ^{18}F-FDG uptake throughout the spleen and liver. Both were massively enlarged, combined with a lower ^{18}F-FDG uptake in the bone marrow of the central skeleton, being a reflection of the patients' MF [43]. Patients with MDS also show diffuse bone marrow ^{18}F-FDG uptake. The latter was also found in patients who underwent ^{18}F-FDG-PET for other reasons. So, these cases demonstrate that diffuse ^{18}F-FDG uptake by bone marrow likely suggests neoplastic disease of the hematopoietic tissue. [44] ^{18}F-FDG-PET has shown efficacy for the detection of bone marrow metastases from several malignancies including lung carcinoma, breast carcinoma, and lymphoma [45-49]. It is unclear to which extent lesions are involved in bone marrow and bone metastases. A recent study of 21 patients with diffuse large B-cell lymphoma (DLBCL) and bone marrow involvement, showed that the bone marrow uptake of ^{18}F-FDG depends on the histological type of the cell infiltrate. In this study, ^{18}F-FDG-PET showed abnormal foci of uptake in most patients with concordant bone marrow involvement (prominent diffuse large- B-cell lymphoma), whereas ^{18}F-FDG uptake was normal in most patients with discordant bone marrow involvement (prominent indolent lymphoma) [50]. Another study demonstrated at initial staging of Hodgkin Lymphoma (HL) that diffuse bone marrow uptake without splenic involvement could be due to HL related bone marrow involvement. However, these observations are more likely to be due to bone marrow inflammatory changes. In contrast, diffuse spleen uptake in combination with bone marrow uptake is probably more associated with disease involvement than with inflammatory changes [51]. Moreover, a report which describes the role of ^{18}F-FDG as a tracer to visualize bone marrow metastases in 257 patients with newly diagnosed lung cancer, the accuracy, sensitivity and specificity of ^{18}F-FDG-PET and bone scintigraphy were 94% vs 85%, 91% vs 75%, and 96% vs 95%, respectively [45].

A previous study investigating the bone marrow status in 112 breast cancer patients with N0 or N1 disease (who had undergone bone marrow aspiration twice) demonstrated that tumor cells are present in the bone marrow in 83% of the cases at the time of primary surgery. The latter was reduced to 24%, 12 months after initiation of adjuvant systemic chemotherapy [52]. This supports the concept that systemic treatment is effective in reducing the number of tumor cells within the bone marrow. Further studies are warranted to investigate this differential response to systemic therapy. When metastases are mainly confined to the bone marrow compared to those that involve the bone matrix, this would

further enhance the role of metabolic imaging of bone marrow metastases by ^{18}F-FDG-PET in various malignant disorders.

^{18}F-FDG-PET can also be used for the evaluation of chronic myeloid leukemia (CML) or acute lymphoblastic leukemia (ALL) [53,54]. Follow-up ^{18}F-FDG-PET scans were performed in patients with CML after termination of treatment [54]. ^{18}F-FDG-PET findings showed reduced ^{18}F-FDG uptake in the bone marrow. Also localized relapse of ALL in bone marrow can be visualized with ^{18}F-FDG-PET [53]. ^{18}F-FDG-PET has already been shown to be useful in the initial staging of multiple myeloma (MM) patients (fig. 2). As well, it was demonstrated to be valuable in patients with solitary plasmacytoma in bone as well as in patients suffering from extramedullary plasmacytoma [55]. Somatostatin receptor scintigraphy (SRS) using ^{111}In-pentetreotide may also be a good alternative to study the presence of the malignant plasma cells in MM and plasmacytoma patient, especially at relapse [56]. ^{99m}Tc-sestamibi has also been proposed as a potential tracer in patients with MM [57]. The patterns of ^{99m}Tc-sestamibi uptake in patients with MM are related to both the clinical status and the stage of disease. The presence of focal uptake or of intense diffuse bone marrow uptake suggests that the patient has active and advanced stage disease, while a negative scan in a patient with MM clearly indicates remission [57]. Compared with ^{99m}Tc-sestamibi ^{18}F-FDG-PET-CT performed better in the detection of focal lesions, whereas ^{99m}Tc-sestamibi was superior in the visualization of diffuse disease. In the spine and pelvis [58]. Finally, it is evident that ^{18}F-FDG-PET may become useful in the initial staging, follow-up, and restaging of patients with bone marrow malignancy.

Figure 2: FDG PET in a patient with multiple myeloma. Lesions are visible in the ribs, right scapula en sternum.

Imaging of the proliferative activity

The thymidine analogue 3-deoxy-3-^{18}F-fluorothymidine (^{18}F-FLT) has been developed as a PET tracer to image cell proliferation [59]. The pyrimidine analogue thymidine is incorporated in DNA and undergoes the same first metabolic step as thymidine. ^{18}F-FLT is taken up by the cell by both passive diffusion as well as facilitated transport by Na^+-dependent carriers. Subsequently, ^{18}F-FLT is phosphorylated by thymidine kinase 1 (TK1) into ^{18}F-FLT-monophosphate, after which it is trapped in the cell. The phosphorylation by TK1 forms the basis of ^{18}F-FLT as a proliferation tracer. As a result of this behavior, reduced ^{18}F-FLT uptake is seen in the affected area after radiotherapy (fig. 3). Accordingly, increased ^{18}F-FLT uptake in bone marrow and spleen is seen in patients with AML. This uptake was significantly higher in patients with relapsed, refractory, or

untreated leukemia [60]. Therefore, ^{18}F-FLT could be an imaging biomarker of disease activity. EMH lesions can also be seen with ^{18}F-FLT-PET (fig. 4E).

In a pilot study, we recently demonstrated ^{18}F-FLT distribution in hematologic disorders [61]. There is increased ^{18}F-FLT uptake in the bone marrow areas compared with healthy control subjects and a significant expansion of the bone marrow compartment in patients with MDS (fig. 4B). MPDs showed remarkable expansion of bone marrow with high uptake (fig. 4C). Despite the large size of liver and spleen in two patients with MPD, ^{18}F-FLT uptake in these organs was not elevated. Significantly higher uptake in the spleen and liver with distinct hepatosplenomegaly was characteristic of MF, with bone marrow uptake significantly reduced and expansion may be seen (fig. 4D). ^{18}F-FLT may also be a valuable tool to visualize the bone marrow compartment and identifies solitary areas of increased proliferative activity that can frequently be recognized in patients with AA (fig. 4A). Increased ^{18}F-FLT uptake is demonstrated after stem cell transplantation in a group of patients with lymphoma. At the same time there is an extension of bone marrow activity in the peripheral skeleton. These findings correlated with in vitro data showing a higher proliferative activity of hematopoietic progenitor cells [62]. ^{18}F-FLT-PET may be a promising method for non invasive evaluation of bone marrow activity after bone marrow transplantation.

^{11}C-methionine is another PET compound that can be used for imaging the amino acid activity in highly proliferative tissues, such as bone marrow [63]. The mechanism of increased uptake of ^{11}C-methionine in bone marrow has been described as an expression of increased cellular proliferation and protein synthesis [64]. MM is a process that is characterized by neoplastic proliferation of plasma cells, and these cells produce nearly always complete monoclonal immunoglobulins or monoclonal immunoglobulin light chains. The unrestricted expansion of a plasma cell clone and the excessive synthesis of monoclonal immunoglobulins result in extensive skeletal destruction and anemia. ^{11}C-methionine incorporation into immunoglobulins of the malignant plasma cell clone in vivo can be assumed. On the basis of increased methionine uptake in plasma cells, active MM can be imaged with ^{11}C-methionine PET [64]. Nunez et al., compared ^{11}C-methionine with ^{18}F-FDG-PET in 12 metastatic prostate cancer patients. The authors reported that ^{11}C-methionine PET was more effective than ^{18}F-FDG-PET for detecting bone metastases, including bone marrow involvement in this patient population [63].

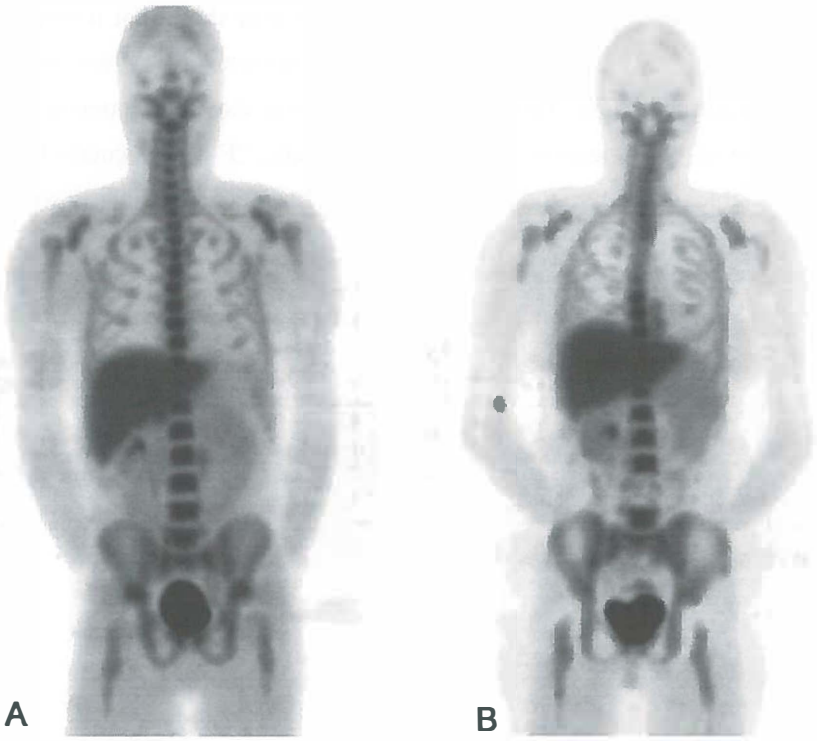

Figure 3: Normal distribution of ^{18}F-FLT PET (A); the effect of radiotherapy on bone marrow activity on the 4th lumbar vertebra and mid-thoracic vertebrae (B).

The potential advantages of PET using radiolabeled phospholipids, such as ^{11}C- and ^{18}F-labeled choline, in the assessment of prostate cancer patients have been emphasized in previous studies [65,66]. Choline uptake seems to be a marker of cell proliferation in prostate cancer, as malignancies are commonly characterized by increased proliferative activity. The second explanation proposed is upregulation of choline kinase in cancer cells: overexpression of choline kinase has been found in cancer cell lines, including human-derived prostate cancer [67]. Cimitan et al., examined 100 postoperative prostate cancer patients with persistent increased serum PSA levels, suggestive of local recurrences or distant metastases. ^{18}F-choline PET-CT correctly detected bone involvement in 21% of patients; also 76% of them were undergoing hormone therapy [65]. Bone marrow metastases were not scored separately in this study, but ^{18}F-choline may be an interesting PET tracer for this purpose.

^{11}C-acetate has also been used for the imaging of prostate cancer and the genitourinary system during the last few years and shows preferable characteristics for visualizing the pelvis due to its lack of urinary excretion and its acceptable tumor to background contrast

[68,69]. The value of ^{11}C-acetate PET in previously published data show that it might have significant potential for the detection of recurrences and bone metastases when using more advanced PET/CT equipment [70]. Probably ^{11}C-acetate may also be an interesting PET tracer for evaluation of bone marrow metastases. Recently, ^{18}F-fluoroacetate has been introduced as a possible alternative to ^{11}C-acetate for PET imaging, especially with respect to its longer half-life [71].

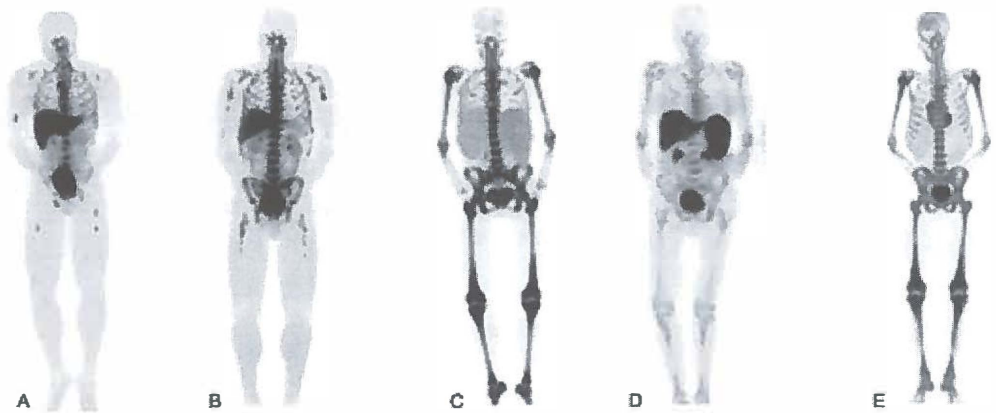

Figure 4: Different bone marrow patterns in 18F-FLT PET. A) A patient with AA. Several patchy hot lesions with increased proliferative activity are visible in the spine and femora, and mainly higher liver uptake compared to controls. B) A patient with MDS shows a relatively homogeneous 18F-FLT PET pattern in the bone marrow of the spine and relative heterogeneous expansion in the extremities, but the extremities can also be homogeneous. There is normal uptake in the liver and spleen. C) A patient with MPD shows homogeneously increased uptake and extensive peripheral bone marrow expansion into extremity bones and no elevated uptake in the liver or (enlarged) spleen. D) A patient with MF shows low uptake in the bone marrow compartment. Elevated uptake in the enlarged spleen and moderate elevated uptake in the liver as a result of extramedullary haematopoiesis. E) A patient with thoracic paravertebral EMH with β-thalassaemia.

Future perspectives and conclusion

Several patterns of bone marrow uptake can be identified depending on the hematopoietic activity, the underlying disorder and the radiopharmaceutical used. The appearance of the bone marrow activity can be more or less identical recognized with gamma- or PET cameras. However, differences were noted in the resolution and quality, and PET offers the ability of SUV quantification of the bone marrow activity. Different targets can be used for imaging the total normal and diseased bone marrow compartment. This is an advantage compared to a bone marrow biopsy by which 1-2 cm of the bone marrow compartment is evaluated. Imaging may help to differentiate in various bone marrow diseases and may play a part in monitoring treatment and bone marrow transplantation effect. New developments in PET tracers are entering our field of nuclear medicine. Imaging of hypoxia and programmed cell death of the bone marrow compartment are two features that can be studied in the future for monitoring disease activity or for studying the effects of therapy including chemotherapy, kinase inhibitors or radiotherapy [72]. A number of agents exploit the low oxygen tension in hypoxic tissues to permit intercellular trapping by reductive mechanisms. [^{18}F]Fluoromisonidazole-3-fluoro-1-(2 □-nitro-1 □-imidazolyl)-2-propanol (^{18}F-MISO) and ^{64}Cu-diacetyl-bis(N^4-methylthiosemicarbazone (^{64}Cu-ATSM), and the recently introduced [^{18}F]fluoroazomycinarabinoside (^{18}F-FAZA) are the lead contenders for human application. This promise is based on their non invasive nature, ease of use and robustness, measurement of hypoxia status, validity, ability to demonstrate heterogeneity and general availability [72,73]. ^{18}F-FAZA uptake by normal bone marrow cells is relative low, but may potentially increase during hypoxic circumstances [72]. Apoptosis or programmed cell death visualized with ^{18}F-annexin A5 may be of use to study the effectiveness of treatment in leukemia, MM or myeloproliferative disorders [74].

In future, ^{18}F-Immuno-PET or labeled with the longer living PET-label ^{89}Zr is of interest for the determination of CD66 distribution in the bone marrow especially for the evaluation of leukemia [75]. The CD66 antigen is expressed at the cell surface of mature myeloid cells including promyelocytes and granulocytes. It is therefore an attractive target for the detection of the extent of the monotonous population of leukemic cells in the bone marrow and probably also of value to monitor minimal residual disease following treatment. Anti-CD66 monoclonal antibodies (mAbs) labeled with beta-emitting nuclides (^{188}Re and ^{90}Y) have already been introduced and are suited as part

of treatment in high risk leukemia [76]. Neovascularisation is also a prominent feature of malignant transformation. Recently different agents have been introduced in the clinical practice including monoclonal antibodies against VEGF or kinase inhibitors of the VEGF receptor. New imaging tools with ^{89}Zr-bevacizumab have become available in solid tumors for visualization of neovascularisation [77]. This might be also an attractive approach for hematological disorders since enhanced neovascularisation is also a prominent feature in AML [78]. In conclusion, a variety of bone marrow targets can be imaged with radionuclide imaging, where PET offers the opportunity of absolute quantification of bone marrow activity. Imaging may help to differentiate in various bone marrow diseases and can play a role in monitoring treatment effect.

Acknowledgement

We thank Jan Pruim, Douwe Buiter and Albertus Piers for technical assistance.

REFERENCES

1. *Rubin R, Strayer DS. Rubin's Pathology: Clinicopathologic Foundations of Medicine. Lippincott Williams & Wilkins, 2007.*
2. *Rizo A, Vellenga E, de Haan G, Schuringa JJ. Signaling pathways in self-renewing hematopoietic and leukemic stem cells: do all stem cells need a niche? Hum Mol Genet 2006; 15 Spec No 2:R210-R219.*
3. *Johnsen HE, Kjeldsen MK, Urup T, Fogd K, Pilgaard L, Boegsted M et al. Cancer stem cells and the cellular hierarchy in haematological malignancies. Eur J Cancer 2009; 45 Suppl 1:194-201.*
4. *Vardimann JW. Myelodysplastic/Myeloproliferative Diseases. In: Finn WG, Peterson LC, editors. Hematopathology in Oncology. Springer US, 2004: 13-43.*
5. *Schepers H, van Gosliga D, Wierenga AT, Eggen BJ, Schuringa JJ, Vellenga E. STAT5 is required for long-term maintenance of normal and leukemic human stem/progenitor cells. Blood 2007; 110:2880-2888.*
6. *Koch CA, Li CY, Mesa RA, Tefferi A. Nonhepatosplenic extramedullary hematopoiesis: associated diseases, pathology, clinical course, and treatment. Mayo Clin Proc 2003; 78:1223-1233.*
7. *Charache S, Page DL. Infarction of bone marrow in the sickle cell disorders. Ann Intern Med 1967; 67:1195-1200.*
8. *Lutzker LG, Alavi A. Bone and marrow imaging in sickle cell disease: diagnosis of infarction. Semin Nucl Med 1976; 6:83-93.*
9. *Swardlow SH, Campo E, Harris NL, Jaffe ES, Pileri SA, Stein H et al. The revised (4th edition) of the World Health Organisation (WHO) classification of tumors of hematopoietic and lymphoid tissue. 2009.*
10. *Delhommeau F, Dupont S, Della Valle V, James C, Trannoy S, Masse A et al. Mutation in TET2 in myeloid cancers. N Engl J Med 2009; 360:2289-2301.*
11. *Jaffe ES, Harris NL, Stein H, Vardiman JW. Tumours of haematopoietic and lymphoid tissue, pathology and genetics. World Health Organization Classification of Tumours. IARC Press, 2001.*

12. *Tefferi A, Spivak JL. Polycythemia vera: scientific advances and current practice. Semin Hematol 2005; 42:206-220.*

13. *Tennvall J, Brans B. EANM procedure guideline for 32P phosphate treatment of myeloproliferative diseases. Eur J Nucl Med Mol Imaging 2007; 34:1324-1327.*

14. *Tam CS, Kantarjian H, Cortes J, Lynn A, Pierce S, Zhou L et al. Dynamic model for predicting death within 12 months in patients with primary or post-polycythemia vera/essential thrombocythemia myelofibrosis. J Clin Oncol 2009; 27:5587-5593.*

15. *Greenberg P, Anderson J, de Witte T, Estey E, Fenaux P, Gupta P et al. Problematic WHO reclassification of myelodysplastic syndromes. Members of the International MDS Study Group. J Clin Oncol 2000; 18:3447-3452.*

16. *Williamson PJ, Kruger AR, Reynolds PJ, Hamblin TJ, Oscier DG. Establishing the incidence of myelodysplastic syndrome. Br J Haematol 1994; 87:743-745.*

17. *Greenberg P, Anderson J, de Witte T, Estey E, Fenaux P, Gupta P et al. Problematic WHO reclassification of myelodysplastic syndromes. Members of the International MDS Study Group. J Clin Oncol 2000; 18:3447-3452.*

18. *Young NS. Acquired aplastic anemia. Ann Intern Med 2002; 136:534-546.*

19. *Young NS, Scheinberg P, Calado RT. Aplastic anemia. Curr Opin Hematol 2008; 15:162-168.*

20. *Pitcher LA, Hann IM, Evans JP, Veys P, Chessells JM, Webb DK. Improved prognosis for acquired aplastic anaemia. Arch Dis Child 1999; 80:158-162.*

21. *Desai AG, Thakur ML. Radiopharmaceuticals for spleen and bone marrow studies. Semin Nucl Med 1985; 15:229-238.*

22. *Reske SN. Recent advances in bone marrow scanning. Eur J Nucl Med 1991; 18:203-221.*

23. *Milner PF, Brown M. Bone marrow infarction in sickle cell anemia: correlation with hematologic profiles. Blood 1982; 60:1411-1419.*

24. *Blebea JS, Houseni M, Torigian DA, Fan C, Mavi A, Zhuge Y et al. Structural and functional imaging of normal bone marrow and evaluation of its age-related changes. Semin Nucl Med 2007; 37:185-194.*

25. *Ferrant A, Rodhain J, Leners N, Cogneau M, Verwilghen RL, Michaux JL et al. Quantitative assessment of erythropoiesis in bone marrow expansion areas using 52Fe. Br J Haematol 1986; 62:247-255.*

26. *Datz FL, Taylor A, Jr. The clinical use of radionuclide bone marrow imaging. Semin Nucl Med 1985; 15:239-259*

27. *Itoh H, Kanamori M, Takahashi N. Dissociation between In-111 chloride and Tc-99m colloid bone marrow scintigraphy in refractory anemia with excess blasts. Clin Nucl Med 1990; 15:124-125.*

28. *Sayle BA, Helmer RE, III, Birdsong BA, Balachandran S, Gardner FH. Bone-marrow imaging with indium-111 chloride in aplastic anemia and myelofibrosis: concise communication. J Nucl Med 1982; 23:121-125.*

29. *Rain JD, Najean Y. Bone marrow scintigraphy in myelofibrosis. Nouv Rev Fr Hematol 1993; 35:101-102.*

30. *McNeil BJ, Rappeport JM, Nathan DG. Indium chloride scintigraphy: an index of severity in patients with aplastic anaemia. Br J Haematol 1976; 34:599-604.*

31. *Hotta T, Murate T, Inoue C, Kagami T, Tsushita K, Wang JY et al. Patchy haemopoiesis in long-term remission of idiopathic aplastic anaemia. Eur J Haematol 1990; 45:73-77.*

32. *Huic D, Ivancevic V, Richter WS, Munz DL. Immunoscintigraphy of the bone marrow: normal uptake values of technetium-99m-labeled monoclonal antigranulocyte antibodies. J Nucl Med 1997; 38:1755-1758.*

33. *Wahren B, Gahrton G, Hammarstrom S. Nonspecific cross-reacting antigen in normal and leukemic myeloid cells and serum of leukemic patients. Cancer Res 1980; 40:2039-2044.*

34. *Becker W, Borst U, Fischbach W, Pasurka B, Schafer R, Borner W. Kinetic data of in-vivo labeled granulocytes in humans with a murine Tc-99m-labelled monoclonal antibody. Eur J Nucl Med 1989; 15:361-366.*

35. *Reske SN, Karstens JH, Gloeckner W, Steinstrasser A, Schwarz A, Ammon J et al. Radioimmunoimaging for diagnosis of bone marrow involvement in breast cancer and malignant lymphoma. Lancet 1989; 1:299-301.*

36. *Munz DL, Voth E, Emrich D. Different approaches to determine the uptake ratio of bone-marrow-seeking radiopharmaceuticals for classifying the scintigraphic bone marrow status. Nuc Compact 1987; 18:192-194.*

37. *Bonner H. Pathology. Chapter: The blood and the lymphoid organs. Lipincott, Philadelphia, 2009.*

38. *Inoue K, Goto R, Okada K, Kinomura S, Fukuda H. A bone marrow F-18 FDG uptake exceeding the liver uptake may indicate bone marrow hyperactivity. Ann Nucl Med 2009; 23:643-649.*

39. *Sugawara Y, Fisher SJ, Zasadny KR, Kison PV, Baker LH, Wahl RL. Preclinical and clinical studies of bone marrow uptake of fluorine-1-fluorodeoxyglucose with or without granulocyte colony-stimulating factor during chemotherapy. J Clin Oncol 1998; 16:173-180.*

40. *Knopp MV, Bischoff H, Rimac A, Oberdorfer F, van Kaick G. Bone marrow uptake of fluorine-18-fluorodeoxyglucose following treatment with hematopoietic growth factors: initial evaluation. Nucl Med Biol 1996; 23:845-849.*

41. *Basu S, Asopa R, Peshwe H, Mohandas KM. Diffuse intense FDG uptake in the bone marrow in gastrointestinal stromal tumor with coexistent polycythemia rubra vera. Clin Nucl Med 2008; 33:782-783.*

42. *Quarles van Ufford HM, de Jong JA, Baarslag HJ, de Haas MJ, Oud K, de Klerk JM. F-18 FDG PET in a patient with polycythemia vera. Clin Nucl Med 2008; 33:780-781.*

43. *Burrell SC, Fischman AJ. Myelofibrosis on F-18 FDG PET Imaging. Clin Nucl Med 2005; 30:674.*

44. *Inoue K, Okada K, Harigae H, Taki Y, Goto R, Kinomura S et al. Diffuse bone marrow uptake on F-18 FDG PET in patients with myelodysplastic syndromes. Clin Nucl Med 2006; 31:721-723.*

45. *Cheran SK, Herndon JE, Patz EF, Jr. Comparison of whole-body FDG-PET to bone scan for detection of bone metastases in patients with a new diagnosis of lung cancer. Lung Cancer 2004; 44:317-325.*

46. *Kumar R, Alavi A. Fluorodeoxyglucose-PET in the management of breast cancer. Radiol Clin North Am 2004; 42:1113-22, ix.*

47. *Kumar R, Maillard I, Schuster SJ, Alavi A. Utility of fluorodeoxyglucose-PET imaging in the management of patients with Hodgkin's and non-Hodgkin's lymphomas. Radiol Clin North Am 2004; 42:1083-1100.*

48. *Mavi A, Lakhani P, Zhuang H, Gupta NC, Alavi A. Fluorodeoxyglucose-PET in characterizing solitary pulmonary nodules, assessing pleural diseases, and the initial staging, restaging, therapy planning, and monitoring response of lung cancer. Radiol Clin North Am 2005; 43:1-21, ix.*

49. *Moog F, Bangerter M, Kotzerke J, Guhlmann A, Frickhofen N, Reske SN. 18-F-fluorodeoxyglucose-positron emission tomography as a new approach to detect lymphomatous bone marrow. J Clin Oncol 1998; 16:603-609.*

50. *Paone G, Itti E, Haioun C, Gaulard P, Dupuis J, Lin C et al. Bone marrow involvement in diffuse large B-cell lymphoma: correlation between FDG-PET uptake and type of cellular infiltrate. Eur J Nucl Med Mol Imaging 2009; 36:745-750.*

51. *Salaun PY, Gastinne T, Bodet-Milin C, Campion L, Cambefort P, Moreau A et al. Analysis of 18F-FDG PET diffuse bone marrow uptake and splenic uptake in staging of Hodgkin's lymphoma: a reflection of disease infiltration or just inflammation? Eur J Nucl Med Mol Imaging 2009; 36:1813-1821.*

52. *Becker S, Becker-Pergola G, Wallwiener D, Solomayer EF, Fehm T. Detection of cytokeratin-positive cells in the bone marrow of breast cancer patients undergoing adjuvant therapy. Breast Cancer Res Treat 2006; 97:91-96.*

53. *Endo T, Sato N, Koizumi K, Nishio M, Fujimoto K, Sakai T et al. Localized relapse in bone marrow of extremities after allogeneic stem cell transplantation for acute lymphoblastic leukemia. Am J Hematol 2004; 76:279-282.*

54. *Nakajo M, Jinnouchi S, Inoue H, Otsuka M, Matsumoto T, Kukita T et al. FDG PET findings of chronic myeloid leukemia in the chronic phase before and after treatment. Clin Nucl Med 2007; 32:775-778.*

55. *Jadvar H, Conti PS. Diagnostic utility of FDG PET in multiple myeloma. Skeletal Radiol 2002; 31:690-694.*

56. *Agool A, Slart RH, Dierckx RA, Kluin PM, Visser L, Jager PL et al. Somatostatin receptor scintigraphy might be useful for detecting skeleton abnormalities in*

patients with multiple myeloma and plasmacytoma. Eur J Nucl Med Mol Imaging 2010; 37:124-130.

57. *Pace L, Catalano L, Pinto A, De Renzo A, Di Gennaro F, Califano C et al. Different patterns of technetium-99m sestamibi uptake in multiple myeloma. Eur J Nucl Med 1998; 25:714-720.*

58. *Fonti R, Salvatore B, Quarantelli M, Sirignano C, Segreto S, Petruzziello F et al. 18F-FDG PET/CT, 99mTc-MIBI, and MRI in evaluation of patients with multiple myeloma. J Nucl Med 2008; 49:195-200.*

59. *Shields AF, Grierson JR, Dohmen BM, Machulla HJ, Stayanoff JC, Lawhorn-Crews JM et al. Imaging proliferation in vivo with [F-18]FLT and positron emission tomography. Nat Med 1998; 4:1334-1336.*

60. *Buck AK, Bommer M, Juweid ME, Glatting G, Stilgenbauer S, Mottaghy FM et al. First demonstration of leukemia imaging with the proliferation marker 18F-fluorodeoxythymidine. J Nucl Med 2008; 49:1756-1762.*

61. *Agool A, Schot BW, Jager PL, Vellenga E. 18F-FLT PET in hematologic disorders: a novel technique to analyze the bone marrow compartment. J Nucl Med 2006; 47:1592-1598.*

62. *Woolthuis C, Agool A, Olthof S, Slart RH, Huls G, Smid WM et al. Auto-SCT induces a phenotypic shift from CMP to GMP progenitors, reduces clonogenic potential and enhances in vitro and in vivo cycling activity defined by (18)F-FLT PET scanning. Bone Marrow Transplant 2010;*

63. *Nunez R, Macapinlac HA, Yeung HW, Akhurst T, Cai S, Osman I et al. Combined 18F-FDG and 11C-methionine PET scans in patients with newly progressive metastatic prostate cancer. J Nucl Med 2002; 43:46-55.*

64. *Dankerl A, Liebisch P, Glatting G, Friesen C, Blumstein NM, Kocot D et al. Multiple Myeloma: Molecular Imaging with 11C-Methionine PET/CT--Initial Experience. Radiology 2007; 242:498-508.*

65. *Cimitan M, Bortolus R, Morassut S, Canzonieri V, Garbeglio A, Baresic T et al. [18F]fluorocholine PET/CT imaging for the detection of recurrent prostate cancer at PSA relapse: experience in 100 consecutive patients. Eur J Nucl Med Mol Imaging 2006; 33:1387-1398.*

66. *Kwee SA, Thibault GP, Stack RS, Coel MN, Furusato B, Sesterhenn IA. Use of step-section histopathology to evaluate 18F-fluorocholine PET sextant localization of prostate cancer. Mol Imaging 2008; 7:12-20.*

67. *Zheng QH, Gardner TA, Raikwar S, Kao C, Stone KL, Martinez TD et al. [11C] Choline as a PET biomarker for assessment of prostate cancer tumor models. Bioorg Med Chem 2004; 12:2887-2893.*

68. *de Jong IJ, Pruim J, Elsinga PH, Vaalburg W, Mensink HJ. Visualization of prostate cancer with 11C-choline positron emission tomography. Eur Urol 2002; 42:18-23.*

69. *Shreve P, Chiao PC, Humes HD, Schwaiger M, Gross MD. Carbon-11-acetate PET imaging in renal disease. J Nucl Med 1995; 36:1595-1601.*

70. *Albrecht S, Buchegger F, Soloviev D, Zaidi H, Vees H, Khan HG et al. (11) C-acetate PET in the early evaluation of prostate cancer recurrence. Eur J Nucl Med Mol Imaging 2007; 34:185-196.*

71. *Ponde DE, Dence CS, Oyama N, Kim J, Tai YC, Laforest R et al. 18F-fluoroacetate: a potential acetate analog for prostate tumor imaging--in vivo evaluation of 18F-fluoroacetate versus 11C-acetate. J Nucl Med 2007; 48:420-428.*

72. *Souvatzoglou M, Grosu AL, Roper B, Krause BJ, Beck R, Reischl G et al. Tumour hypoxia imaging with [18F]FAZA PET in head and neck cancer patients: a pilot study. Eur J Nucl Med Mol Imaging 2007; 34:1566-1575.*

73. *Padhani A. PET imaging of tumour hypoxia. Cancer Imaging 2006; 6:S117-S121.*

74. *Baumann P, Mandl-Weber S, Volkl A, Adam C, Bumeder I, Oduncu F et al. Dihydroorotate dehydrogenase inhibitor A771726 (leflunomide) induces apoptosis and diminishes proliferation of multiple myeloma cells. Mol Cancer Ther 2009; 8:366-375.*

75. *Neumaier B, Mottaghy FM, Buck AK, Glatting G, Blumstein NM, Mahren B et al. (18)F-Immuno-PET: Determination of Anti-CD66 Biodistribution in a Patient with High-Risk Leukemia. Cancer Biother Radiopharm 2008;*

76. *Ringhoffer M, Blumstein N, Neumaier B, Glatting G, von Harsdorf S, Buchmann I et al. 188Re or 90Y-labelled anti-CD66 antibody as part of a dose-reduced conditioning regimen for patients with acute leukaemia or myelodysplastic*

syndrome over the age of 55: results of a phase I-II study. Br J Haematol 2005; 130:604-613.

77. *Nagengast WB, de Vries EG, Hospers GA, Mulder NH, de Jong JR, Hollema H et al. In vivo VEGF imaging with radiolabeled bevacizumab in a human ovarian tumor xenograft. J Nucl Med 2007; 48:1313-1319.*

78. *de Bont ES, Rosati S, Jacobs S, Kamps WA, Vellenga E. Increased bone marrow vascularization in patients with acute myeloid leukaemia: a possible role for vascular endothelial growth factor. Br J Haematol 2001; 113:296-304.*

Chapter 3

^{18}F-FLT-PET In haematological disorders: A novel technique to analyze the bone marrow compartment.

Ali Agool[1], Bart W. Schot[2], Pieter L. Jager[1], Edo Vellenga[2]

Departments of Nuclear Medicine and Molecular Imaging[1] ; Haematology[2].
University of Groningen and University Medical Center Groningen,
The Netherlands.

The Journal of Nuclear Medicine. 2006;47:1592-1598

Abstract

Few diagnostic procedures are available to determine the degree of bone marrow cellularity and the numbers of cycling cells in patients with bone marrow disorders. Non-invasive imaging of the bone marrow compartment may be helpful. The PET tracer [18F]-3'-fluoro-3'-deoxy-L-thymidine (^{18}F-FLT) has been developed recently. ^{18}F-FLT uptake is related to the rate of DNA synthesis and increases with higher proliferation rates in many types of cancer. Background uptake of ^{18}F-FLT in bone marrow is common. ^{18}F-FLT-PET might, therefore, visualise the high cycling activity of haematopoietic cells in the bone marrow compartment. Therefore, we investigated the feasibility of visualisation and quantification of the activity of the bone marrow compartment with ^{18}F-FLT-PET to distinguish different haematological disorders. ***Methods*** Clinical and laboratory data of 18 patients with myelodysplasia (MDS), chronic myeloproliferative disorders, myelofibrosis (MF), aplastic anemia (AA) or multiple myeloma (MM) were correlated with the results of ^{18}F-FLT-PET imaging using visual analysis and the standardized uptake value (SUV). Findings were compared with those of healthy control subjects (n=14). ***Result***s With SUV and visual analysis a distinction could be made between MDS (N=9), chronic myeloproliferative disorders (N=3) and myelofibrosis (n=3) compared with healthy control subjects. A significant increase in ^{18}F-FLT uptake was observed in all the studied patients with MDS and myeloproliferative disorders. In contrast, patients with MF and AA (n=1) demonstrated a decline in bone marrow ^{18}F-FLT uptake compared with healthy control subjects. Comparable results were observed in osteolytic lesions of patients with MM (n=2). ***Conclusion*** ^{18}F-FLT-PET can be used to visualize the proliferative activity of the bone marrow compartment and may be helpful to distinguish separate haematological disorders.

Introduction

In the management of patients with a haematological disorder, limited diagnostic procedures are available to determine the degree of bone marrow cellularity and the numbers of cycling cells. Primarily a bone marrow biopsy is performed in conjunction with microscopic evaluation. With these methods the bone marrow composition and cellularity can be analyzed. In addition, specific staining procedures can be performed to demonstrate the number of cycling cells. This procedure has distinct limitations: the procedure is invasive and only a very small proportion of the total bone marrow content is investigated, which carries the risk of sampling error. Also, the staining of the bone marrow cells with the monoclonal antibody Ki67, which reflects the number of cycling cells, is an in vitro procedure [1]. This might not always reflect the in vivo situation.

Non-invasive imaging of the bone marrow cellularity has been pursued using many tracer methods. Bone marrow scintigraphy can be divided into 3 categories based on the three target cell systems: red cell precursors, white cell precursors, and tracers for the reticuloendothelial system (RES). For example, in the past, ^{52}Fe was used for imaging of the erythropoietic precursor and ^{59}Fe for kinetic studies [2-4]. The exact target of ^{111}In-chloride, frequently used in the 1970s and 1980s, is unknown [5-6]. Recently, ^{99m}Tc-labeled antigranulocyte antibodies have been proposed to assess activity of granulocytic cells [7-9]. Finally, the activity of the RES can be assessed using ^{99m}Tc-labeled colloids. Important problems, however, with all of these agents appear to be non-specific couptake in RES (monocytes, macrophages, and so forth), the formation of human antimonoclonal antibodies or less desirable imaging properties (^{59}Fe and ^{52}Fe).

The DNA precursor 3'-fluoro-3'-deoxy-L-thymidine (^{18}F-FLT) has been developed Recently. Uptake of this tracer is directly related to the rate of DNA synthesis [10]. Preliminary results with this tracer in several types of cancer patients have demonstrated a high 'background' activity in the bone marrow compartment [11]. This might reflect the high cycling activity of haematopoietic cells in the bone marrow. However, the exact mechanism of ^{18}F-FLT uptake in bone marrow is still unclear. In several tumor types a relation between ^{18}F-FLT uptake and the proliferation rate has been found, suggesting that the same mechanism could be responsible for the bone marrow uptake [11].

The suggested specificity of ^{18}F-FLT uptake for cycling cells, the whole body imaging aspect, the high resolution of PET, and the quantification possibilities may support the relevance of ^{18}F-FLT-PET as diagnostic procedure in haematological disorders with bone

marrow abnormalities. These aspects could be of great advantage over ^{18}F-FDG-PET, which only has a minor uptake in normal bone marrow and might, therefore, be less sensitive. This is the rationale of our study. Patients with myelodysplasia (MDS), chronic myeloproliferative disorders, and myelofibrosis (MF) in conjunction with healthy control subjects were studied using the degree of ^{18}F-FLT uptake and the distribution pattern as the main study parameters.

Materials and Methods

Patients

Consecutive patients with haematological disorders were eligible for this study. The precise diagnosis was derived from clinical information and bone marrow biopsies. Patients were divided in 4 groups: MDS, chronic myeloproliferative disorders, MF and a miscellaneous group of patients. Patients with severe renal dysfunction, peripheral neuropathy, or severe elevation of liver enzymes were excluded. All patients provided written informed consent, and the study was approved by the local Medical Ethics Committee of the Groningen University Medical Center.

Controls

Patients with untreated non-small cell lung cancer (NSCLC) or testicular cancer, who had undergone ^{18}F-FLT-PET for other studies, were considered as the control subjects. Before inclusion, they were required to have normal blood hematology values, and no signs of bone marrow metastases at presentation or during 6 month follow-up. In addition the patients had to be free of chemotherapeutic or radiotherapeutic treatment.

Table 1: Patient characteristics.

Patient no	*Diagnosis*	*Hb*	*Leuco.*	Thrombo.
Ref. values		**7.5-9.9 mmol/l**	**4-10x10^9/l**	**150-0x10^9/l**
Myelodysplasia				
1	CMMoL	7.2	5	161
2	RARS	6.4	8.7	214
3	RA	5.4	1.1	108
4	RA	7.8	4.6	89
5	RA	6.5	6.5	218
6	RA	5.6	9.4	490
7	RARS	5.9	3.2	199
8	RAEB	6.5	10	68
9	RA	5.3	5.9	436
Myeloprolifertive				
10		5.7	20.2	244
11		6.5	4.6	404
12		5.2	11.6	170
Myelofibrosis				
13		4.1	1.9	11
14		7.2	7.1	132
15		6.1	16.9	110
Miscellaneouss				
16	MM	8.5	4.5	190
17	MM	8.4	4.8	177
18	AA	6.6	1.9	14

*RA = refractory anemia, RARS = refractory anemia with ringsideroblasts, RAEB = refractory anemia with blast excess, CMML = chronic myelo-monocytic leukemia, MM= multiple myeloma, AA = aplastic anemia.

Table 2: FLT findings in different bone marrow disorders.

Patient	*Visual FLT assessment*				*SUV FLT*								
	Liver	Spleen	Expansion	General	FemR	FemL	CrR	CrL	L4	T6	Li	Spine	Sp
Myelodysplasia													
1	+	+	5	Homogeneous	4.4	4.9	3.3	3.6	5.6	7.1	2.1	7.3	0.8
2	+	-	11	Homogeneous	5.8	5.8	6.8	6.9	8.6	6.6	1.9	8.2	0.9
3	+	+	16	Homogeneous, hepatosplenomegaly	6.8	6.8	7.8	7.6	10.2	9.6	2.1	9.9	2.4
4	++	+	5	Homogeneous, patchy expansion	2.2	1.6	2.4	5.2	9.2	6.9	5.0	8.2	1.3
5	+	+	10	homogeneous	2.7	2.6	5.3	5.2	5.2	6.6	3.2	6.2	1.5
6	+	-	7	Homogeneous	-	4.6	5.8	5.3	7.1	8.0	2.0	7.8	0.8
7	+	+	2	Homogeneous	8.3	-	5.6	5.7	7.2	7.5	1.9	8.2	1.5
8	+	+	7	Homogeneous	1.8	1.5	4.1	4.3	6.9	8.0	3.8	8.1	0.9
9	+	-	8	Homogeneous	3.0	3.0	4.3	3.9	5.7	6.6	2.2	6.5	1.2
Myeloproliferative													
10	+	+	22	Homogeneous, hepatosplenomegaly	3.8	4.0	3.3	3.2	4.0	3.2	1.2	4.0	1.0
11	+	+	8	Homogeneous	4.0	4.4	5.5	6.8	10.2	8.8	2.4	8.7	1.5
12	+	+	22	Homogeneous, hepatosplenomegaly	5.1	4.9	3.7	3.7	5.0	4.4	1.5	6.0	1.5
Myelofibrosis													
13	+++	+++	20	Inhomogeneous, splenomegaly	1.0	1.0	1.2	1.2	1.8	1.6	4.0	2.0	8.0
14	+++	+++	3	Homogeneous, hepatosplenomegaly	0.9	1.0	1.3	1.4	2.3	3.1	4.0	3.4	6.2
15	+++	+++	10	Homogeneous, hepatosplenomegaly	2.7	2.3	1.4	1.1	3.3	3.3	3.8	3.2	4.0
Miscellaneous													
16	+	+	0	Homogeneous, MM scapula R									
17	+	-	0	Homogeneous, MM crista									
18	+++	+	1	Homogeneous	0.5	0.5	0.8	1.8	1.7	2.8	4.6	3.1	1.1

*FemR=right femur , FemL=left femur, Cr=crista, L4=lumbar 4 vertebral body, T6= thoracic 6 vertebral body, Spl=spleen, Liv=liver, MM = multiple myeloma.

Table 3: Mean uptake values of ^{18}F-FLT in various patient groups and healthy control subjects.

Group	*Expansion*	*FemR*	*FemL*	*CrR*	*CrL*	*L4*	*T6*	*Liv*	*Spine*	*Spleen*
Controls (n=14)	0	1.41 ± 0.73	1.39 ± 0.68	2.50 ± 0.74	2.50 ± 0.74	3.38 ± 1.05	3.52 ± 1.12	2.33 ± 0.74	4.56 ± 1.36	1.46 ± 0.41
MDS (n=9)	8.2 ± 4.1†	4.36 ± 2.36†	3.84 ± 1.97†	5.03 ± 1.68†	5.29 ± 1.29†	7.29 ± 1.71†	7.43 ± 1.00†	2.69 ± 1.08	7.81 ± 1.08†	1.27 ± 0.56
MP (n=3)	17.3 ± 9.2†	4.29 ± 0.69*	4.45 ± 0.46*	4.17 ± 1.21*	4.57 ± 1.91*	6.41 ± 3.35*	5.47 ± 2.94	1.69 ± 0.61	6.22 ± 2.38	1.50 ± 0.03
MF (n=3)	11 ± 5.0†	1.51 ± 0.98	1.44 ± 0.77	1.32 ± 0.11*	1.23 ± 0.13*	2.44 ± 0.77	2.65 ± 0.91	3.95 ± 0.11*	2.87 ± 0.75*	6.00 ± 2.17†

† $P < 0.001$, * $P < 0.05$ for comparison with controls. MP= Myeloproliferative, MF=Myelofibrosis.

Bone marrow examination

Bone marrow biopsy was performed on all patients before ^{18}F-FLT-PET, with a maximal interval of one month and a minimal interval of 2 weeks. Cellular proliferation was determined in a subgroup using Ki-67 immunostaining with MIB-1 (Ki-67 index) in a selected number of patients [12].

^{18}F-FLT-PET

^{18}F-FLT was produced according to the method described by Grierson et al with a radiochemical purity of >95% and a specific activity of >10 TBq/mmol [13]. Patients were instructed to fast at least six hours before investigation, with the exception of free access to water and normal medication. ^{18}F-FLT in a dose of 400 MBq (±10%) was administered intravenously.

Approximately 60 minutes after the ^{18}F-FLT injection, the patient was placed in the camera and emission scans of 5 minutes per bed position and transmission scans of 3 minutes per bed position were acquired over ~12 bed positions to cover the whole body. An ECAT EXACT HR+ scanner (Siemens Medical Systems) was used for all PET studies. Images were acquired in the three-dimentional acquisition mode.

Data analysis

two nuclear physicians who were unaware of the results of bone marrow biopsy and the clinical diagnosis performed visual and quantitative analysis of ^{18}F-FLT-PET images. As this is a new application of ^{18}F-FLT-PET, the first readings were independent and a consensus reading was carried out afterwards. In visual analysis the overall scan pattern was recorded, the intensity of bone marrow uptake as well as the degree of bone marrow expansion were evaluated. To quantify bone marrow expansion, we developed a simple scoring system in which one point is given for expansion in every one third of the long bones, based on the well known distribution of ^{18}F-FLT in the central skeleton and ultra-proximal part of femora and humera. Also the liver and spleen size and uptake intensity were evaluated qualitatively: + denotes minor uptake intensity, ++ denotes intermediate uptake, +++ denotes strong uptake intensity.

We also quantified FLT uptake using standard SUV analysis in patients and control subjects. We selected several sites of the axial skeleton to sample ^{18}F-FLT activity. These sites were the proximal femur (left and right) at the level of the trochanter major, the iliac crest on both sides, the corpus of lumbar vertebra 4 and thoracic vertebra 6. In case of

enlargement, also SUV of the liver or spleen was also determined. The region of interests used in SUV analysis were three-dimensional and were based on the mean value within the 50% isocontour's boundaries using a Siemens Leonardo workstation.

Statistics

For analysis of overall and individual group differences, we used Kruskall- Wallis and Mann-Whitney *U* tests. For correlations, we used Spearman's ϱ. *P* values < 0.05 were considered significant.

Results

Patients

Eighteen patients were included in this study, 10 men (mean age 69 y) and 8 women (mean age 64 y). Patients groups included MDS (n=9), according to International Prognosis Scoring System score belonging to the low-risk or low-intermediate risk group [14], chronic myeloproliferative disorders (n=3), MF(n=3) and a miscellaneous group of patients (AA n=1, MM n=2)(Table 1 and 2). Fourteen untreated patients known with NSCLC or testis carcinoma were used as the control group. None of the patients had bone marrow involvement and none had undergone chemotherapy or radiotherapy and had normal peripheral blood cell counts.

Visual analysis and SUV of ^{18}F-FLT-PET in controls

All healthy control subjects were verified to have a qualitatively normal ^{18}F-FLT scan with homogenous tracer distribution, as known from all previous ^{18}F-FLT studies (Fig. 1) [15-20]. No bone marrow expansion was observed beyond the axial skeleton, and the size of liver and spleen was within the normal range. Within the group of healthy control subjects no difference was observed for ^{18}F-FLT uptake between the right or left uptake from the same area (Table 3). The lowest uptake was observed in the femura (1.41 ± 0.73) and the highest uptake in the thoracic and lumbar vertebral body (3.52 ± 1.12; 3.38 ± 1.05).

Visual analysis and SUV of ^{18}F-FLT-PET in patient groups

Overall, significant differences were found between the patient groups for all sites of ^{18}F-FLT uptake (Kruskal-Wallis test, *P* values between 0.003 – 0.001) and the expansion score ($P < 0.0001$) (Fig. 2).

MDS groups

Visual analysis in 8 MDS patients demonstrated a homogenous ^{18}F-FLT pattern in the bone marrow (Fig. 3). In one patient ^{18}F-FLT-PET showed a patchy uptake with hot spots distributed over the skeleton. SUV analysis of the total MDS group demonstrated significantly increased ^{18}F-FLT uptake in all of the tested bone marrow areas compared with healthy control subjects ($P < 0.001$, Table 3). In addition, a significant expansion of the bone marrow compartment was shown ($P < 0.001$). Liver and splenic uptake were similar to the ^{18}F-FLT uptake in control subjects.

Chronic myeloproliferative group

^{18}F-FLT uptake in these 3 patients was homogenous, with hepatosplenomegaly in two (Fig. 4). As expected, this group of patients had remarkable expansion of bone marrow uptake with a mean expansion score of 17.3 ± 8 ($P < 0.0001$ vs control subjects). This was also higher compared with the MDS group but the difference was not significant. Despite the large size of liver and spleen in two, ^{18}F-FLT uptake in these organs was not elevated. SUV analysis in this small subgroup yielded higher values than those in the control group in the right femur, both iliac crests, and L4 vertebral body. Values were highest in L4 and T6 but no significant difference was observed in comparison with the MDS group. In this patient group, liver and splenic uptake were similar to the uptake in controls.

Myelofibrosis group

^{18}F-FLT uptake was homogenous in two patients but was irregular in one patient. Significantly higher uptake in the spleen and liver with distinct hepatosplenomegaly was characteristic of this subgroup compared with healthy control subjects (Liver: 3.95 ± 0.11 vs 2.33 ± 0.74, $P < 0.05$; Spleen 6.0 ± 2.2 vs 1.46 ± 0.41) (Fig. 5). Bone marrow expansion was also observed, with a mean expansion score of 6.5 ± 5.0. Expansion was significant in one and moderate in the additional 2 patients. A significant reduced

[18]F-FLT uptake was found for left and right crista, and fore the spine (2.87 ± 0.75 vs 4.56 ± 1.36, $P < 0.05$).

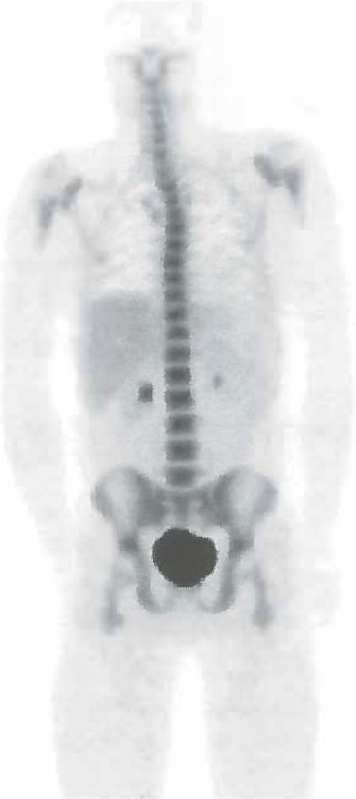

Figure 1: Normal [18]F-FLT PET projection image shows uptake in bone marrow in the central skeletal compartment limited to the ultraproximal extremity bones.

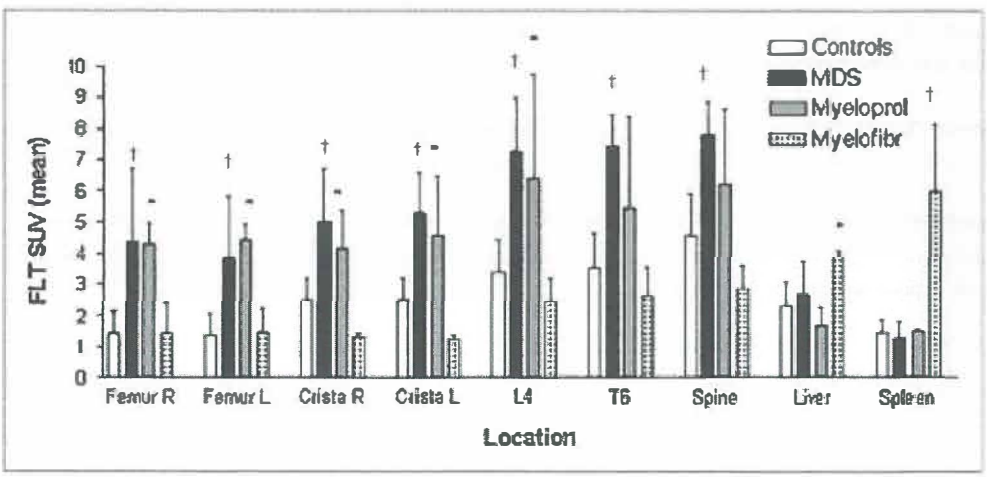

Figure 2: Bar graph showing [18]F-FLT uptake values (SUVmean) at various locations. * $P < 0.05$, † $P < 0.001$ for comparison to controls. Myeloprol = Myeloproliferative disorder; Myelofibr = myelofibrosis.

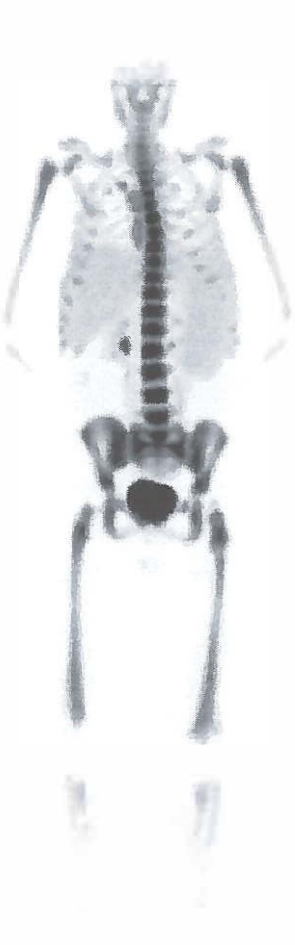

Figure 3

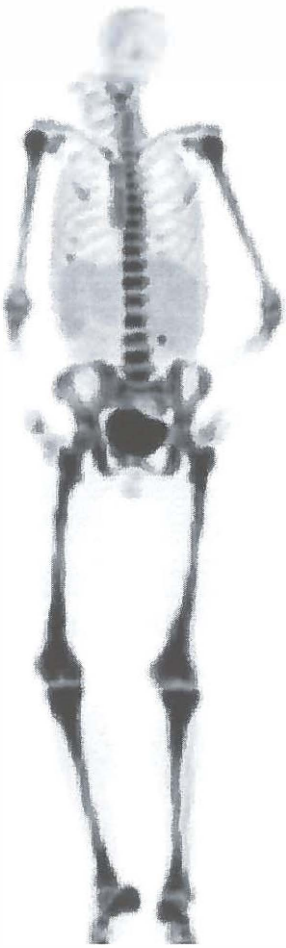

Figure 4

Figure 5

Figure3: ^{18}F-FLT PET in patient with myelodysplasia, shows homogeneously increased uptake and modest peripheral bone marrow expansion into the peripheral bones.

Figure4: ^{18}F-FLT PET in patient with myeloproliferative disorder shows homogeneously increased uptake and extensive peripheral bone marrow expansion into the extremity bones.

Figure5: ^{18}F-FLT PET in patient with myelofibrosis shows low uptake in the bone marrow compartment, hepatosplenomegaly with increased uptake as a result of extramedullary hematopoiesis and minor bone marrow expansion into the extremity bones.

Miscellaneous group

To underscore further that the ^{18}F-FLT uptake is a reflection of the proliferative activity of the bone marrow compartment, one patient with AA was studied. In addition, osteolytic lesions of 2 MM patients were analyzed, as it is known that this malignant plasma cell population has a low proliferative activity. In the patient with AA, a strongly reduced ^{18}F-FLT uptake was observed (Table 2). In the MM patients, the affected area demonstrated a low ^{18}F-FLT uptake.

Correlations With ^{18}F-FLT uptake parameters

In the 10 MDS patients Ki-67 staining of the bone marrow was available. No correlation was found between ^{18}F-FLT uptake and Ki-67 positivity. For most locations significant and moderate correlation coefficients (varying between 0.52 and 0.77) between ^{18}F-FLT uptake and the bone marrow expansion scores were found. In addition, a moderate negative correlation of –0.77 was found between ^{18}F-FLT expansion score and hemoglobulin level.

Discussion

This feasibility study appears to confirm the value of ^{18}F-FLT-PET in various haematological bone marrow disorders. Compared with control subjects, bone marrow uptake of ^{18}F-FLT was clearly higher in patients with MDS and myeloproliferative disorders but was lower in patients with MF, MM and AA, in agreement with the cycling activity of the bone marrow compartment of the affected areas. In addition, bone marrow expansion into the peripheral bones was clearly visualized in various degrees in all patients. The combined use of visual analysis and SUV could help distinguish separate haematologic disorders and might be of value for the diagnostic follow-up of this group of patients. In this way, ^{18}F-FLT-PET may provide additional information to data from bone marrow biopsies. ^{18}F-FLT-PET, especially, provides a detailed analysis on the entire bone marrow compartment.

In MDS, the increased proliferative activity of erythroid and myeloid cells appears to be followed by an increased programmed cell death [21,22] and, as consequences, peripheral pancytopenia. The increased uptake of ^{18}F-FLT in our MDS patients is in agreement with

the high proliferative activity of the progenitor cells in the bone marrow compartment [21]. Although comparable high ^{18}F-FLT SUV values are observed in patients with myeloproliferative disorders, the underlying defects are different. High peripheral blood cell counts are observed frequently in this patient group, which excludes the possibility of increased programmed cell death in the bone marrow compartment.

Although in most patients ^{18}F-FLT uptake was homogenous, there was one MDS patient who had a clear patchy ^{18}F-FLT appearance with focal hot spots, possibly indicating 'islands' with high bone marrow activity.

In MF, the number of cycling bone marrow cells is reduced due to excessive fibrosis, which is in accordance with the low ^{18}F-FLT uptake. In contrast high SUV values were observed in liver and spleen because of extramedullary hematopoiesis, reflecting proliferative activity of the erythroid and myeloid cells.

The mechanisms governing the uptake of ^{18}F-FLT in bone marrow are not fully clarified. In many tumor types, good correlations between proliferative activity and ^{18}F-FLT uptake have been demonstrated [11]. Uptake of ^{18}F-FLT appears to be related to the activity of the thymidine-kinase-1 enzyme, which is expressed higher in tumor cells, especially during the S-phase of the cell cycle [23]. Presumably the same mechanism accounts for the high uptake in the bone marrow compartment with its high proliferative activity. Uptake of ^{18}F-FLT by RES is less likely. This assumption is based on previous studies in both patients and laboratory animals, in which only minor uptake of ^{18}F-FLT in inflammatory lesions was observed [11,24]. However, this assumption needs further validation. No correlation was found with Ki-67 staining. Besides sampling errors, this finding may also be due to the fact that this marker is more suitable to demonstrate a reduced proliferation than an increased proliferation, as normal bone marrow cells already demonstrate high proliferative activity [12].

Studies Comparable as the present study have been performed in the past, using a multitude of tracers, such as iron isotopes for imaging and turnover studies of the erythropoietic precursor [2-4], ^{99m}Tc-labeled antigranulocyte antibodies for imaging of myeloid cells [7-9], radiocolloids for RES cell activity, and ^{111}In-choride. Compared with those methods, ^{18}F-FLT-PET has a considerably higher resolution, produces tomographic information and allows better quantification. Moreover, it might provide more specific information about the bone marrow compartment than a reflection of the functional activity of the RES .

Conclusion

^{18}F-FLT-PET provides visual and quantitative information on the entire bone marrow compartment studied in a limited number of patients with haematologic disorders. This might help in distinguishing various bone marrow disorders and be of value in the diagnostic follow-up of these patients.

Acknowledgment

We thank Philip Elsinga, PhD and his radiochemical staff for providing ^{18}F-FLT.

REFERENCES

1. *Palutke M, Tabaczka PM, Kukuruga DL, Kantor NL. A method for measuring lymphocyte proliferation in mixed lymphocyte cultures using a nuclear proliferation antigen, Ki-67, and flow cytometry. Am J Clin Pathol. 1989;91:417-421.*

2. *Kahn E, Aubert B, Parmentier C, Di Paola R. Feasibility of a 59Fe ferrokinetic study based on bone-marrow scans. Eur J Nucl Med. 1983;8:312-316.*

3. *Ferrant A, Rodhain J, Leners N, Cogneau M, Verwilghen RL, Michaux JL, Sokal G. Quantitative assessment of erythropoiesis in bone marrow expansion areas using 52Fe. Br J Haematol. 1986;62:247-255.*

4. *Lubberink M, Tolmachev V, Beshara S, Lundqvist H. Quantification aspects of patient studies with 52Fe in positron emission tomography. Appl Radiat Isot. 1999;51:707-715.*

5. *Horn NL, Bennett LR, Marciano D. Evaluation of aplastic anemia with indium chloride In 111 scanning. Arch Intern Med. 1980;40:1299-1303.*

6. *Pauwels EK, Hermans J, Jurgens PJ, Tjon Pian Gi CE, Haak HL, te Velde J. Scintigraphic aspects of 111In-chloride bone marrow scintigraphy in aplastic anaemia. Diagn Imaging. 1981;50:269-276.*

7. *Jamar F, Field C, Leners N, Ferrant A. Scintigraphic evaluation of the haemopoietic bone arrow using a 99mTc-anti-granulocyte antibody: a validation study with 52Fe. Br J Haematol. 1995;90:22-30.*

8. *Chung JK, Yeo J, Lee DS, Park S, Lee MC, Kim BK, Koh CS. Bone marrow scintigraphy using technetium-99m-antigranulocyte antibody in hematologic disorders. J Nucl Med. 1996;37:978-982.*

9. *Huic D, Ivancevic V, Richter WS, Munz DL. Immunoscintigraphy of the bone marrow: normal uptake values of technetium-99m-labeled monoclonal antigranulocyte antibodies. J Nucl Med. 1997;38:1755-1758.*

10. *Shields AF, Grierson JR, Dohmen BM, Machulla HJ, Stayanoff JC, Lawhorn-Crews JM, et al. Imaging proliferation in vivo with [F-18]FLT and positron emission tomography. Nature Med 1998;4:1334-1336.*

11. *Been LB, Suurmeijer AJ, Cobben DC, Jager PL, Hoekstra HJ, Elsinga PH. [18F] FLT-PET in oncology: current status and opportunities. Eur J Nucl Med Mol Imaging. 2004;31:1659-1672.*

12. *Brada SJ, van de Loosdrecht AA, Koudstaal J, de Wolf JT, Vellenga E. Limited numbers of apoptotic cells in fresh paraffin embedded bone marrow samples of patients with myelodysplastic syndrome. Leuk Res. 2004;28:921-925.*

13. *Grierson John R, Shields Anthony F. Radiosynthesis of 3'-Deoxy-3'-[^{18}F] fluorothymidine: [^{18}F]FLT for imaging of cellular profileration in vivo. Nuclear Medicine & Biology. 2000;27:143-156.*

14. *Greenberg P, Cox C, LeBeau MM, Fenaux P, Morel P, Sanz G, et al. International scoring system for evaluating prognosis in myelodysplastic syndromes. Blood. 1997;89:2079-2088.*

15. *Been LB, Elsinga PH, de Vries J, Cobben DC, Jager PL, Hoekstra HJ et al. Positron emission tomography in patients with breast cancer using (18)F-3'-deoxy-3'-fluoro-l-thymidine ((18)F-FLT)-a pilot study. Eur J Surg Oncol. 2006;32:39-43.*

16. *van Westreenen HL, Cobben DC, Jager PL, van Dullemen HM, Wesseling J, Elsinga Ph, et al. Comparison of 18F-FLT PET and 18F-FDG PET in esophageal cancer. J Nucl Med. 2005;46:400-404.*

17. *Cobben DC, Elsinga PH, Hoekstra HJ, Suurmeijer AJ, Vaalburg W, Maas B,et al. Is 18F-3'-fluoro-3'-deoxy-L-thymidine useful for the staging and restaging of non-small cell lung cancer? J Nucl Med. 2004;45:1677-1682.*

18. *Cobben DC, Elsinga PH, Suurmeijer AJ, Vaalburg W, Maas B, Jager PL et al. Detection and grading of soft tissue sarcomas of the extremities with (18)F-3'-fluoro-3'-deoxy-L-thymidine. Clin Cancer Res. 2004;10:1685-1690.*

19. *Cobben DC, van der Laan BF, Maas B, Vaalburg W, Suurmeijer AJ, Hoekstra HJ et al. 18F-FLT PET for visualization of laryngeal cancer: comparison with 18F-FDG PET. J Nucl Med. 2004;45:226-231.*

20. *Cobben DC, Jager PL, Elsinga PH, Maas B, Suurmeijer AJ, Hoekstra HJ. 3'-18F-fluoro-3'-deoxy-L-thymidine: a new tracer for staging metastatic melanoma? J Nucl Med. 2003 44:1927-1932.*

21. *Span LF, Vierwinden G, Pennings AH, Boezeman JB, Raymakers RA, de Witte T. Programmed cell death is an intrinsic feature of MDS progenitors, predominantly found in the cluster-forming cells. Exp Hematol. 2005;33:435-442.*

22. *Houwerzijl EJ, Blom NR, van der Want JJ, Louwes H, Esselink MT, Smit JW et al. Increased peripheral platelet destruction and caspase-3-independent programmed cell death of bone marrow megakaryocytes in myelodysplastic patients. Blood. 2005;105:3472-3479.*

23. *Barthel H, Perumal M, Latigo J, He Q, Brady F, Luthra SK et al. The uptake of 3'-deoxy-3'-[18F]fluorothymidine into L5178Y tumors in vivo is dependent on thymidine kinase 1 protein levels. Eur J Nucl Med Mol Imaging. 2005;32:257-263.*

24. *Van Waarde A, Cobben DC, Suurmeijer AJ, Maas B, Vaalburg W, de Vries EF, et al. Selectivity of 18F-FLT and 18F-FDG for differentiating tumor from inflammation in a rodent model. J Nucl Med. 2004;45:695-700.*

Chapter 4

Auto-SCT induces a phenotypic shift from CMP to GMP progenitors, reduces clonogenic potential and enhances in vitro and *in vivo* cycling activity defined by ^{18}F-FLT-PET scanning

Carolien Woolthuis[1], Ali Agool[2], Sandra Olthof[1], Riemer H.J.A. Slart[2], Gerwin Huls[1], Martin Smit[3], Jan J. Schuringa[1], Edo Vellenga[1]

[1]Department of Hematology, [2]Department of Nuclear Medicine and Molecular Imaging, [3]Sanquin, University of Groningen and University Medical Center Groningen, Groningen, The Netherlands

Bone Marrow Transplantation (In press)

Abstract

Autologous SCT (auto-SCT) introduces a reduced tolerance to chemotherapy even in patients with adequate engraftment, suggesting long-term effects of the transplantation procedure on the BM capacity. To study the hematopoietic cell compartment after auto-SCT, $CD34^+$ BM cells (n=16) from patients at 6–9 months after auto-SCT were studied with regard to the progenitor subsets, colony frequency and cell cycle status. The BM compartments were studied in vivo using PET tracer 3-fluoro-3-deoxy-Lthymidine (^{18}F-FLT-PET). BM $CD34^+$ cells after auto-SCT were compared with normal $CD34^+$ cells and showed a phenotypic shift from common myeloid progenitor (CMP mean percentage 3.7 vs 19.4%, P=0.001) to granulocyte–macrophage progenitor (GMP mean percentage 51.8 vs 27.6%, P=0.01). In addition, a reduced clonogenic potential and higher cycling activity especially of the GMP fraction (41%±4 in G2/S phase vs 19%±2, P=0.03) were observed in BM after auto-SCT compared with normal. The enhanced cycling activity was confirmed in vivo by showing a significantly higher uptake of the ^{18}F-FLT-PET tracer by the BM compartment. This study shows that auto-SCT results in defects of the hematopoietic compartment at least 6 months after auto-SCT, characterized by changes in the composition of progenitor subsets and enhanced in vitro and in vivo cycling activity.

Introduction

Auto-SCT is a frequently applied treatment modality for patients with multiple myeloma and relapsing lymphoma [1,2]. However, in 30–50% of the patients the underlying malignant disorder relapses within 2–5 years after auto-SCT. Treatment options are then limited not only because of drug resistance of the tumor, but also because of the severe concurrent chemotherapy-induced pancytopenia. Several in vitro studies have shown that the impaired BM capacity might be related to intrinsic defects of the hematopoietic compartment reflected by a reduced clonogenic potential of the long-term culture initiating cells in conjunction with a shortening of telomeres [3-5].After allo-SCT also a higher mitotic activity of BM $CD34^+/CD90^+$ cells has been shown [6].

Recent studies in mice and humans have shown that the compartments of the hematopoietic stem cell and progenitor cells (common myeloid progenitor (CMP), granulocyte–macrophage progenitor (GMP) and megakaryocyte–erythroid progenitor (MEP)) can be defined phenotypically with certain surface markers [7,8]. These phenotypically defined subpopulations are also verified by in vitro colony assays. In these assays the CMP fraction provided myeloid and erythroid colony formation whereas the GMP fraction generated exclusively myeloid colony formation [9]. In addition, the progenitors and more differentiated hematopoietic cells can be studied in vivo. Recent studies have shown that the cycling activity of the BM compartment can be visualized by using the PET tracer 3-fluoro-3-deoxy-Lthymidine (^{18}F-FLT-PET) [10,11]. Distinct patterns of uptake have been shown. In myelodysplasia a significantly higher cycling activity of the BM compartment was noticed whereas in aplastic anemia a significant reduction in cycling activity was shown [10]. Combining both in vitro and in vivo experiments, important information can be obtained regarding the functionality of the hematopoietic stem cell compartment after auto-SCT.

The results of this study show that BM $CD34^+$ cells at 6–9 months after auto-SCT show a shift from CMP to a more GMP-enriched phenotype, a reduced colony frequency and a higher cycling activity compared with normal $CD34^+$ cells. These results were validated in vivo by showing a significantly higher uptake of ^{18}F-FLT in the BM compartment after auto-SCT.

Materials and Methods

Patients

BM samples from patients and normal controls were obtained after informed consent according to institutional guide lines. $CD34^+$ cells were isolated by EasySep immunomagnetic cell selection (StemCell Technologies, Vancouver, Canada) according to manufacture's instructions.

Flowcytometry analysis and sorting procedures

Sorting of the $CD34^+$ cells into progenitor fractions was performed on the basis of the combinatorial expression of cell surface Ags as previously reported [9]. CMPs were defined as $CD34^+$ $CD38^+CD110^+CD45RA^+$, GMPs as $CD34^+CD38^+$ $CD110^-CD45RA^+$ and MEP as $CD34^+CD38^+CD110^+CD45RA^-$. The FACS analyses were performed on a FACS Calibur (Becton Dickinson (BD), Alphen a/d Rijn, The Netherlands). Antibodies were obtained from BD. Data were analysed using WinList 3D (Verity Software House, Topsham, ME, USA) and FlowJo (Tri Star, Inc, Ashland, OR, USA) software.

CFC progenitor assays

The colony forming cell (CFC) assays were performed in 1.2% methylcellulose containing 30% FCS, 57.2 μM β-mercaptoethanol, and 2 mM Glutamine, supplemented with 20 ng/ml IL-3, 20 ng/ml IL-6, 20 ng/ml G-CSF, 20 ng/ml c-Kit ligand and 1 U/ml EPO (Cilag: Eprex; Brussels, Belgium) as previously described [12]. To define the *in vitro* cycling activity of the CFC's, $CD34^+$ cells were incubated with variable concentrations of cytarabin (Faulding Pharmaceuticals, Brussels, Belgium), that is, 5 x 10^{-6}M, 1 x 10^{-6}M, 5 x 10^{-6}M, 7.5 x 10^{-6}M, 1 x 10^{-5}M, 5 x 10^{-5}M, and 1 x 10^{-4}M during 24 hrs and subsequently plated in the CFC assay. After 14 days the CFC colony number was counted with an inverted microscope.

Cell cycle analysis

For cell cycle analysis, Hoechst staining was performed. In brief, cells were resuspended at 1 x 10^6/mL in warm hematopoietic progenitor growth medium, 5 μg/mL Hoechst 33 342 (Sigma-Aldrich, Zwijndrecht, The Netherlands) was added and cells were incubated at 37°C for 45 min. Medium was removed and cells were stained with antibodies for progenitor analysis. Washed cells were kept on ice until FACS analysis.

^{18}F-FLT-PET

^{18}F-FLT was produced with a radiochemical purity of >95% and a specific activity of >10 TBq/mmol. ^{18}F-FLT in a dose of 400 MBq (±10%) was administered intravenously as described [10]. To quantify BM expansion, we developed a simple scoring system in which one point is given for expansion in every one third of the long bones, based on the well known distribution of ^{18}F-FLT in the central skeleton and ultra-proximal part of femoral and humeral bones. The ^{18}F-FLT uptake was also quantified using standard SUV analysis in patients and control subjects. We selected several sites of the axial skeleton to sample ^{18}F-FLT activity. The region of interests used in standarized uptake value analysis were based on the mean value within the 50% isocontour's boundaries using a Siemens Leonardo workstation Forchheim, Germany. The control patients were patients with untreated non-small cell lung cancer or testicular cancer who had undergone 18F-FLT-PET for other studies with normal blood hematology values and had no signs of BM metastases at presentation or during 6 months of follow-up. In addition, the patients were free of chemotherapeutic or radiotherapeutic treatment. The protocols were approved by the institutional medical ethical committee of the University Medical Center Groningen.

Statistics

For analysis of overall and individual group differences, we used Kruskall–Wallis and Mann–Whitney *U* tests. For correlations, we used Spearman. Differences with a *P*-value ≤ 0.05 were considered statistically significant.

Table 1: Patient characteristics and peripheral blood cell counts

Patient no	*Clinical diagnosis*	*Age (yrs)*	*Hb (mmol/l)*	*Leuco ($x10^9$/l)*	*Granulo ($x10^9$/l)*	*Trombo ($x10^9$/l)*
1	MM	62	7.1	5.5	3.3	179
2	MM	52	7.1	5.1	2.1	214
3	MM	42	8.4	7.3	5.5	147
4	MM	52	7.7	3.4	2.4	111
5	MM	48	8.3	7.0	3.5	211
6	MM	62	7.9	8.1	5.8	212
7	MM	61	7.6	7.4	4.5	312
8	MM	62	6.9	6.1	4.2	318
9	MM	52	6.5	9.0	4.5	313
10	MM	63	6.7	4.7	2.3	217
11	MM	52	7.3	5.8	2.9	170
12	NHL	59	8.1	6.7	4.7	199
13	NHL	59	7.7	4.3	2.15	126
14	MH	50	7.2	15	11.4	276
15	NHL	48	8.1	6.4	4.0	80
16	NHL	46	8.7	10.1	7.6	154

MM: Multiple Myeloma; NHL: Non Hodgkin Lymphoma; MH: M. Hodgkin; Hb: haemoglobulin (n: 7.5-9.9 mmol/l); Leuco: leucocytes (n: 4.0-10.0x10^9/l); Granulo: granulocytes (n: 2.1-7.5x10^9/l); Trombo: trombocytes (n: 150-400x10^9/l); *in vitro* colony formation (CFC) assays or ^{18}F-FLT-Pet were performed (+) or not (-).

Results

Patients

This study included patients with relapsing lymphoma (n=5) treated with intensive chemotherapy and auto-SCT using BEAM as conditioning regimen, and MM patients (n=11) treated with chemotherapy and auto-SCT using high dose melphalan (200 mg/m^2) as conditioning regimen. The infused auto-SCT consisted of at least 4 x 10^6 CD34$^+$ cells/kg (range 4.3-12.3 x 10^6) with only three patients receiving <5 x 10^6 CD34$^+$ cells/kg. The studied patients were analyzed at 6-9 months following auto-SCT. The peripheral blood cells counts showed a mean Hb level of 7.6 mmol/ L (range 6.5-8.7), a mean leucocytes count of 6.9 x 10^9/L (3.4-15 x 10^9/L), a mean granulocyte count of 4.4 x 10^9/L (2.1-11.4 x 10^9/L) and a mean platelet count of 202 x 10^9/L (80-318 x 10^9/L). Patient characteristics are depicted in table 1. BM cytology showed no abnormalities. There was no significant difference in age between patients after auto-SCT (median 52 years, range 42–63)) and controls (median 48 years, range 29–68) (P=0.1).

Bone marrow CD34$^+$ progenitor subsets after auto-SCT

The isolated CD34$^+$ BM cells (n=8) were phenotypically characterized for the percentage of CMP, GMP and MEP and compared with the distribution pattern of normal BM CD34$^+$ cells (n=7). No significant difference was observed in the percentage of MEP in BM after auto-SCT vs normal controls (mean percentage 4.3%, 95% confidence interval (CI) 2.1–6.5 vs 2.6%, 95% CI 0.8-4.5, P=0.3). However, a significantly increased percentage of phenotypically defined GMP (mean percentage 51.8%, 95% CI 39.6–64.2 vs 27.6%, 95% CI 19.6–35.5, P=0.01) was observed, whereas a reduction in the phenotypically defined CMP fraction (mean percentage 3.7% 95% CI 0.7–6.9 vs 19.4% 95% CI 11.3–27.6, P=0.001) was shown after auto-SCT. A representative experiment is depicted in Figure 1. Comparable results were observed in a limited number of patients studied with a follow-up time of 43 years as shown for a patient 10 years after auto-SCT (Supplementary Figure). No distinct difference in progenitor subsets was observed between multiple myeloma or lymphoma patients.

To further characterize the CD34$^+$ cell fraction after auto-SCT, progenitor frequency was tested using the in vitro CFC assay. A decrease in CFC frequency per 10^3 plated CD34$^+$ cells was shown compared with normal CD34$^+$ BM cells (109±52 vs 185±56, P=0.008). In these CFC assays no significant difference was found in the colony distribution of

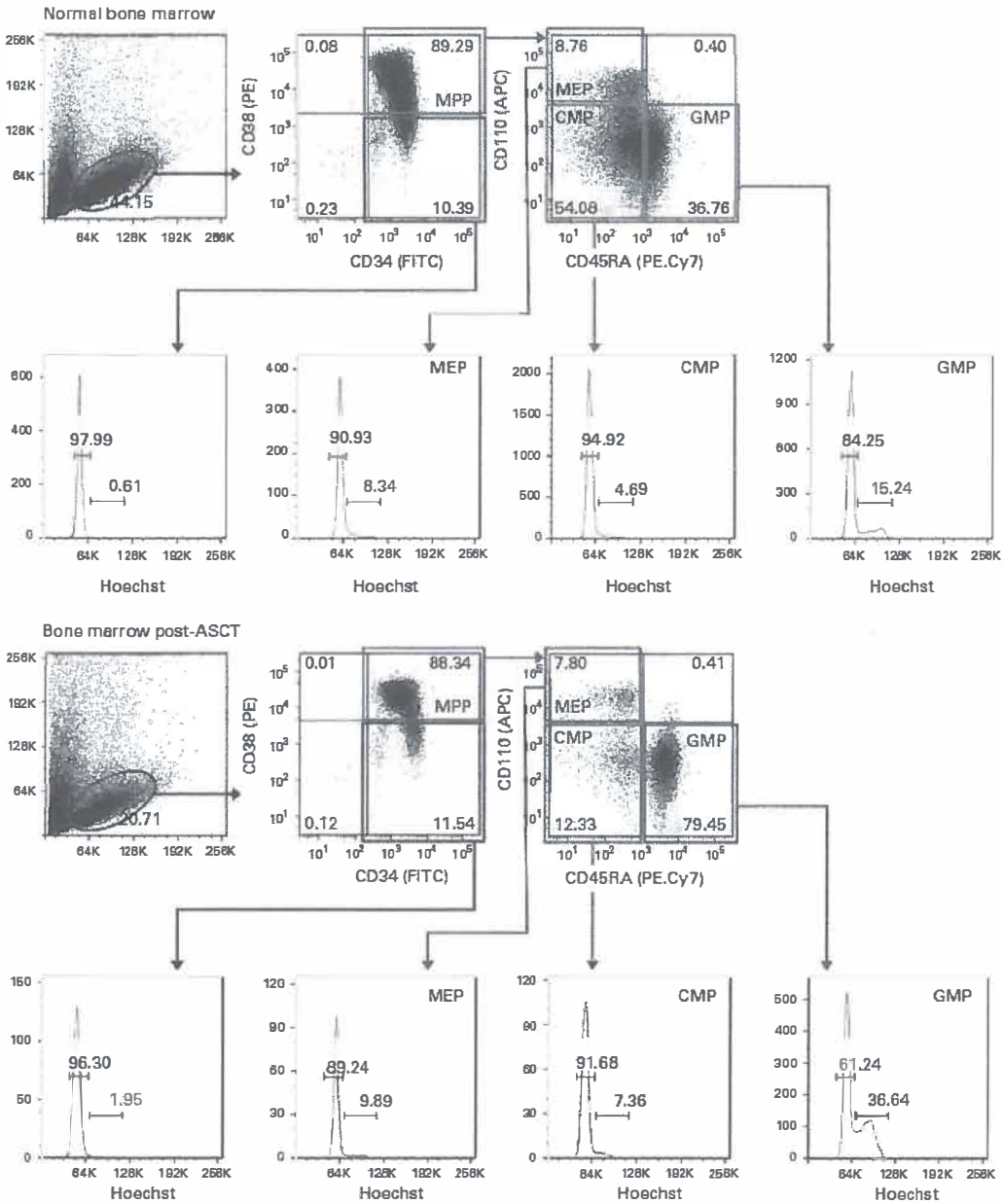

Figure 1: Shift to a GMP-enriched phenotype in the BM compartment after auto-SCT. Representative FACS dot plots showing progenitor subsets of normal BM and BM at 6--9 months after auto-SCT. In BM after auto-SCT, the percentage of phenotypically defined GMP was increased, whereas a reduced percentage was observed in the CMP fraction. With Hoechst staining a higher cycling activity was observed in the CD34þ/ CD38low and GMP subfractions of BM after auto-SCT compared with normal.

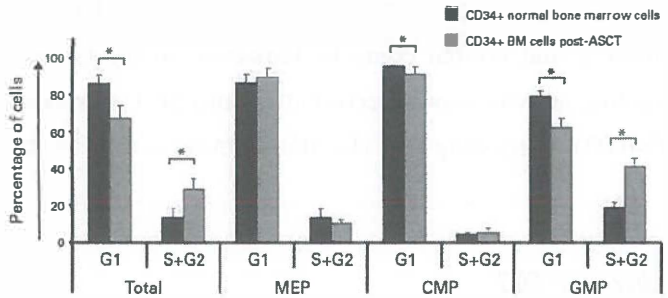

Figure 2: Cell cycle analysis of CD34þ cells of patients after auto-SCT (n¼3) compared with normal CD34þ BM cells (n¼3). Both the total CD34þ cell fractions as well as the progenitor subsets (MEP, CMP and GMP) were analyzed. BM after auto-SCT showed a significantly higher fraction of cells in S/G2 phase compared with normal BM in both the total CD34þ and the GMP fraction. Significant differences are marked by an asterisk.

colony-forming unit granulocyte/monocyte and erythroid burst-forming units in BM after auto-SCT compared with normal BM. In CFC assays from BM after auto-SCT, the percentage of colony-forming unit granulocyte/monocyte colonies was 60.4% (compared with 55.5% for normal BM, P=0.67) and 39.1% for erythroid burst-forming unit colonies (compared with 41.4% for normal BM, P=0.78). The decrease in CFC frequency from CD34$^+$ cells after auto-SCT was not due to an impaired proliferative activity. Cell cycle analysis revealed a significantly higher fraction of CD34$^+$ cells in G2/S phase (mean 29%, 95% CI 19.1–38.4 vs 14%, 95% CI 1.6–25.7, P=0.03) and a reduced percentage of cells in G1 phase (mean 67%, 95% CI 56.4–78.2 vs 86%, 95% CI 73.9–98.4, P=0.03) compared with normal CD34$^+$ cells (Fig. 2). It seemed that especially the GMP fraction of CD34$^+$ cells after auto-SCT showed a higher cycling activity (mean percentage 35%, 95% CI 27.7–43.0 in G2/S phase vs 19%, 95% CI 13.0–25.7, P=0.03), whereas no significant differences were observed for the MEP and CMP fractions. The higher cycling activity of the GMP fraction was also

observed in BM cells of patients with a longer follow-up time. Analysis of the GMP fraction in a patient at 10 years after auto-SCT showed 36.7% of cells in G2/S phase. To verify whether the progenitor fraction within the CD34$^+$ fraction had an enhanced cycle activity and therefore would be more susceptible to chemotherapy-induced apoptosis, CD34$^+$ cells were incubated in vitro with variable concentrations of Ara-C (range $5x10^{-7}$ M to $3x10^{-3}$ M) for 24 h and subsequently cultured in the CFC assay. Normal CD34$^+$ cells showed a 45% reduction in CFC frequency at a concentration of $5x10^{-5}$ M (n=4). Comparable results were observed with CD34$^+$ cells after auto-SCT (n=3) (reduction of

39%; NS). No significant difference was observed in the percentage of $CD34^+/CD38^{low}$ cells between patients after auto-SCT and normal controls. However, in the $CD34^+/CD38^{low}$ fraction also a higher cycling activity was observed after auto-SCT compared with normal controls (Fig. 1) (P=0.03), suggesting that also this fraction is affected by the auto-SCT procedure.

^{18}F-FLT-PET scans in patients after auto-SCT

Recent studies have shown that ^{18}F-FLT-PET scan can be used to visualize the cycling activity of the BM by which the degree of uptake is a reflection of the rate of DNA synthesis[10,11]. The ^{18}F-FLT-PET scans in 10 patients after auto-SCT showed a significant increase in standardized uptake values measured at different points of the BM compartment (fig. 3). The mean values of the left and right area were obtained in comparison to normal controls: Femur 3.6 ± 0.7 versus 1.2 ± 0.5, $P < 0.001$; Crista 3.9 ± 0.6 versus 2.2 ± 0.5, $P < 0.001$; Lumbar 4 vertebral body 4.9 ± 1.3 versus 3.1 ± 0.9, $P < 0.005$; Thoracic 6 vertebral body 5.0 ± 0.6 versus 3.2 ± 0.9, $P < 0.001$; Spine 4.7 ± 2.5 versus 3.9 ± 0.7, $P < 0.005$. Moreover, a significant expansion of the BM compartment was noticed (expansion factor of 6 ± 2.5). representative ^{18}F-FLT-PET scans of a patient after auto-SCT and of s normal individual are shown in Figure 3B.

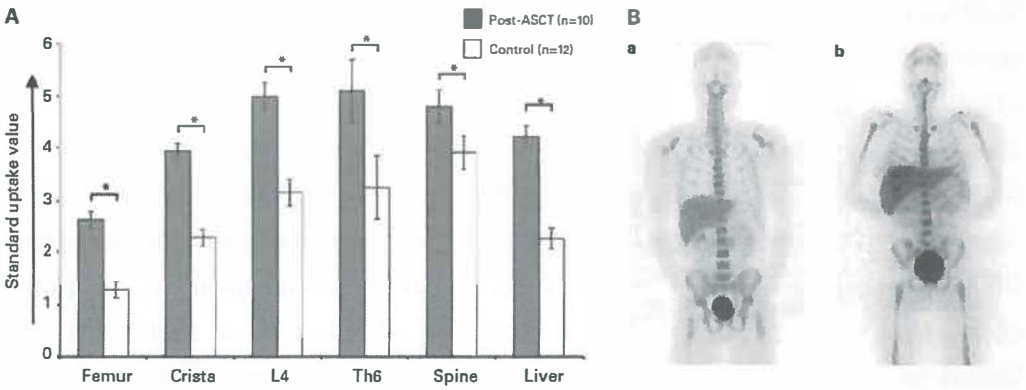

Figure 3: Standard uptake value (SUV) of ^{18}F-FLT-scans of normal individuals and patients after auto-SCT. (A) The mean of the left and right SUV was calculated from femur, crista, lumbar 4 vertebral body (L4), thoracic 6 vertebral body (Th6), spine and liver showing a significant increase ($P < 0.005$) of SUV for each location in patients after auto-SCT compared with normal individuals. Significant differences are marked by an asterisk. (B) ^{18}F-FLT-PET scan of a normal individual (a) and of a patient after auto-SCT (b).

Discussion

This study shows that the auto-SCT procedure results in defects of myeloid progenitors at different levels. BM CD34$^+$ cells after auto-SCT show a phenotypic shift from CMP to GMP progenitors and have a reduced clonogenic potential. Moreover, these cells show an enhanced cycling activity *in vitro* by ^{18}F-FLT-PET scanning.

It is remarkable that even though we observe enhanced proliferation of myeloid cells as determined by ^{18}F-FLT-PET scanning as well as by cell cycle analysis of the GMP fraction, the steady-state peripheral blood cell counts seem to be almost normal at 6–9 months after auto-SCT. Thus, there seems to be an imbalance in the hematopoietic compartment, by which under steady-state conditions the peripheral blood cell counts can be maintained up to normal levels, but at the expense of an increased proliferation rate. Although molecular mechanisms remain to be determined, it is conceivable that cell intrinsic as well as extrinsic factors are contributing to the observed phenotypes after auto-SCT. So far, no enhanced apoptosis was observed in BM cells after auto-SCT as determined by EM studies (E Vellenga, 2009 unpublished data). Several studies have shown an enhanced decline of telomere length after auto-SCT predominantly of the myeloid lineage [5,13]. In aging telomerase knockout mice, enhanced proliferation and cycling activity of myeloid progenitors have been shown in conjunction with a preferential differentiation along the myeloid lineage with a significant increase in the

GMP fraction [14-16]. Therefore, chemotherapy application and the auto-SCT procedure might have fastened the aging process in patients after auto-SCT, resulting in the shift to a GMP phenotype.

The enhanced cycling activity by $CD34^+$ cells is not restricted to auto-SCT. Patients at 6–12 months after allo-SCT also have an enhanced cycling activity of the $CD34^+$ cells, suggesting that the enhanced cycling activity is not only associated with the exposure of DNA-damaging agents [6]. It is therefore conceivable that the hematopoietic compartment undergoes a replicative stress response because of the infusion and engraftment of a limited number of cells. It is of interest whether alternative transplantation strategies might improve this situation by increasing the number of hematopoietic stem cells in the BM cavity by direct infusion of the SCT in the BM. Indeed studies in mice have shown that direct infusion of the stem cell transplant in the BM cavity has advantages compared with infusion i.v. [17,18]. Comparable results have been shown with cord blood transplantation in the setting of allo-SCT [19,20]. Whether this approach will also reduce the replicative stress response in the auto-SCT setting requires further study.

In summary, this study shows that auto-SCT results in defects of the hematopoietic compartment after auto-SCT, characterized by a shift to a GMP-enriched phenotype, reduced clonogenic potential and enhanced *in vitro* and *in vivo* cycling activity.

Acknowledgements

The study was supported by a grant of the Tekke Huizenga Fonds.

REFERENCES

1. *Lokhorst HM, Schmidt-Wolf I, Sonneveld P, et al. Thalidomide in induction treatment increases the very good partial response rate before and after high-dose therapy in previously untreated multiple myeloma. Haematologica. 2008;93:124-127.*

2. *Vellenga E, van Putten WL, van 't Veer MB, et al. Rituximab improves the treatment results of DHAP-VIM-DHAP and ASCT in relapsed/progressive aggressive CD20+ NHL: a prospective randomized HOVON trial. Blood. 2008;111:537-543.*

3. *Noach EJ, Ausema A, van Os R, et al. Chemotherapy prior to autologous bone marrow transplantation impairs long-term engraftment in mice. Exp Hematol. 2003;31:528-534.*

4. *Domenech J, Linassier C, Gihana E, et al. Prolonged impairment of hematopoiesis after high-dose therapy followed by autologous bone marrow transplantation. Blood. 1995;85:3320-3327.*

5. *Widmann T, Kneer H, König J, Herrmann M, Pfreundschuh M. Sustained telomere erosion due to increased stem cell turnover during triple autologous hematopoietic stem cell transplantation. Exp Hematol. 2008;36:104-110.*

6. *Thornley I, Sutherland DR, Nayar R, Sung L, Freedman MH, Messner HA. Replicative stress after allogeneic bone marrow transplantation: changes in cycling of CD34+CD90+ and CD34+CD90- hematopoietic progenitors. Blood. 2001;97:1876-1878.*

7. *Manz MG, Miyamoto T, Akashi K, Weissman IL, Prospective isolation of human clonogenic commen myeloid progenitors. Proc Natl Ascd Sci USA 2002; 99:11872-11877.*

8. *Edvardsson L, Dykes J, Olofsson T. Isolation and characterization of human myeloid progenitor populations – TpoR as discriminator between common myeloid and megakaryocyte/erythroid progenitors. Exp Hematol. 2006;34:599-609.*

9. *Olthof SG, Fatrai S, Drayer AL, Tyl MR, Vellenga E, Schuringa JJ. Downregulation of STAT5 in CD34+ Cells Promotes Megakaryocytic Development while Activation of STAT5 Drives Erythropoiesis. Stem Cells. 2008;26:1732-1742.*

10. *Shields AF, Grierson JR, Dohmen BM, et al. Imaging proliferation in vivo with [F-18]FLT and positron emission tomography. Nat Med. 1998;4:1334-1336.*

11. *Agool A, Schot BW, Jager PL, Vellenga E. ^{18}F-FLT PET in hematologic disorders: a novel technique to analyze the bone marrow compartment. J Nucl Med. 2006;47:1592-1598.*

12. *Schepers H, van Gosliga D, Wierenga AT, Eggen BJ, Schuringa JJ, Vellenga E. STAT5 is required for long-term maintenance of normal and leukemic human stem/progenitor cells. Blood. 2007;110:2880-2888.*

13. *Bhatia R, Van Heijzen K, Palmer A, Komiya A, Slovak ML, Chang KL. Longitudinal assessment of hematopoietic abnormalities after autologous hematopoietic cell transplantation for lymphoma. J Clin Oncol 2005; 23:6699-6711.*

14. *Rossi DJ, Bryder D, Zahn JM, Ahlenius H, Sonu R, Wagers AJ, et al. Cell intrinsic alterations underlie hematopoietic stem cell aging. Proc Natl Acad Sci U S A. 2005;102:9194-9199.*

15. *Rossi DJ, Bryder D, Seita J, Nussenzweig A, Hoeijmakers J, Weissman IL. Deficiencies in DNA damage repair limit the function of haematopoietic stem cells with age. Nature. 2007;447: 725-9.*

16. *Ju Z, Jiang H, Jaworski M, Rathinam C, Gompf A, Klein C, et al. Telomere dysfunction induces environmental alterations limiting hematopoietic stem cell function and engraftment. Nat Med. 2007;13:742-747.*

17. *Kimura T, Asada R, Wang J, Kimura T, Morioka M, Matsui K, et a. Identification of long-term repopulating potential of human cord blood-derived CD34-flt3- severe combined immunodeficiency-repopulating cells by intra-bone marrow injection. Stem Cells. 2007;25:1348-1355.*

18. *Li Q, Hisha H, Yasumizu R, Fan TX, Yang GX, Li Q, et al. Analyses of very early hemopoietic regeneration after bone marrow transplantation: comparison of intravenous and intrabone marrow routes. Stem Cells. 2007;25:1186-1194.*

19. *Frassoni F, Gualandi F, Podestà M, Raiola AM, Ibatici A, Piaggio G, et al. Direct intrabone transplant of unrelated cord-blood cells in acute leukaemia: a phase I/II study. Lancet Oncol. 2008;9(9):831-9.*

20. *Castello S, Podestà M, Menditto VG, Ibatici A, Pitto A, Figari O, et al. Intra-bone marrow injection of bone marrow and cord blood cells: an alternative way of transplantation associated with a higher seeding efficiency. Exp Hematol. 2004;32:782-787.*

Chapter 5

^{18}F-FLT-PET: a non-invasive diagnostic tool for visualization the bone marrow compartment in patients with aplastic anemia

Ali Agool[1], Riemer H.J.A. Slart[1], Philip M. Kluin[3], Rudi A.J.O. Dierckx[1], Joost T.M. de Wolf[2], Edo Vellenga[2]

University Medical Center Groningen, University of Groningen, [1]Department of Nuclear Medicine and Molecular Imaging, [2]Department of Hematology, [3]Department of Pathology, The Netherlands

Clinical Nuclear Medicine (In press)

Abstract

Rationale A discordant relationship between bone marrow cellularity and peripheral blood findings are regular noticed in patients with aplastic anemia (AA). Therefore the feasibility of 3-^{18}F-fluoro-3-deoxy-L-thymidine (^{18}F-FLT) ^{18}F-FLT-PET was tested as a non-invasive tool to visualize the total distribution of the hematopoietic bone marrow compartment in AA at presentation or following treatment. *Methods* In-vivo scanning was performed with ^{18}F-FLT-PET in AA patients (n=17) including patients upfront (n=11) and following treatment (n=6) in addition to peripheral blood cell counts and a bone marrow biopsy. ***Results*** A striking abnormal ^{18}F-FLT scan was observed in all patients upfront treatment in particular a reduced uptake of the pelvis was shown, the area that is biopsied for the bone marrow biopsy. Following treatment a number of solitary lesions with increased proliferative activity outside the pelvis was noticed in patients with partial response while patients with a complete remission showed a homogenous uptake throughout the skeleton. ***Conclusion*** This pilot study demonstrates that ^{18}F-FLT scan provides a highly distinctive overview of the bone marrow compartment in AA that might be helpful for making a proper diagnosis and treatment response of AA patients.

Keywords: ^{18}F-FLT, aplastic anemia, bone marrow distribution

Introduction

Aplastic anemia (AA) is a rare hematological disorder characterized by peripheral pancytopenia in association with a decreased bone marrow cellularity [1]. A number of causative agents have been identified that might be responsible for the bone marrow failure but in the majority of cases no definitive cause can be identified [1]. A bone marrow specimen is a prerequisite for a proper diagnosis of AA. Histological evaluation demonstrates hypocellularity or aplasia with an increased number of fat cells. Moreover, some patients manifest with patchy areas of often aberrant hematopoiesis in the bone marrow specimen called "hot spots" which might be responsible for a discordant relationship between bone marrow cellularity and peripheral blood findings [2,3]. Therefore, a more global investigation of the bone marrow compartment as a whole could be of value for making a proper diagnosis of AA.

PET using ^{18}F-labeled DNA precursors has a potential for specific imaging of proliferation in vivo. In the past 3'-deoxy-3'-^{18}F-fluorothymidine (^{18}F-FLT) was introduced as a thymidine analog that is resistant to in vivo degradation and accumulates predominantly in proliferating tissues [4]. Results with ^{18}F-FLT in several types of cancer patients have demonstrated a high background activity by the bone marrow compartment reflecting the high proliferative activity of hematopoietic cells [5-7]. This is in line with the enhanced bone marrow ^{18}F-FLT uptake in patients with myelodysplasia and myelofibrosis and patients following autologous stem cell transplantation [8,9]. Based on these findings we studied the bone marrow compartment in patients with AA and compared the results with clinical parameters.

Materials and methods

^{18}F-FLT-PET

^{18}F-FLT was synthesized by the method of Grierson et al [10]. ^{18}F-FLT was produced by fluorination with ^{18}F-fluoride of the 4,4'-dimethoxytrityl–protected anhydrothymidine and then a deprotection step. After purification by reversed-phase high-performance liquid chromatography, the product was made isotonic and passed through a 0.22-μm filter. ^{18}F-FLT was produced with a radiochemical purity of greater than 95% and a specific activity of greater than 10 TBq/mmol. The radiochemical yield was 8.8%± 3.7% (decay corrected).

Patients were instructed to fast at least six hours before investigation, with exception of free access to water and usual medication. ^{18}F-FLT in a dose of 400 MBq (±10%) was administered intravenously. Approximately 60 minutes after the FLT injection, the patient was placed in the camera and emission scans of 5 minutes per bed position and transmission scans of 3 minutes per bed position were acquired over ~12 bed positions in order to cover the whole body. A Siemens ECAT EXACT HR+ (Siemens Medical Systems, Knoxville, TN) was used for all PET studies. Images were acquired in the 3-D acquisition mode. Three-minute transmission scans with a ^{68}Ge/^{68}Ga ring source were obtained for attenuation correction after tracer application. Images were reconstructed using an iterative reconstruction algorithm. Emission data were corrected for randoms, scatter, and attenuation.

Controls

Patients (n=10) with untreated non-small cell lung cancer (NSCLC) or testicular cancer, who had undergone ^{18}F-FLT-PET for other studies, were considered as controls [6-8]. Before inclusion, they were required to have normal blood hematology values, lack of signs of bone marrow metastases at presentation or during 6 month follow up. In addition the patients had to be free of chemotherapeutic or radiotherapeutic treatment.

Data analysis

Two independent nuclear physicians prospectively evaluated the PET scans. Visual and quantitative analysis of ^{18}F-FLT-PET images was performed. In visual analysis the overall scan pattern was recorded, the intensity of bone marrow uptake was evaluated as well as the degree of bone marrow expansion. We used the same expansion scoring

system which is developed to assess different bone marrow disorders in short: one point is given for expansion in every one third of the long bones, based on the well known distribution of ^{18}F-FLT in the central skeleton and ultra-proximal part of femora and humera [8]. Also the spleen size and uptake intensity was qualitatively evaluated.

We also counted the lesions in the axial skeleton and quantified ^{18}F-FLT uptake using maximal standard uptake value (SUVmax) analysis. Also SUV of the spleen was determined. The region of interests using in SUV analysis were three-dimensional and based on the mean value within the 50% isocontours boundaries using a Siemens Leonardo workstation. Data was expressed as mean ± standard deviation (SD). For analysis of group differences, the Mann-Whitney U test was used. $P < 0.05$ was considered significant.

Table 1: Clinical characteristics of the studied aplastic anaemia patients

Patient no.	*Hb (mmol/l)*	*Leuco's ($x10^9$/l)*	*Granuloc ($x10^9$/l)*	*Platelets ($x10^9$/l)*	*Bone marrow histology*	*Clinical diagnosis*
1	Transf.	1.1	0.6	8	Aplasia	AA
2	6.7	4.6	2	7	Aplasia	Relapse AA
3	5.5	2.0	1.0	13	Severe hypocellular	AA
4	4.9	3.7	1.8	11	Aplasia	AA
5	6.0	3.2	0.9	32	Hypocellular	Relapse AA
6	Transf.	4.2	0.8	9	Aplasia	AA
7	Transf.	2.4	0.45	4	Aplasia	AA
8	Transf.	4.5	1.5	40	Aplasia	AA
9	6.1	5.8	2.7	34	Hypocellular	AA
10	Transf.	5.6	2.4	20	Aplasia	AA
11	Transf.	2.4	0.2	2	Aplasia	Relapse AA
12	8.3	4.1	1.5	185	n.d.	AA; PR following ATG/CSP
13	7.9	5.2	2.6	258	Hypo-normocellular	AA; PR following ATG/CSP
14	5.4	5.2	1.8	40	Hypo-normocellular	AA; PR following ATG/CSP
15	9.0	6.6	4.2	161	n.d.	AA; CR following ATG/CSP
16	8.0	4.5	2.8	167	Normocellular	AA; CR following allogeneic SCT
17	8.0	6.4	3.9	201	Normocellular	AA; CR following allogeneic SCT
Normal	8.0-10.5	4.0-10.0	2.0-7.5	150-350		

Aplastic anemia (AA) patients; transf.: transfusion dependent; ATG: anti-thymocyte globulin; CSP: cyclosporine; CR: complete remission; PR: partial remission; Granuloc: granulocytes; SCT: stem cell transplantation

Table 2: Characteristics of ^{18}F-FLT scan in patients with aplastic anemia

Patient no	*Expansion factor*	*Total no of lesions*	*Spine*		*Cristae*		*Sternum*		*Spleen*
			*No lesions**	*SUV***	*No lesions**	*SUV***	*No lesions**	*SUV***	
1	0	5	2	4.6	0	**1.8**	1	3.6	1.4
2	3	10	4	4.6	0	**2.9**	1	4.9	1.4
3	0	2	1	4.3	0	**2.0**	0	**2.7**	1.0
4	2	7	4	5.4	0	**2.2**	1	3.3	1.9
5	1	12	7	6.0	1	3.7	1	5.3	1.9
6	1	15	5	3.7	1	3	1	2.5	5.3
7	0	14	6	2	3	1.8	0	0.9	3
8	0	0	0	3.7	0	3.5	0	3	1.7
9	8	17	4	6.5	4	4.3	3	3.2	1.6
10	2	9	4	4.8	2	3.8	1	6.2	3
11	0	4	0	2.1	0	2.1	1	2.7	1.9
12	6	34	9	6.6	1	8.0	3	5.0	2.2
13	2	18	2	4.8	1	7.7	2	5.3	1.6
14	12	10	9	5.1	0	3.6	2	5.2	1.4
15	0	0	0	5.1	0	3.5	0	4.1	1.4
16	2	0	0	4	0	2.9	0	2.8	1.8
17	8	0	0	4.1	0	3.3	0	3.2	1.4
Normal	0	0	0	3.7±0.65	0	3.1±0.34	0	2.3±0.1	1.7±0.8

*No lesions: number of lesions identified on the ^{18}F-FLT scan; ** SUV: standard uptake values of the identified hot spot(s) at specific areas. **Bold text**: reflects the residual hematopoietic activity in the cristae or sternum. Patient number corresponds with patient number from table 1.

Results

Patients

17 patients were included, 11 male and 6 female with a median age of 54 year (range of 20 - 84 year). The diagnosis of aplastic anemia was based on peripheral blood cell counts and bone marrow biopsy. The patients were studied at presentation (n=8) or relapse (n=3) and 6 patients were studied after having achieved a partial or complete normalization of peripheral blood cells following therapy with prednisolone, anti-thymocyte globulin (ATG) and cyclosporine or after an allogeneic stem cell transplantation (table 1). None of the patients were treated with colony stimulating factors. In 15 patients a bone marrow biopsy was performed at the same time that the ^{18}F-FLT scan was performed. In patients (no. 1-11) with moderate to severe AA at presentation or relapse, the findings of the the bone marrow biopsy corresponded with the peripheral blood cell counts: severe peripheral pancytopenia in association with aplasia or (severe) hypocellularity of the bone marrow biopsy. In patients (no. 12-17) with a partial or complete normalization of peripheral blood cell counts following treatment, the bone marrow specimen demonstrated hypocellularity to normocellularity in 4 of the 6 patients studied.

^{18}F-FLT-PET

In patients with presenting AA a significant abnormal ^{18}F-FLT scan was observed. Of the studied patients no 7 and 16 are the same patient before and following therapy. In all untreated patients a significant reduced uptake of the pelvic area was shown unless a hotspot was present, while the vertebral column showed patchy areas that varied between 2-15 spots, and corresponded with the histological findings in the bone marrow biopsy which is taken from this area (table 2, fig. 1B). The patchy areas showed increased uptake (SUVmax 4.3 ± 1.4) compared to normal controls (3.7 ± 0.65, $P = 0.021$, fig. 1A and 1B). Six patients (no.12-17) were studied following immune suppressive therapy or allogeneic stem cell transplantation. Three patients (no.12-14) had a partial response (PR) based on the findings of the peripheral blood cell counts and bone marrow histology (Fig. 2). The ^{18}F-FLT scan in these patients demonstrated hot spots and increased uptake that included the peripheral skeleton. The amount of spots varied between 10-34. The pelvic area showed normal to high ^{18}F-FLT uptake (SUVmax 3.6-8) compared to the untreated patients (SUVmax 2.8 ± 0.9, $P = 0.05$). The patients in CR showed a

homogenous [18]F-FLT uptake throughout the skeleton without hot-spots but with a certain degree of expansion. In almost all the patients a normal uptake of the spleen was shown.

Figure 1: (A) Normal [18]F-FLT distribution in the bone marrow compartment. Central skeletal uptake and limited to the bones of the proximal extremities.
(B) [18]F-FLT in untreated aplastic anemia patient (no 8, table 1) showing several solitary lesions of increased proliferative activity in the central skeleton with extension of the lesions to the proximal extremities. Relative low [18]F-FLT uptake in the pelvis.

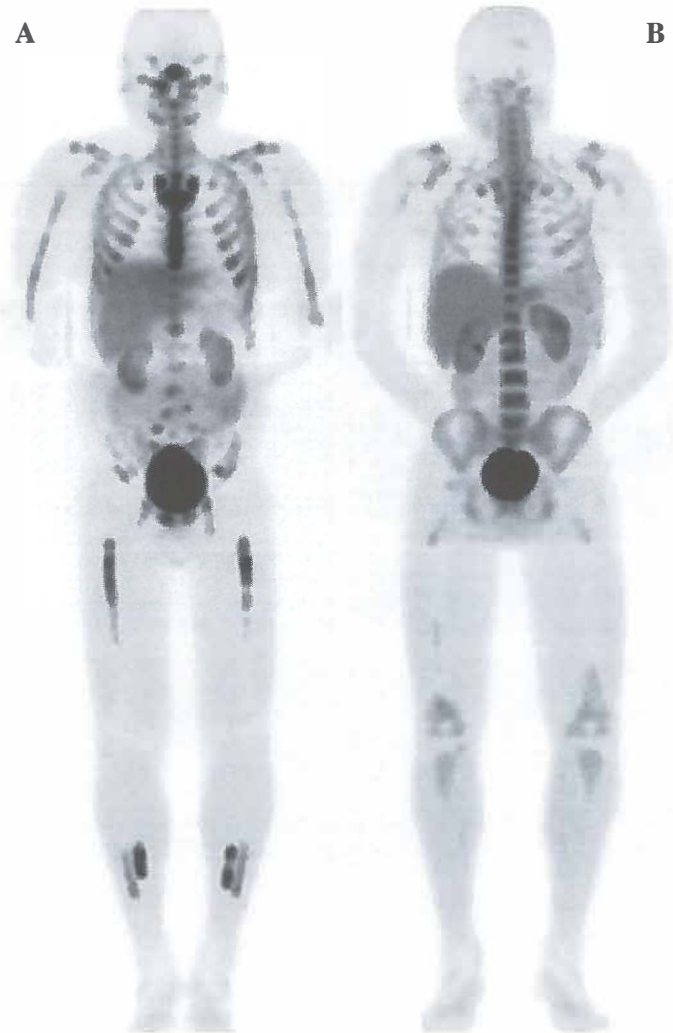

Figure 2: A: ^{18}F-FLT scan in a patient (no 14) in partial remission following treatment with ATG and cyclosporine. The scan was performed 7 months following this treatment; B: ^{18}F-FLT scan in a patient (no 16) in complete remission following treatment with an allogeneic stem cell transplantation by using a reduced intensity conditioning. The scan was performed 4 months following this treatment.

Discussion

The results of this pilot study demonstrate that ^{18}F-FLT can be a helpful tool to visualize the bone marrow compartment and identifies solitary areas of increased proliferative activity that can frequently be recognized in patients with AA. In most patients with active disease no activity of ^{18}F-FLT was shown in the pelvis which corresponds with the histological findings in the bone marrow biopsy which is taken from this area. Furthermore it appeared that within the bone marrow compartment certain areas with increased or reduced activity can be recognized in connection with an extension to the long tubular bones of more peripheral areas. These solitary areas of increased proliferative activity probably augment following treatment in patients with PR and might be responsible for the improvements in peripheral blood cell counts. Apparently the impairment of the bone marrow compartment is not a general event but is restricted to certain areas with an increased vulnerability for the noxious agents. This is illustrated in a number of patients where solitary lesions of increased ^{18}F-FLT uptake were found in the skull, lower legs and upper arms. In contrast patients in CR following therapy demonstrated a homogenous uptake throughout the skeleton. It is likely that the defined "hot spots" in the bone marrow biopsy of AA patients are linked to the areas of increased ^{18}F-FLT uptake. However, the ^{18}F-FLT scan recognizes only the proliferative activity and is not informative regarding the cell lineages involved.

The scans obtained in these patients are highly distinctive from that of patients with myelodysplasia or myelofibrosis or normal controls [7-9]. In myelodysplasia a homogenous elevated ^{18}F-FLT uptake of the bone marrow compartment was demonstrated while in myelofibrosis a highly increased uptake of the spleen was seen as result of extramedullary hematopoiesis [8]. Therefore, ^{18}F-FLT-PET may be helpful in differentiating between these hematological disorders.

The mechanisms governing the uptake of ^{18}F-FLT in bone marrow are not fully clarified. In many tumor types, good correlations between proliferative activity and ^{18}F-FLT uptake have been demonstrated [9]. ^{18}F-FLT acts as a chain terminator and is only marginally incorporated into DNA and therefore not a direct measure of proliferation [12]. In vitro studies indicate that ^{18}F-FLT uptake is closely related to thymidine kinase 1 activity, as well as to expression of nucleoside transporters in the cellular membrane and reflects S-phase fraction rather than DNA synthesis [13,14].

Studies comparable to the present study have been performed in the past, using a multitude of tracers, such as iron isotopes for imaging, and turnover studies of the erythropoietic precursor, ^{99m}Tc-labeled antigranulocyte antibodies for imaging of myeloid cells [15], radiocolloids for RES cell activity, and ^{111}In-choride [15-17]. Compared with those methods, ^{18}F-FLT-PET has a considerably higher resolution, produces tomographic information, and allows better quantification. Moreover, it might provide more specific information about the hematopoietic bone marrow compartment than a reflection of the functional activity of the RES. To our knowledge this is the first ^{18}F-FLT-PET study concerning the evaluation of bone marrow proliferation.

In conclusion, this study demonstrates that the ^{18}F-FLT scan is a novel non-invasive tool to visualize the hematopoeitic bone marrow compartment and provides a highly distinctive picture that might be helpful to distinguish AA patients from other hematological bone marrow disorders. In addition it might be helpful to monitor the treatment response in future clinical studies.

REFERENCES

1. *Young NS, Calado RT, Sc-heinberg P. Current concepts in the pathophysiology and treatment of aplastic anemia. Blood. 2006;108:2509-2519.*
2. *Fong TP, Okafor LA, Schmitz TH, Thomas W, Westerman MP. An evaluation of cellularity in various types of bone marrow specimens. Am J of Clin Path. 1979;72:812-816.*
3. *Kansu E, Erslev AJ. Aplastic anaemia with 'hot pockets'. Scand J Haematol. 1976;17:326-334.*
4. *Shields AF, Grierson JR, Dohmen BM, Machulla HJ, Stayanoff JC, Lawhorn-Crews JM, et al. Imaging proliferation in vivo with [F-18]FLT and positron emission tomography. Nat Med. 1998;4:1334-1336.*
5. *Been LB, Elsinga PH, de Vries J, Cobben DC, Jager PL, Hoekstra HJ et al. Positron emission tomography in patients with breast cancer using 18F-39-deoxyf-39-fluoro-l-thymidine (18F-FLT): a pilot study. Eur J Surg Oncol. 2006;32:39-43.*
6. *van Westreenen HL, Cobben DC, Jager PL, van Dullemen HM, Wesseling J, Elsinga PH et al. Comparison of 18F-FLT PET and 18F-FDG-PET in esophageal cancer. J Nucl Med. 2005;46:400-404.*
7. *Cobben DC, van der Laan BF, Maas B, Vaalburg W, Suurmeijer AJ, Hoekstra HJ et al. 18F-FLT PET for visualization of laryngeal cancer: comparison with 18F-FDG PET. J Nucl Med. 2004;45:226-231.*
8. *Agool A, Schot BW, Jager PL, Vellenga E. [18]F-FLT PET in hematologic disorders: a novel technique to analyze the bone marrow compartment. J of Nucl Med. 2006;47:1592-1598.*
9. *Woolthuis C, Agool A, Olthof S, Slart RHJA, Huls G, W. Smid WM, Schuringa JJ, Vellenga E. Autologous stem cell transplantation induces a phenotypical shift from CMP to GMP progenitors, reduces clonogenic potential and enhances in vitro and in vivo cycling activity defined by [18]F-FLT PET scanning. Bone Marrow Transpl. In press.*

10. *Grierson JR, Shields AF. Radiosynthesis of 39-deoxy-39-[18F]fluorothymidine: [18F]FLT for imaging of cellular profileration in vivo. Nucl Med Biol. 2000; 27:143–156.*

11. *Been LB, Suurmeijer AJ, Cobben DC, Jager PL, Hoekstra HJ, Elsinga PH. ^{18}F-FLT-PET in oncology: current status and opportunities. Eur J Nucl Med Mol Imaging. 2004;31:1659–1672.*

12. *Rasey JS, Grierson JR, Wiens LW, Kolb PD, Schwartz JL. Validation of FLT uptake as a measure of thymidine kinase-1 activity in A549 carcinoma cells. J Nucl Med. 2002;43:1210–1217.*

13. *Barthel H, Perumal M, Latigo J, He Q, Brady F, Luthra SK et al. The uptake of 3'-deoxy-3'-[18F]fluorothymidine into L5178Y tumours in vivo is dependent on thymidine kinase 1 protein levels. Eur J Nucl Med Mol Imaging. 2005;32:257–263.*

14. *Perumal M, Pillai RG, Barthel H, Leyton J, Latigo JR, Forster M et al. Redistribution of nucleoside transporters to the cell membrane provides a novel approach for imaging thymidylate synthase inhibition by positron emission tomography. Cancer Res. 2006;66:8558–8564.*

15. *Jamar F, Field C, Leners N, Ferrant. A.Scintigraphic evaluation of the haemopoietic bone marrow using a 99mTc-anti-granulocyte antibody: a validation study with 52Fe. Br J Haematol. 1995;90:22-30.*

16. *Chung JK, Yeo J, Lee DS, Park S, Lee MC, Kim BK et al. Bone marrow scintigraphy using technetium-99m-antigranulocyte antibody in hematologic disorders.J Nucl Med. 1996;37:978-982.*

17. *Horn NL, Bennett LR, Marciano D. Evaluation of aplastic anemia with indium chloride In 111 scanning. Arch Intern Med. 1980;40:1299–1303.*

Chapter 6

Effect of radiotherapy and chemotherapy on bone marrow activity: a ^{18}F-FLT-PET study

Ali Agool[1], Riemer H.J.A. Slart [1],Kristin K. Thorp[2], Andor W.J.M. Glaudemans[1], David C.P. Cobben[3], Lukas B. Been[4], Fred R. Burlage[5],Rudi A.J.O. Dierckx[1], Edo Vellenga[6], Jennifer L. Holter[2]

[1] Department of Nuclear Medicine and Molecular Imaging, Department of [5]Radiotherapy, [6]Department of Hematology, [4]Department of Surgery, University of Groningen and University Medical Center Groningen, Groningen, The Netherlands; [3]Department of Radiotherapy, University Medical Center Maastricht, The Netherlands, [2]Section of Hematology/Oncology, Department of Internal Medicine, University of Oklahoma Health Sciences Center, U.S.A.

Nuclear Medicine Communications. 2011; 32:17-22

Abstract

Radiotherapy and chemotherapy are important treatment modalities for a variety of malignant tumor types. During therapy for malignant diseases, often the limitation for further therapy is determined by the capability of the bone marrow to withstand radiochemotherapeutic effects. Evaluation of hematologic toxicity is commonly done with peripheral blood counts, and occasionally, sampling of marrow via a bone marrow biopsy. Neither method provides a comprehensive assessment, bone marrow biopsy is invasive, and both are subject to sampling variability. 3'-fluoro-3'-deoxy-L-thymidine (^{18}F-PET) is a non-invasive method and related to the rate of DNA synthesis and visualizes the high cycling activity of hematopoietic cells in the bone marrow compartment. In order to prove clinical consistency of marrow function and imaging, we investigated populations of patients typically seen in clinical practice, post radiation and post chemotherapy. In this feasibility study populations were evaluated on 1) to prove the ability of visualization and quantification of the activity of the bone marrow compartment with ^{18}F-FLT-PET and 2) to evaluate the effect of radiotherapy and chemotherapy on bone marrow activity and the correlation with clinical findings. ***Methods*** Bone marrow activity in the cervical region of 10 patients with laryngeal carcinoma that received a mean total dose of 68 Gy (range 30-41 fractions) was evaluated with ^{18}F-FLT-PET before and 6 months after radiotherapy. Whole Body ^{18}F-FLT-PET were assessed in 9 patients with non-seminomatous testicular germ cell tumors before and 4 months after the last chemotherapy consisting of 4 courses of bleomycin, cisplatin, and etoposide. Maximal standardized uptake value (SUVmax) was used to quantify FLT uptake in bone marrow at standard bone marrow regions. ***Results*** A significant decrease in ^{18}F-FLT-PET uptake was observed in all of the studied laryngeal carcinoma patients in the cervical region after RT of the adjacent bone marrow compartment. Tumor stage and additional field of view of RT was inversely related to the FLT uptake in bone marrow. The mean ^{18}F-FLT SUVmax before RT was 3.0 ± 1.34 and after RT 1.94 ± 0.60 (P= 0.013). The mean ^{18}F-FLT SUVmax of the spine (Th5-Th12) regions outside the field of view of RT were stable and reproducible and not significantly different (5.56 ± 1.56 versus 5.16 ± 1.35, P = 0.16). Chemotherapy did not result in a significant difference of whole body SUVmax value, with a mean SUVmax of 4.99 ± 1.15 pre-chemo, and a mean SUVmax of 5.28 ± 1.0 post-chemo (P = 0.21). Laboratory analysis of hematologic parameters confirmed repopulation of bone marrow. ***Conclusion*** Radiotherapy decreases ^{18}F-FLT

uptake in bone marrow, but not following chemotherapy. We conclude that ^{18}F-FLT-PET is a potential non-invasive tool that can be used in the assessment of quantification of cellular division in the hematopoetic organ.

Introduction

Hematologic toxicity is often the limiting factor in the use of cytotoxic chemotherapy. The introduction of multi-agent chemotherapy has improved management of a variety of solid and hematologic malignancies. However, chemotherapy may result in depressed bone marrow activity resulting in impaired progenitor blood cell proliferation. Depressed bone marrow reserve hampers the use of further cytotoxic chemotherapy. Although limited radiation rarely causes significant impact on marrow capacity, when directed regionally toward highly active marrow sites systemic marrow activity can be affected. Currently, marrow activity is evaluated systemically utilizing peripheral blood counts, and occasionally bone marrow biopsies. Although useful as indirect methods of systemic marrow capacity, both are limited by high of rates sampling errors and accuracy is dependent on limited systemic inflammatory changes. Although MRI and ^{18}F-FDG-PET can provide information about marrow content, they are non-specific and often confounded by inflammatory changes in the marrow. For this reason, a tool that could objectively assess the bone marrow compartment that is both clinically consistent and reproducible would be useful. The PET tracer 3'-fluoro-3'-deoxy-L-thymidine (^{18}F-FLT-PET), by its incorporation into DNA during S phase, shows increased uptake in highly proliferative tissues. It is currently being evaluated for tumor staging in a multitude of malignancies (Table 1).

^{18}F-FLT-PET has been used in several studies to visualize the cellular proliferative rate of the bone marrow compartment [1-3]. In several bone marrow disorders a relation between ^{18}F-FLT-PET uptake and the proliferation rate has been found, suggesting that the same mechanism could be responsible for the bone marrow uptake [29]. The specificity with ^{18}F-FLT-PET uptake for cycling cells, the ability to assess the entire hematopoietic compartment, the high resolution of PET, and the quantification possibilities may support the relevance of ^{18}F-FLT-PET as a diagnostic procedure. In this investigation, we have evaluated two populations where we can objectively evaluate the use of common toxic insults on marrow capacity, namely radiation and chemotherapy. Therefore, we studied in

this feasibility study the effect of regional radiotherapy (RT) and systemic chemotherapy on bone marrow activity in patients with laryngeal carcinoma and non-seminomatous testicular germ cell tumors, respectively, with ^{18}F-FLT-PET.

Table 1. Evaluation of malignancy with ^{18}FLT -PET Imaging

References	*Tumor type*	*N*	*Comment*
[1-5]	Malignant Glioma	115	Useful for imaging high grade lesions and predicting treatment response
[6-8]	Colorectal	37	Low sensitivity, especially for liver metastasis. Not useful for assessing response to treatment.
[9-11]	Non-Hodgkin's Lymphoma	63	Useful for both staging and assessing treatment response.
[12-14]	Breast	41	Useful for staging, with some limitations in sensitivity. Useful for predicting response to treatment.
[15,16]	Head/neck	31	Sensitivity high, but poor specificity. Not useful.
[17,18]	Sarcoma	29	Useful for imaging both primary tumors and metastatic disease. SUV correlates well with mitotic index. Predicts response to therapy.
[11, 19-24]	Lung	92	Low sensitivity but high specificity, perhaps useful as an adjunct to FDG-PET.
[25]	Esophageal	10	Low sensitivity and high specificity, limited usefulness.
[26]	Melanoma	10	Reasonably useful in tumor staging.
[27,28]	Acute Leukemia	16	May be useful in predicting response to therapy

Materials and methods

Patients

Patients with laryngeal carcinoma and non-seminomatous testicular germ cell tumors that visited the hospital between 2002 and 2005 were retrospectively included for this study. Patients with severe renal dysfunction, peripheral neuropathy, severe elevation of liver enzymes and metastasized disease were excluded. All patients provided written informed consent, and the study was approved by the local Medical Ethics Committee of the Groningen University Medical Center.

^{18}F-FLT-PET

^{18}F-FLT-PET was produced according to the method described by Grierson et al. with a radiochemical purity of >95% and a specific activity of >10 TBq/mmol [31]. Patients were instructed to fast for at least 6 h before investigation, with the exception of free access to water and normal medication. ^{18}F-FLT-PET in a dose of 400 MBq (±10%) was administered intravenously. Approximately 60 min after the ^{18}F-FLT injection, the patient was placed in the camera, and emission scans of 5 min per bed position and transmission scans of 3 min per bed position were acquired over 12 bed positions to cover the whole body. An ECAT EXACT HR+scanner (Siemens Medical Systems) was used for all PET studies. Images were acquired in the 3-dimensional acquisition mode. All ^{18}F-FLT-PET scans were fused with the planning CT scans of the RT on Leonardo Siemens workstation (Siemens Medical Systems) for delineation of the vertebrae.

Radiotherapy

10 patients (all men, mean age 68.1 ± 9.4 yr) with laryngeal carcinoma underwent a ^{18}F-FLT-PET for tumor activity assessment before and one month after finishing RT at a dose of 70 Gy (range 30-41 fractions). None of the patients had bone marrow involvement and none had undergone chemotherapy or radiotherapy in the past and all had normal peripheral blood cell counts prior to the therapy. The tumor classification of the laryngeal carcinoma ranged from T1 to T4 (table 1).

Chemotherapy

9 patients (mean age 27.4 ± 5.3 yr) with metastatic non-seminomatous testicular germ cell tumor were treated with 4 courses of chemotherapy (with bleomycin, cisplatin, and etoposide). These patients underwent a ^{18}F-FLT-PET for tumor activity assessment one week before and 6 months after finishing chemotherapy. None of the patients had bone marrow involvement and none had undergone chemotherapy or radiotherapy in the past. All had normal peripheral blood cell counts prior to the therapy and after therapy.

Table 2: Stage, radiation dose and site of radiation in patients with pre-and post irradiation FLT measurements.

Patient	*TNM classification*	*RT dose (Gy)*	*Number of fractions*	*RT cervical spine level*	*SUVmax pre RT*	*SUVmax post RT*
1	T2NOMO	70	35	CI-C7	2.91	1.20
2	TlNOMO	64	41	C2-C6	2.87	1.59
3	T4NOMO	70	35	CI-C4	1.36	1.57
4	T2NOMO	70	35	C4-C6	4.16	2.73
5	TlbNOMO	66	33	C4-C6	3.81	2.55
6	T2NOMO	70	35	C4-C7	2.39	1.84
7	T2NOMO	70	35	C4-C7	1.56	1.21
8	T3NOMO	60	30	C3-C6	1.56	1.64
9	T2NOMO	68	34	C2-C5	5.40	2.80
10	T2NOMO	70	35	C3-C6	4.15	2.27
Mean±SD		67.8±3.4			2.89±1.28	1.94±0.60

RT: Radiotherpy; Gy: Gray; SUVmax: standardized uptake value maximum.

Data Analysis

We quantified ^{18}F-FLT-PET uptake using the maximal standardized uptake value (SUVmax) analysis in all patients. The region of interests used in SUV analysis were 3-dimensional and were based on the mean value within the 50% isocontour's boundaries using a Siemens Leonardo workstation. Regional mean SUVmax was calculated for cervical (level 1-7), thoracic (level 1-12) and lumbar vertebrae (level 1-5), sternum, and pelvis (crista iliaca both sides). Bone marrow in the field of view of RT in the cervical spine region was determined from the planings CT. The meanSUVmax of the thoracic vertebrae (level 5-12) in RT patients were used as control. Liver and spleen were also analysed using SUVmax. As previous expansion into appendicular skeleton was noted in patients with myelodysplasia, a known complication of chemoradiotherapy, expansion to the appendicular skeleton was analyzed visually.

Statistics

For analysis of SUVmax value differences before and after therapy Wilcoxon rank test was used. $P < 0.05$ was considered significant. All analyses were performed using SPSS software, version 17.0.

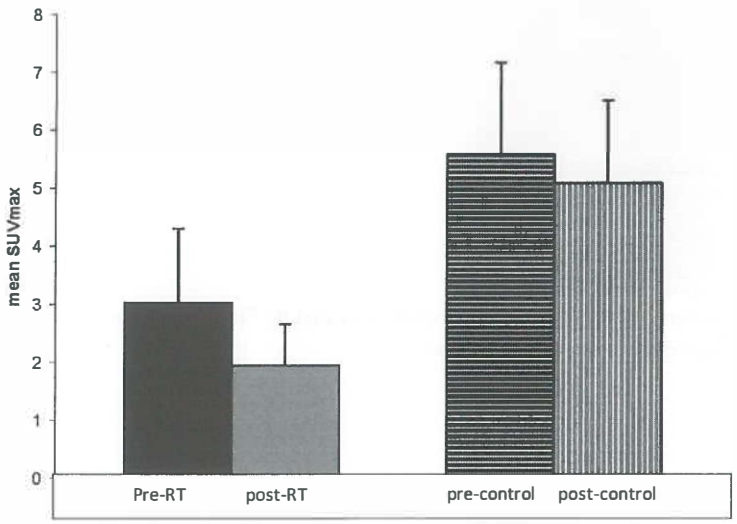

Figure 1: Figure 1: Mean ^{18}FLT-PET SUVmax value of the cervical bone marrow area before (black bar) and after radiotherapy (horizontal lined bar), and mean ^{18}FLT -PET SUVmax value of bone marrow outside the field of radiotherapy (thoracic spine) before (solid grey bar) and after radiotherapy (vertical lined bar).

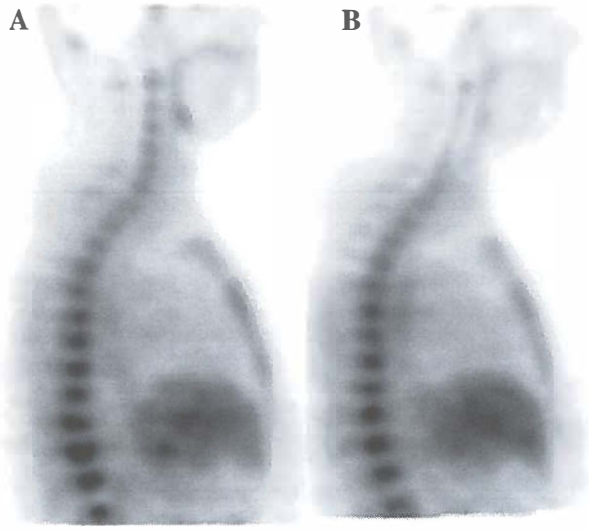

Figure 2: Images represent pre-radiation (panel A) and post radiation (panel B) ^{18}F-FLT studies in cervical bone marrow region after receiving 68Gy for laryngeal carcinoma

Figure 3: Images represent pre-therapy(panel A) and post-therapy(panel B) in representative patient undergoing chemotherapy for non-seminomatous testicular germ cell carcinoma with no significant difference in ^{18}F-FLT uptake.

Results

^{18}F-FLT-PET

No bone marrow expansion was observed beyond the axial skeleton. The size and uptake of the liver and spleen was within the normal range.

Radiotherapy patients

A significant decrease in ^{18}F-FLT-PET uptake was observed in all of the studied laryngeal carcinoma patients in the cervical region after RT of adjacent bone marrow compartment. Tumor stage and additional field of view of RT was inversely related to the ^{18}F-FLT uptake in bone marrow. The mean ^{18}F-FLT-PET SUVmax before RT was 3.0 ± 1.34 and after RT 1.94 ± 0.60 ($P = 0.013$) The mean ^{18}F-FLT-PET SUVmax of the spine (Th5-Th12) regions outside the field of view of RT were stable and reproducible and not significantly different (5.56 ± 1.56 versus 5.16 ± 1.35, $P = 0.16$, fig. 1). All patients had normal peripheral blood cell counts prior to the therapy and remained stable after RT (pre-RT: mean value white blood cells (WBC) 6.74 ± 2.91 10e9/L, hemaglobin (Hb) 8.82 ± 0.57 mmol/L, platelets (plat)269 ± 103 10e9/L; post-RT (< 1 week ^{18}F-FLT-PET scanning): WBC 5.44 ±1.88 10e9/L, Hb 8.14 ± 0.99 mmol/L, platelets 212 ±77 10e9/L). Figure 2 shows representative images of pre and post radiation images.

Chemotherapy patients

Chemotherapy did not result in a significant difference of SUVmax value, with a mean SUVmax of 4.99 ± 1.15 pre-chemo, and a mean SUVmax of 5.28 ± 1.0 post-chemo ($P = 0.21$).

Table 3: Stage, hematologic paramaters, and ^{18}F-FLT uptake in pretreatment and post therapy patients with non-seminomatous testicular germ cell carcinoma treated with bleomycin, etoposide and platinum therapy.

Patient	*Stage*	*SUVmax pre chemo*	*Hb*	*WBC*	*Plat*	*SUVmax post chemo*	*Hb*	*WBC*	*Plat*
1	II	6.87	9.7	5.3	162	4.88	8.3	4.9	141
2	II	4.16	9.1	6.2	151	3.90	8.7	5.3	129
3	II	4.06	9.0	9.3	210	4.95	7.1	3.4	215
4	II	5.43	9.7	7.2	259	6.61	7.4	2.8	256
5	IV	4.82	8.4	3.6	210	5.97	9.0	4.1	232
6	II	5.47	9.1	5.3	257	6.01	7.8	3.8	177
7	II	5.47	9.0	6.8	176	4.71	5.7	4.0	128
8	II	6.49	8.6	7.5	334	6.41	7.2	7.9	484
9	II	3.79	10.2	5.5	304	4.10	8.3	6.3	220
Mean		4.99	9.20	6.30	229	5.28	7.72	4.72	220
±SD		±1.15	±0.57	±1.63	±63	±1.0	±1.0	±1.58	±109

Hb: Hemaglobin; WBC: total white blood count; Plat: platelets; chemo: chemotherapy.

Discussion

The ability to quantify the effect of radiation therapy on cellular division within the bone marrow compartment is an important initial step in advancing our understanding of bone marrow kinetics. ^{18}F-FLT-PET has already been used in a few patients [27,29] to study acute leukemia and other hematologic disorders. However, ^{18}F-FLT-PET has not yet been used to visualize the effect of therapy-related bone marrow toxicity in patients being treated for malignancy. This feasibility study provides evidence that we can quantify and visualize the amount of hematologic toxicity the patient will be subjected to with a given therapy. Our data indicate that radiation therapy with a mean dose of 68 Gy does diminish ^{18}F-FLT-PET uptake in the cervical region that may represent reduced hematopoeitic activity. Data show that the chemotherapeutic effect on bone marrow capacity is stable, and ^{18}F-FLT-PET measurements do not change from pre-chemotherapy assessment. The stability of marrow compartment assessment allows for greater use of ^{18}F-FLT-PET as an objective measure of bone marrow capacity over time. In addition, the absence of expansion following chemotherapy can distinguish post-chemotherapy ^{18}F-FLT uptake from myelodysplasia expansion decribed previously [29]. As myelodysplasia is a complication of chemoradiotherapy, this could clinically allow for prediction of early

risk for treatment associated myelodysplasia, which is often fatal. It is entirely possible that ^{18}F-FLT-PET could be used as a technique to monitor hematopoietic reserve over the course of the patient's chemotherapy. A noted decrease in activity after repeated courses of chemotherapy may represent a diminished number of cycling progenitor stem cells, that might prompt earlier referral for stem cell collection in cases of disease in which bone marrow transplant is a treatment option. ^{18}F-FLT-PET may be a quantitative and descriptive tool for evaluation of the bone marrow capacity during chemo- and/or radiotherapeutic treatment.

Conclusion

Radiotherapy decreases ^{18}F-FLT uptake in bone marrow, but not following chemotherapy. We conclude that ^{18}F-FLT-PET is may be a potential non-invasive tool that can be used in the assessment of quantification of cellular division in the hematopoetic organ.

REFERENCES

1. *Chen W, Cloughesy T, Kamdar N, et al. Imaging proliferation in brain tumors with 18FFLT PET: comparison with 18F-FDG. Journal of Nuclear Medicine. 2005;46:945-952.*

2. *Yamamoto Y, Wong TZ, Turkington TG, et al. 3'-Deoxy-3'-[F-18]fluorothymidine positron emission tomography in patients with recurrent glioblastoma multiforme: comparison with Gd-DTPA enhanced magnetic resonance imaging. Molecular Imaging & Biology.2006;8:340-347.*

3. *Muzi M, Spence AM, O'Sullivan F, et al. Kinetic analysis of 3'-deoxy-3'-18Ffluorothymidine in patients with gliomas. Journal of Nuclear Medicine. 2006;47:16121621.*

4. *Jacobs AH, Thomas A, Kracht LW, et al. 18F-fluoro-L-thymidine and 11C-methylmethionine as markers of increased transport and proliferation in brain tumors. Journal of Nuclear Medicine. 2005;46:1948-1958.*

5. *Choi SJ, Kim JS, Kim JH, et al. [18F]3'-deoxy-3'-fluorothymidine PET for the diagnosis and grading of brain tumors. European Journal of Nuclear Medicine & Molecular Imaging. 2005;32:653-659.*

6. *Wieder HA, Geinitz H, Rosenberg R, et al. PET imaging with [18F]3'-deoxy-3'fluorothymidine for prediction of response to neoadjuvant treatment in patients with rectal cancer. European Journal of Nuclear Medicine & Molecular Imaging. 2007;34:878-883.*

7. *Francis DL, Freeman A, Visvikis D, et al. In vivo imaging of cellular proliferation in colorectal cancer using positron emission tomography. Gut. 2003;52:1602-1606.*

8. *Francis DL, Visvikis D, Costa DC, et al. Potential impact of [18F]3'-deoxy-3'-fluorothymidine versus [18F]fluoro-2-deoxy-D-glucose in positron emission tomography for colorectal cancer. European Journal of Nuclear Medicine & Molecular Imaging. 2003;30:988-994.*

9. *Herrmann K, Wieder HA, Buck AK, et al. Early response assessment using 3'-deoxy-3'-[18F]fluorothymidine-positron emission tomography in high-grade non-Hodgkin's lymphoma. Clinical Cancer Research. 2007;13:3552-3558.*

10. *Buck AK, Bommer M, Stilgenbauer S, et al. Molecular imaging of proliferation in malignant lymphoma. Cancer Research. 2006;66:11055-11061.*

11. *Buchmann I, Neumaier B, Schreckenberger M, et al. [18F]3'-deoxy-3'-fluorothymidine-PET in NHL patients: whole-body biodistribution and imaging of lymphoma manifestations--a pilot study. Cancer Biotherapy & Radiopharmaceuticals. 2004;19:436-442.*

12. *Pio BS, Park CK, Pietras R, et al. Usefulness of 3'-[F-18]fluoro-3'-deoxythymidine with positron emission tomography in predicting breast cancer response to therapy. Molecular Imaging & Biology. 2006;8:36-42.*

13. *Kenny L, Coombes RC, Vigushin DM, et al. Imaging early changes in proliferation at 1 week post chemotherapy: a pilot study in breast cancer patients with 3'-deoxy-3'[18F]fluorothymidine positron emission tomography.[see comment]. European Journal of Nuclear Medicine & Molecular Imaging.2007;34:1339-1347.*

14. *Smyczek-Gargya B, Fersis N, Dittmann H, et al. PET with [18F]fluorothymidine for imaging of primary breast cancer: a pilot study. European Journal of Nuclear Medicine & Molecular Imaging. 2004;31:720-724.*

15. *Troost EG, Vogel WV, Merkx MA, et al. F18-FLT does not discriminate between reactive and metastatic lymph nodes in primary head and neck cancer patients. Journal of Nuclear Medicine. 2007;48:726-735.*

16. *Cobben DC, van der Laan BF, Maas B, et al. F18-FLT for visualization of laryngeal cancer: comparison with 18F-FDG PET. Journal of Nuclear Medicine.2004;45:226-231.*

17. *Been LB, Suurmeijer AJ, Elsinga PH, et al. 18F-fluorodeoxythymidine PET for evaluating the response to hyperthermic isolated limb perfusion for locally advanced soft-tissue sarcomas. Journal of Nuclear Medicine.2007;48:367-372.*

18. *Cobben DC, Elsinga PH, Suurmeijer AJ, et al. Detection and grading of soft tissue sarcomas of the extremities with (18)F-3'-fluoro-3'-deoxy-L-thymidine. Clinical Cancer Research.2004;10:1685-1690.*

19. *Cobben DC, Elsinga PH, Hoekstra HJ, et al. Is 18F-3'-fluoro-3'-deoxy-L-thymidine useful for the staging and restaging of non-small cell lung cancer? Journal of Nuclear Medicine. 2004;45:1677-1682.*

20. *Muzi M, Vesselle H, Grierson JR, et al. Kinetic analysis of 3'-deoxy-3'-fluorothymidine PET studies: validation studies in patients with lung cancer. Journal of Nuclear Medicine 2005;46:274-282.*

21. *Yap CS, Czernin J, Fishbein MC, et al. Evaluation of thoracic tumors with 18F-fluorothymidine and 18F-fluorodeoxyglucose-positron emission tomography. Chest. 2006;129:393-401.*

22. *Halter G, Buck A, Schirrmeister H. 3-deoxy-3'-fluorothymidine positron emission tomography: alternative of diagnostic adjunct to 2-[18F]-fluoro-2-deoxy-D-glucose positron emission tomography in the workup of suspicious central focal lesions? Journal of Thoracic and Cardiovascular Surgery. 2004 2004;127:1093-1099.*

23. *Dittmann H, Dohmen BM, Paulsen F, et al. [18F]FLT PET for diagnosis and staging of thoracic tumours. European Journal of Nuclear Medicine & Molecular Imaging. 2003;30:1407-1412.*

24. *Buck AK, Halter G, Schirrmeister H, et al. Imaging proliferation in lung tumors with PET: 18F-FLT versus 18F-FDG.[see comment]. Journal of Nuclear Medicine. 2003;44:14261431.*

25. *van Westreenen HL, Cobben DC, Jager PL, et al. Comparison of F18-FLTand 18FFDG PET in esophageal cancer. Journal of Nuclear Medicine. 2005;46:400-404.*

26. *Cobben DC, Jager PL, Elsinga PH, et al. 3'-18F-fluoro-3'-deoxy-L-thymidine: a new tracer for staging metastatic melanoma? Journal of Nuclear Medicine. 2003;44:1927-1932.*

27. *Buck A, Bommer M, Juweid M, et al. First Demonstration of Leukemia Imaging with the Proliferation Marker 18F-Fluorodeoxythymidine. Journal of Nuclear Medicine. 2008;49:1756-1762.*

28. *Vanderhoek M. Early assessment of treatment response in hematopoietic disease using [18F]FLT PET imaging. American Association of Physicists in Medicine [Abstract] Abstract.*

29. *Agool A, Schot BW, Jager PL, et al. F18-FLTin hematologic disorders: a novel technique to analyze the bone marrow compartment. Journal of Nuclear Medicine. 2006;47:1592-1598.*

30. *Awasthi VH, J. Thorp, K. Anderson, S. Epstein, R. 18F-Fluorothymidine-PET evaluation of Bone Marrow Transplant in a Rat Model. Nuclear Medicine Communications. 2010;31:152-8.*

31. *Grierson JSA. Radiosynthesis of 3'-deoxy-3'-[(18)F]fluorothymidine: [(18)F]FLT for imaging of cellular proliferation in vivo. Nucl Med Biol. 2000;27:143-156.*

Chapter 7

Extramedullary hematopoiesis imaging with ^{18}F-FLT-PET

Ali Agool[1, 2], Rudi A.J.O. Dierckx[2], Joost T.M. de Wolf[3], Edo Vellenga[3], Riemer H.J.A. Slart[2]

[1]Department of Nuclear Medicine, Medical Center Twente, the Netherlands
[2]Department of Nuclear Medicine and Molecular Imaging, University Medical Center Groningen, University of Groningen, Groningen, the Netherlands
[3]Department of Haematology, University Medical Center Groningen, University of Groningen, Groningen, the Netherlands.

European Journal of Nuclear Medicine and Molecular Imaging. 2010;37:1620

A 40-year-old Caucasian male known with a history of hemoglobin-E β-thalassemia was presented to our department with progressive back pain referred to the both limbs, disturbed sensibility and weakness. Due to persisting physical complains a MRI of the thorax was performed (Fig. 1A), showing a bilateral paravertebral mass. The combination of the mass configuration and a patient with β-thalassemia makes the presence of extramedullary hematopoiesis (EMH) high ranking in the differential diagnosis, but malignant lymphoma could not be excluded. 3'-^{18}F-fluoro-3'-deoxy-L-thymidine (^{18}F-FLT) is used to detect and assess the hematopoietic bone marrow activity and could be helpful for the diagnosis of EMH [1]. ^{18}F-FLT-PET demonstrated bone marrow expansion to the distal parts of the skeleton, with a homogeneous activity, and an elevated standardized uptake value (SUVmax of spine 4.2; normal 3.7) in bone marrow, but decreased in liver and spleen compared to normal values [1]. Normally no ^{18}F-FLT activity is shown in the distal bones [1]. More importantly, ^{18}F-FLT-PET revealed multiple EMH masses bilateral and paravertebral in the thorax with an elevated SUVmax of 5 (Fig. 2). For optimal delineation of the EMH mass ^{18}F-FLT-PET was fused with a MRI and demonstrated intense ^{18}F-FLT uptake paravertebral in the thorax (Fig. 1B). Due to the observed findings a new bone marrow aspiration was performed and revealed hypercellularity with erythroid hyperplasia as result of a persisting anemia. Patient was treated with blood transfusions and hydroxyuria and showed a considerable relief of his complaints.

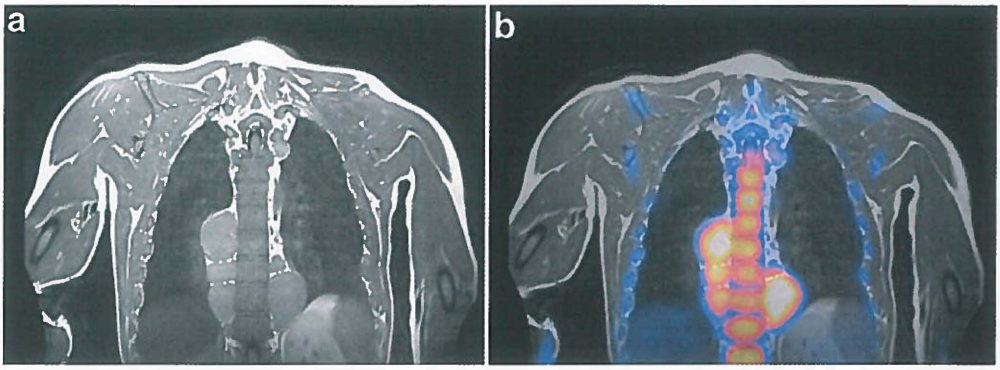

Figure 1: A: MRI thorax with a mass paravertebral, B: Fused ^{18}F-FLT-PET-MRI shows an elevated ^{18}F-FLT uptake paravertebral due to extramedullary hematopoiesis.

Figure 2: Thoracic paravertebral extramedullary hematopoiesis in a patient with β-thalassemia using ^{18}F-FLT-PET.

Discussion

Extramedullary hematopoiesis is a rare disorder and defined as the localization and probably production of myeloid and erythroid cells outside of the bone-marrow cavity. It can be a mechanism to compensate for impaired red cell production or accelatered destruction as in haemolytic anaemia such as spherocytosis or thalassaemia. Alternatively it is shown in response to bone-marrow dysfunction seen in disorders as myelofibrosis or leukaemia [2]. Approximately 5% of the cases with EMH occur outside of the liver and spleen. Of these, the most common sites are surrounding the vertebral column (especially the thoracic region), lymph nodes, retroperitoneum, lung and pleura [2]. A CT-scan is a common preliminary investigation to demonstrate EMH. It usually appears as heterogeneous lobulated solid mass with smooth margins. Based on CT imaging, the differential diagnosis is lymphoma, which tends to produce a pattern of retroperitoneal involvement of lymph nodes surrounding the great vessels [3,4]. An alternative diagnostic tool might be an MRI that often reveals a characteristic well encapsulated tumour with a slightly higher signal intensity than muscle and adjacent marrow of the vertebral bodies on T1 and T2 weighted imaging [5].

The ^{18}F-FDG-PET scan may also reveal mild to moderate FDG activity in multiple paraspinal thoracic masses, just as ^{111}In-chloride, ^{99m}Tc-colloid, ^{201}Thallium, and ^{99m}Tc-sestamibi scintigraphy [6-8], but the SUV value of FDG is in general lower than detected in aggressive lymphoma. ^{18}F-FLT is recently developed to image more specifically the cellular proliferation of different tumours. In particular it can also assess the function and expansion of the hematopoietic bone marrow compartment and shows significant high tracer uptake on PET imaging [1] of the central skeleton. The pyrimidine analogue thymidine is incorporated in DNA and undergoes the same first metabolic step as thymidine, thus, its uptake reflects the DNA synthesis of the affected tissue. Besides being non invasive, PET imaging permits the evaluation of the entire bone marrow compartment overcoming issues of heterogeneity and bone marrow sampling.

In our case EMH was differentiated from malignant lymphoma in a patient that presented large thoracic masses with a familiar red cell disorder. ^{18}F-FLT uptake revealed EMH activity indicating that ^{18}F-FLT-PET is an attractive non-invasive technique for the diagnosis of EMH.

REFERENCES

1. *Agool A, Schot BW, Jager PL, Vellenga E. 18F-FLT PET in hematologic disorders: a novel technique to analyze the bone marrow compartment. J Nucl Med 2006; 47:1592-1598.*
2. *Koch CA, Li CY, Mesa RA, Tefferi A. Nonhepatosplenic extramedullary hematopoiesis: associated diseases, pathology, clinical course, and treatment. Mayo Clin Proc 2003; 78:1223-1233.*
3. *Choi H, David CL, Katz RL, Podoloff DA. Case 69: extramedullary hematopoiesis. Radiology 2004; 231:52-56.*
4. *Georgiades CS, Neyman EG, Francis IR, Sneider MB, Fishman EK. Typical and atypical presentations of extramedullary hemopoiesis. AJR Am J Roentgenol 2002; 179:1239-1243.*
5. *Savader SJ, Otero RR, Savader BL. MR imaging of intrathoracic extramedullary hematopoiesis. J Comput Assist Tomogr 1988; 12:878-880.*
6. *Kakite S, Tanabe Y, Kinoshita F, Harada H, Ogawa T. Clinical usefulness of In-111 chloride and Tc-99m Sn colloid scintigraphy in the diagnosis of intrathoracic extramedullary hematopoiesis. Ann Nucl Med 2005; 19:317-320.*
7. *Mosley C, Jacene HA, Holz A, Grand DJ, Wahl RL. Extramedullary hematopoiesis on F-18 FDG PET/CT in a patient with metastatic colon carcinoma. Clin Nucl Med 2007; 32:878-880.*
8. *Niederkohr RD, Chiu E, Nielsen KR, Maclean M. Extramedullary hematopoiesis within paravertebral masses demonstrating prominent sestamibi and thallium uptake. Clin Nucl Med 2009; 34:506-507.*

Chapter 8

Somatostatin receptor scintigraphy might be useful for detecting skeleton abnormalities in patients with multiple myeloma and plasmacytoma

Ali Agool[1], Riemer H.J.A. Slart[1], Rudi A.J.O. Dierckx[1], Philip M. Kluin[2], Pieter L. Jager[3], Edo Vellenga[4]

Department of Nuclear Medicine and Molecular Imaging[1]; Department of Pathology[2], Department of Internal Medicine, Division of Hematology[4], University of Groningen and University Medical Center Groningen, The Netherlands; Department of Nuclear Medicine[3], Hamilton Health Sciences/McMaster University, Hamilton, Canada.

European Journal of Nuclear Medicine and Molecular Imaging. 2010; 37:124–130

ABSTRACT

Somatostatin receptor expression has been demonstrated on a number of plasma cell lines. Therefore, we questioned whether somatostatin receptor scintigraphy (SRS) can be used to demonstrate in vivo multiple myeloma (MM) activity. ***Methods*** SRS was performed in newly diagnosed (n=9) or relapsing (n=18) MM patients or in patients with plasmacytoma (n=2). The results were compared with radiographic findings. ***Results*** A positive SRS was demonstrated in 44% of the newly diagnosed patients, in 83% of the relapsed patients and in both patients with plasmacytoma. The SRS findings corresponded with radiographic abnormalities in 40% of the patients. However, in relapsed patients 60% demonstrated increased SRS uptake in areas without new radiographic abnormalities. The positive SRS corresponded with histological proven disease activity and responded upon treatment. Moreover, immunohistochemical staining of MM material demonstrated concordant somatostatin receptor-sst3 staining in five of six patients. ***Conclusion*** These results demonstrate that SRS is a valuable tool to detect disease activity, especially in relapsing MM patients.

INTRODUCTION

Multiple Myeloma (MM) is clonal B cell disorder characterized by a monoclonal plasma cell population in bone marrow, with bone pain as result of skeleton abnormalities, hypercalceamia, and kidney dysfunction [1]. In a minority of the patients the disorder is localized and presents as a solitary plasmacytoma. In 60%-70% of the patients skeletal abnormalities are identified by X-ray examination and are characterized by typical osteolytic defects [1]. Following treatment with chemotherapy or radiotherapy the osteolytic defects persist and no clear distinction can be made whether vital tumor cells are present in these lesions. Also in relapsing disease the X-ray examination has a limited value unless progressive defects are observed. Therefore, it would be attractive to have scanning methods that identify the metabolic activity of the malignant plasma cells. Previous studies have shown that ^{18}F-FDG-PET might identify the metabolic activity of the malignant plasma cells. Several small studies have demonstrated that in a high percentage of newly diagnosed MM patients osteolytic lesions are ^{18}F-FDG-PET positive due to their higher metabolic activity [2,3]. An alternative approach would be the use of tracers that identify tumor-specific receptors. In vitro studies with plasma cell lines have shown that the somatostatin receptor is expressed on malignant plasma cells. It wsa shown that all MM cell lines express functional somatostatin receptors (sst) and that the subtypes sst2, sst3 are predominantly sst5 were present [4]. It is therefore conceivable that somatostatin receptor scintigraphy (SRS) using ^{111}In-pentetreotide may be a good alternative to study the presence of the malignant plasma cells [5]. So far SRS have been used for the detection of neuroendocrine tumors (NETs) and aggressive malignant lymphoma especially to define the extent of the disease [6,7]. Based on these findings we performed SRS in patients with MM or plasmacytoma to determine whether SRS can be used as an alternative method to detect disease activity in malignant plasma cell disorders.

Materials and methods

Patients

A total of 29 patients were prospectively included in this study (table 1). The patient group consisted of 22 men and 7 women with a median age of 59 year (range: 40-85 year). MM or plasmacytoma was based on the presence of a monoclonal plasma cell population in the bone marrow biopsy, the presence of a monoclonal Ig protein or free light chains (FLC) in serum according to international defined guidelines [1].

In all patients total whole-body radiography was performed. In a selected number of patients an additional CT-scan or MRI scan was performed based on clinical symptoms. Patients were treated according to ongoing trials for MM patients younger than 65 years or with melphalan/prednisolon [8-10]. Patients (< 65 years) were treated upfront with three cycles of VAD (vincristine, doxorubicin, dexamethasone) or TAD (thalidomide, doxorubicin, dexamethasone). This was followed by peripheral blood stem collection following high-dose cyclophosphamide plus granulocyte colony stimulation factor. Finally autologous stem cell transplantation was performed with high dose melphalan and re-infusion of autologous stem cell. The protocol was approved by the Medical Ethical Committee Groningen, The Netherlands and informed consent was obtained from all patients.

Immunohistochemistry

Bone marrow biopsy or material of extra-osseous localization of MM patients was used for these investigations. In two cases the localization was based on a positive SRS. Tissue specimens were fixed in phosphate-buffered formaldehyde (12–24 h) and decalcified using a mixture of 10% acetic acid and 4% formaldehyde (24–48 h). After standard tissue processing biopsies were embedded in paraffin wax. Four-micrometer sections were cut and floated onto 3-aminopropylethoxysilane (APES)-coated slides. After dewaxing slides were microwaved in 10 mmol/l citrate buffer, pH 6.0, for 15 min at 750 W, allowed to cool to room temperature and washed three times in triethanolaminebuffered saline. The slides were processed using a Techmate Horizon (Dako, Carpinteria, CA, USA) slide processor. Affinity purified polyclonal rabbit antisera specifically directed against sst2 (NB100-74537), sst3 (NLS2622) and sst5 (NLS2639) (1 µg/ml, Novus Biologicals, Littleton, CO, USA) were incubated for 1 h and binding was visualized using a streptavidin-biotin complex reagent (StrepABComplex/HRP Duet, Dako,

Carpinteria, CA, USA). Chromogenic substrate was 3,3′-diaminobenzidine. Slides were counterstained with haematoxylin. Positive control of immunostaining was assessed by immunohistochemistry of normal pancreatic islets. However, on bone marrow trephines, satisfactory results were only obtained for the sst3 staining and not for sst2 and sst5. In general, if possible all myeloma cells were stained. The intensity of the immunostaining of myeloma cells was reported using the following system: 0: no or extremely weak, +: moderate and ++: strong.

Octreotide scintigraphy

Whole body scan SRS was performed 24 hours after intravenously injection of 200 MBq ^{111}In-pentetreotide. A Multispect 2 Siemens double headed gamma camera (Siemens Medical Systems, USA) was used with a matrix of 256x256 and equipped with medium-energy collimator. Patients were positioned supine on the imaging table; subsequently 6 views were obtained anterior and posterior of head/neck/thorax, abdomen and the thighs, 10 min/view. The SRS scan and X-skeleton was performed with a period of 7 days.

SRS were separately examined by 2 experienced nuclear physicians using visual examination with special attention to the skeleton. Any focal tracer accumulation exceeding normal regional tracer uptake levels was rated as a pathological. Subsequently, regions of interest (ROIs) were visually placed over the area with abnormal uptake and tracer uptake was quantified by comparing the average counts per pixel of the focus in comparison with normal background bone activity assessed from a usually symmetrically placed contra lateral background ROI. A simple scoring was developed to grade the uptake in the pathological sites. Uptake was recognized as 'slightly elevated' if the uptake ratio exceeded 1.5 in the lesion, as 'moderate' when uptake ratio was between 1.5 and 2, and as 'high' when over 2. Non focal intestinal uptake changing over time was considered to be physiological background activity. All scintigraphic results were compared with radiographic findings.

Table 1: Patient characteristics at presentation or at relapse.

Patient no	*Age (yrs)*	*Sex*	*Type of underlying disorder*	*Para-prot.*	*SRS*
1	63	f	MM	IgA-κ	+
2	58	f	MM	IgG-κ	-
3	54	m	MM	IgG-λ	-
4	57	m	MM	FLC-κ	+
5	62	m	MM	IgA- κ	+
6	53	m	MM	IgG- κ	-
7	52	m	MM	IgG- κ	+
8	51	m	MM	IgG-λ	-
9	62	m	MM	IgG- κ	-
10	60	m	Plasmacytoma	IgA-λ	+
11	40	m	Plasmacytoma	IgG- κ	+
12	85	m	MM-R	IgA- κ	+
13	56	f	MM-R	IgG- κ	+
14	61	m	MM-R	IgG- κ	-
15	64	m	MM-R	IgG- κ	+
16	55	m	MM-R	FLC- κ	+
17	46	m	MM-R	FLC- κ	+
18	48	m	MM-R	FLC-λ	+
19	70	m	MM-R	FLC- κ	+
20	60	m	MM-R	IgG- κ	+
21	63	m	MM-R	IgG- κ	+
22	63	m	MM-R	IgG- κ	+
23	59	m	MM-R	IgG- κ	+
24	67	f	MM-R	IgG-λ	-
25	48	m	MM-R	FLC- κ	+
26	73	m	MM-R	NS *	-
27	65	f	MM-R	FLC- κ	+
28	60	f	MM-R	FLC-λ	+
29	64	f	MM-R	NS	+

*N.S.: non-secretor; FLC: free light chain in serum; MM (R): multiple myeloma (relapse); SRS: somatostatin receptor scintigraphy with a positive (+) or negative (-)scan

Table 2: Somatostatin receptor scintigraphy in multiple myeloma patients upfront treatment or at relapse.

Patient no	*SRS*			*Correspondig Whole body Radiography Abnormalities (y/n)*	*Whole body radiography*		
	Scan Pos.	*No of lesions*	*uptake ratio*		*No lesions >1cm*	*No lesions <1cm*	*New lytic Lesions at Relapse >1 cm*
2	-	0	-	-	3	Y	
3	-	0	-	-	0	N	
4	+	1	2	Y	3	Y	
5	+	1	2.3	N[a]	0	N	
6	-	0	-	-	1	N	
7	+	2	2.5	Y	0	Y	
8	-	0			0	Y	
9	-	0	-	-	0	N	
10	+	1	2	N[a]	0	N	
11	+	1	1.5	Y	0	N	
12	+	11	2 (1.5-2.5)	N	0	N	0
13	+	2	2 (1.8-2.2)	N	0	N	0
14	-	0	-	-	4	Y	1
15	+	1	2.5	Y	3	N	1
16	+	1	1.5	Y	6	Y	1
17	+	1	2	Y	4	Y	1
18	+	3	3 (2.8-3.2)	Y[b]	3	Y	3
19	+	Diffuse	n.a.	N	0	Y	0
20	+	12	2 (1.5-2.5)	N	3	N	0
21	+	1	1.3	Y[a]	2	Y	1
22	+	1	2	Y	5	Y	1
23	+	3	2 (1.7-2.2)	N	0	N	0
24	-	0	-	-	0	Y	0
25	+	3	2	N	5	N	0
26	-	0	-	-	0	N	0
27	+	1	2	N	5	Y	0
28	+	3	3 (2.6-3.3)	N[b]	3	Y	2
29	+	1	1.4	N[a]	0	Y	0
2	-	0	-	-	3	Y	

Lytic lesions larger than 1 cm; osteolytic defects present (Y) or absent (N)
n.a. not available. [a] No abnormalities on whole body radiography but defects on MRI or CTs-can
[b] Extra ossal localization.

Results

A total of 27 patients with MM and 2 patients with plasmacytoma were studied. Patient characteristics are presented in table 1. Of the 27 patients with MM, 9 patients had newly diagnosed MM and 18 patients had relapsing disease. MM showed production of IgG-k (n=12), IgG-l type (n=3), IgA-l type or IgA-k (n=4) types. In eight patients monoclonal FLCs were demonstrated in the serum.

Whole body radiography demonstrated abnormalities in 14 of the 29 patients.

The type of treatment was dependent on age and whether the patient presented with newly diagnosed or relapsing disease. The newly diagnosed patients (age: 51-63 years) were treated with intensive chemotherapy and autologous stem cell transplantation [9,10]. Relapsing patients (age: 46- 85 years) were treated with variable combinations of dexamethason, cyclophosphamide, thalidomide or bortezomib. The two patients with solitary plasmacytoma (age 40 and 60 yr) were treated with radiotherapy with and without intensive chemotherapy (table 2).

Octreotide scintigraphy

In all patients SRS was performed. In 5 patients a second scan was obtained after 3-5 months of treatment. The number of affected areas on the SRS varied between 1 and 12 per patient. The median uptake ratio was 2.0 (range: 1.3-3.5.). Based on a comparison with the abnormalities seen by whole body radiography, we defined that SRS was only positive in lesions with a diameter of more than 1 cm. In four of the nine [44%, 95% confidence interval (CI):0.12--0.77] newly diagnosed MM patients the SRS was positive, in the other 5 patients the SRS was normal (fig. 1). Two of these 5 patients had distinct abnormalities by whole body radiography. In both patients with solitary plasmacytoma, a positive SRS was obtained of the affected area which was confirmed by X-ray examination and CT-scanning.

SRS was studied in 18 MM patients with relapsing disease. A positive SRS was shown in 15/18 (83%, 95% CI: 0.66-1) of these patients. In 6 of the 15 (40%, 95% CI: 0.15-0.60) evaluable patients the increase in SRS corresponded with new abnormalities on the whole body radiography, whereas in the other 9 patients (60%, 95% CI: 0.35-0.85) enhanced SRS activity was not accompanied by new abnormalities on the whole body radiography.

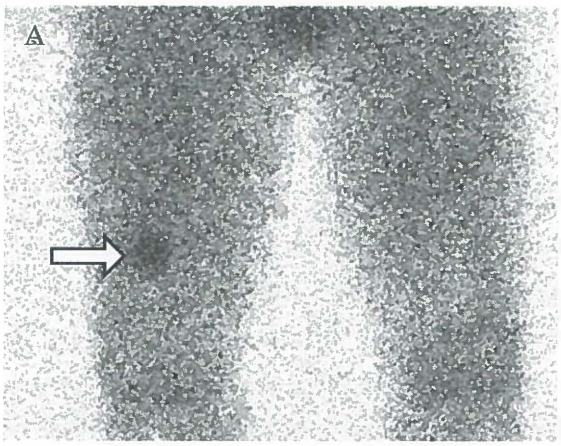

Figure 1: Representative abnormal SRS uptake of the distal femur in combination with the abnormal uptake on the standard skeleton (white arrow). No SRS uptake of the osteolytic lesion of the proximal femur (small black arrow).

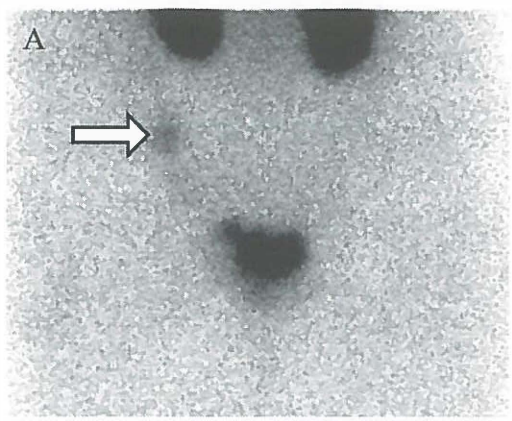

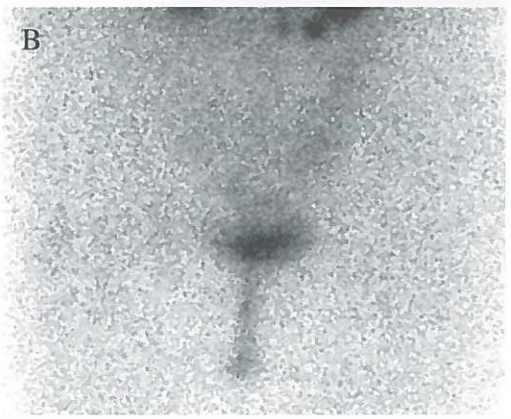

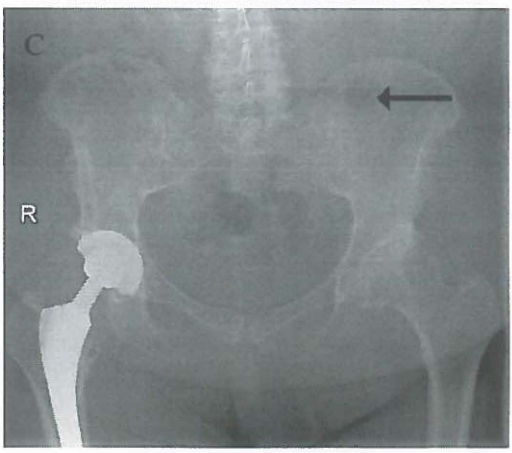

Figure 2: Somatostatin receptors scintigraphy of the pelvis posterior view in patient with multiple myeloma in the iliac bone left, before treatment (A), and after (B). The X-ray (anterior view) show a persistent osteolytic bone lesion (C). Arrow denotes the osteolytic lesion.

To verify that the increased octreotide uptake was related to disease activity, biopsies were performed of the affected areas (pelvis, clavicula) in four patients (no 1, 10, 11, 18). In all four cases histologically proven MM activity was present.

To study the effect of treatment, follow-up scans were performed in five cases. Scans performed after 3-4 months of treatment demonstrated a complete disappearance of lesions in three patients and a decrease in two. These changes corresponded with reduced disease activity including declining paraprotein or FLC levels (table 3).

Finally the somatostatin receptor expression sst3 was studied on biopsy material of patients with MM. It included bone marrow biopsy material and one extra-osseous manifestation of the MM. In total six patients were studied: four patients with a positive SRS scan and two patients with a negative scan. Three of four patients with a positive SRS showed positively stained MM cells, two of them showing strongly positive cells. One patient with a positive showed few strongly positive cells whereas no immunostaining was observed on the majority of the MM cells. One patient with a negative scan showed entirely negative tumour cells, and the other showed occasionally positive cells (table 4, fig. 3). Although the series of patients is very small, we also looked for a possible relationship between the SRS results and tumour load in the biopsies, since negative SRS results might have been caused by a less prominent infiltrate. No such correlation was found (data not shown).

Table 3: Follow-up results of SRS scan after 3-months of treatment.

Patient no	*Type of Paraprot*	*Paraprotiene level*		*SRS*		*Treatment*
		Upfront	*Follow up*	*Upfront*	*Follow up*	
1	FLC-κ	204	2	+	-	VAD
11	IgG-κ	37	4	+	-	VAD
12	IgG-κ	17	3	+	-	Thalid/dexa
18	FLC-λ	885	68	+	+/-	Thalid/dexa
20	FLC-κ	382	40	+	+/-	Thalid/dexa

*Follow-up scan was performed 3 months after start of treatment with: thalidomide (thalid), dexamethason (dexa), or vincristin, adriamycin, dexamethason (VAD). Free light chain (FLC) serum level; normal range: FLC-λ 4.4-32 mg/ml; FLC-κ 2.3-20 mg/ml.

Table 4: Immunohistochemistry for somatostatin receptor subtypes sst3 and sst5.

Patients no	*SRS-scan*	*SST3*	*SST5*
1	Pos	+	+
3	Neg	+	-
6	Neg	+	-
11	Pos	++	+
23	Pos	+++	+
28	Pos	++++	+++

Expression of somatostatin receptor subtypes sst3 and sst5 was studied on bone marrow material of multiple myeloma patients or extra-ossal manifestation of multiple myeloma.
Patients no. reflect the numbers in table 1. sst3 and sst5 staining was quantified semi-quantative as described in material en methods.

DISCUSSION

Several methods are available to demonstrate disease activity and bone lesions in patients with MM. Whole body radiography has been most frequently used so far and demonstrates the characteristic osteolytic lesions in 60%-70% of the patients [1]. By using MRI scanning a further increase in skeletal abnormalities can be demonstrated. Recently, alternative techniques have been developed that make use of an increased metabolic activity of the malignant plasma cells. ^{18}F-FDG-PET as well as ^{99m}Tc-sestamibi scanning have shown that in 80%-90% of the patients abnormal areas of increased uptake can be shown which are frequently associated with abnormal lesions on the whole body radiography [2,3,11,12]. In addition, there is evidence that the increased uptake of the ^{99m}Tc-sestamibi correlates with other measurable parameters of disease activity including C-reactive protein, lactate dehydrogenase and B_2-microglobulin [11,12].

Previous studies have shown that MM cell lines express functional receptors for sst2, sst3 and in particular sst5 and that in vitro growth of myeloma cells can be inhibited by somatostatin and its analogue octreotide [4]. Although the role of these receptors remains enigmatic in lymphoid cells, these findings provided us a rationale to study SRS in the clinical management of myeloma. It has been demonstrated that the currently used radiopharmaceuticals for somatostatin receptor targeting do not bind with high affinity to all presently known somatostatin receptor subtypes. They bind with very high affinity to sst2 and with somewhat lower affinity to sst3 and sst5 but not to sst1 and sst4.

The present study demonstrates that SRS is an alternative method to visualize in vivo MM activity. Although the number of patients with de novo disease is limited, the data in patients with relapsing disease suggest that SRS is more sensitive than other methods. The SRS was abnormal in 82% of the patients whereas conventional whole body radiography revealed new lesions in only 33% of the same patients. Histological analysis in six patients proved that the abnormal lesions as revealed by SRS were tumor related. Moreover, in most patients SRS-positive areas stained at least for the somatostatin receptor subtype sst3. Unfortunately, immunohistochemistry for sst2 and sst5 which was most widely expressed in myeloma cell lines was unsatisfactory [4].

Patients responsive on treatment demonstrated total or partial normalization of the abnormal uptake after 3-4 months of treatment, which correlated with a decline of other disease related parameters. A remarkable finding was the fact that a positive SRS was more frequently noticed in relapsing MM patients than in upfront patients. It is unlikely

that the difference is linked to the number of patients studied. Since we identified several MM cases with histologically massive, diffuse infiltrates that were mainly negative in immunohistochemistry, it is also unlikely that the differences in detection rate by SRS were caused by differences in growth pattern. It is more conceivable that an enhanced somatostatin receptor expression is shown in a more advanced state of the disease. This would be in line with the strong positive somatostatin receptor expression on MM cell lines which reflects also a more aggressive type of MM. Also in two patients with plasmacytoma a localized abnormal SRS could be shown. Although the number of patients studied is limited, these findings suggest that SRS might be a good alternative that verifies whether a localized disease is present. However, the skeletal abnormalities require a certain diameter. In our hands defects ^{3} 1 cm were in general noticed by SRS. Smaller lesions were in general not shown on SRS. Improved localization of the abnormal SRS might further be obtained by combining it with the SPECT-CT scan. Also ^{99m}Tc-labelled somatostatin is a preferable diagnostic radionuclide for higher scan quality because of favourable decay properties (6 h half-life, gamma radiation of 140 KeV) that allow administration of a large dose, to yield high-resolution images, as well as lower cost and easy on-site availability by the ^{99}Mo/^{99m}Tc generator in the clinic. PET labeled somatostatin analogue like ^{68}Ga-DOTANOC are also an interesting option, due to the higher resolution of PET camera systems.

In summary, the results demonstrate that SRS is a valuable tool to detect tumor activity in MM especially in patients with relapsing disease.

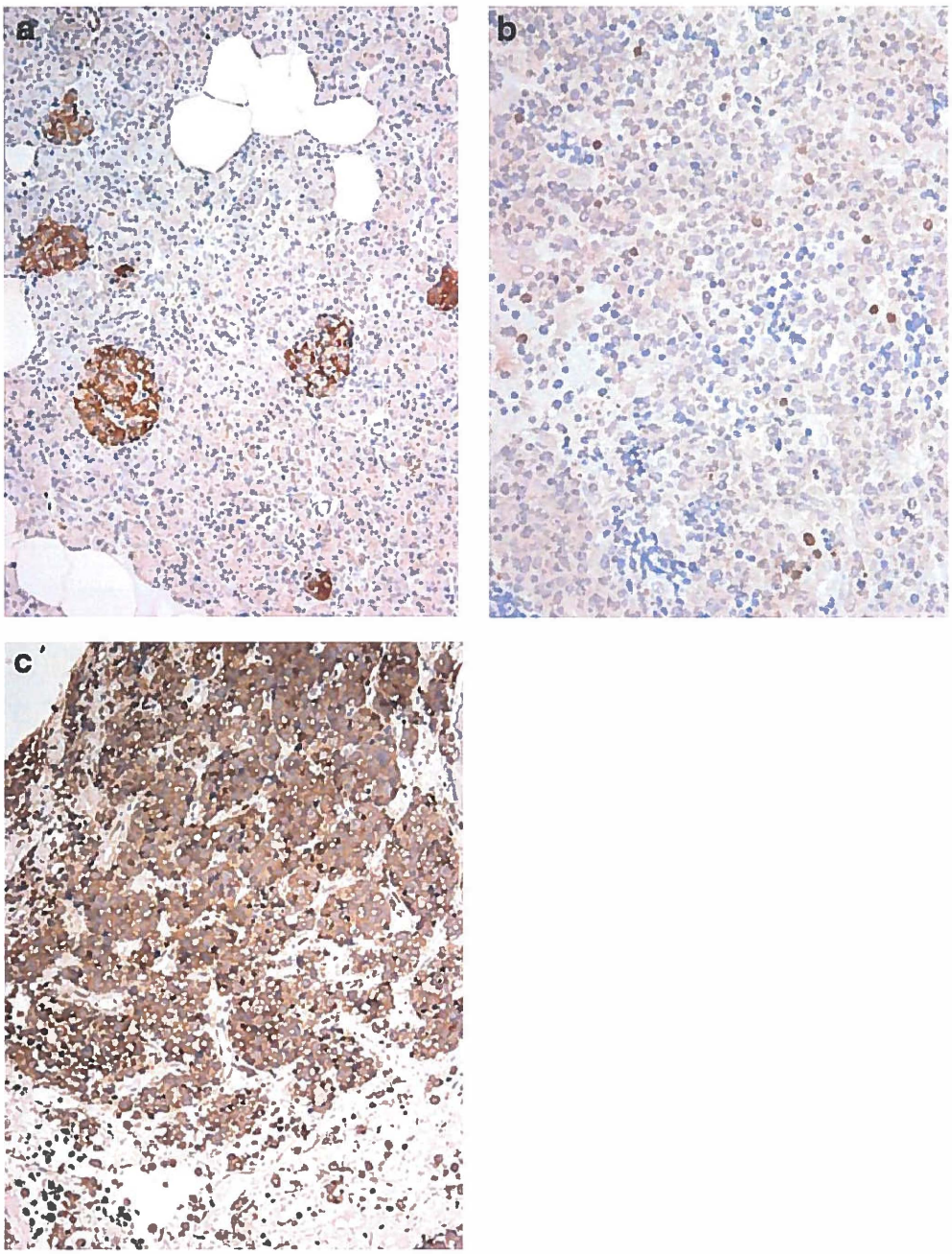

Figure 3: **a** Normal pancreatic tissue showing positive islets and negative exocrine tissue (original magnification ×200). **b** Patient 1 with mainly negative but incidentally strongly positive tumour cells (see also the insert; original magnification ×400). **c** Patient 23 with strongly positive tumour cells.

REFERENCES

1. *Smith A, Wisloff F, Samson D. UK Myeloma Forum; Nordic Myeloma Study Group; British Committee for Standards in Haematology. Guidelines on the diagnosis and management of multiple myeloma 2005. B J Haemat 2006;132:410-451.*

2. *Durie BGM, Waxman AD, D'Agnolo, Williams CM. Whole-body ^{18}F-FDG PET identifies high-risk myeloma. J Nucl Med 2002;43:1457-63.*

3. *Bredella MA, Steinbach L, Caputo G, Segali G, Hawkins R. Value of FDG PET in the assessment of patients with multiple myeloma. Am J Roentgenol 2005;184:1199-204.*

4. *Georgii-Hemming P, Stromberg T, Janson ET, Stridsberg M, Wiklund HJ, Nilsson K. The somatostatin analog octreotide inhibits growth of interleukin-6 (IL-6)-dependent and IL-6-independendt human multiple myeloma cell lines. Blood 1999;93:1724-31.*

5. *Krenning EP, Kwekkeboom DJ, Bakker WH, Breeman WAP, Kooij PPM, Oei HY, et al Somatostatine receptor scintigraphy with [111In-DTPA-D-Phe1]octreotide and [123Tyr3]-octreotide: the Rotterdam experience with more than 1000 patients. Eur J Nucl Med 1993;20:716-731.*

6. *De Jong M, Breeman WA, Bakker WH, Kooij PP, Bernard BF, Hofland LJ, et al. Comparison of (111)In-labeled somatostatin analogues for tumor scintigraphy andradionuclide therapy. Cancer Res 1998;58:437-41.*

7. *Sonneveld P, van der Holt B, Segeren CM, Vellenga E, Croockewit AJ, Verhoef GE, et al. Intermediate-dose melphalan compared with myeloablative treatment in multiple myeloma: long-term follow-up of the Dutch Cooperative Group HOVON 24 trial. Haematologica 2007;92:928-35.*

8. *Lokhorst HM, Schmidt-Wolf I, Sonneveld P, van der Holt B, Martin H, Barge R, et al. Thalidomide in induction treatment increases the very good partial response rate before and after high-dose therapy in previously untreated multiple myeloma. Haematologica 2008;93:124-27.*

9. *Hovenga S, Daenen SM, de Wolf JT, van Imhoff GW, Kluin-Nelemans HC, Sluiter WJ, Vellenga E. Combined thalidomide and cyclophosphamide treatment for refractory*

or relapsed multiple myeloma patients: a prospective phase II study. Ann Hematol 2005;84:311-16.

10. *Mele A, Offidani M, Visani G, Marconi M, Cambioli F, Nonni M, et al. Technetium-99m sestamibi scintigraphy is sensitive and specific for the staging and the follow-up of patients with multiple myeloma: a multicentre study on 397 scans. Br J Haematol. 2007;136:729-35.*

11. *Fallahi B, Saghari M, Fard Esfahani A, Eftekhari M, Iravani M, Beiki D, et al. The value of 99mTc-MIBI whole body scintigraphy in active and in remission multiple myeloma. Hell J Nucl Med. 2005;8:165-8.*

12. *Fonti R, Salvatore B, Quarantelli M, Sirignano C, Segreto S, Petruzziello F, et al. 18F-FDG PET/CT, 99mTc-MIBI, and MRI in evaluation of patients with multiple myeloma. J Nucl Med. 2008;49:195-200.*

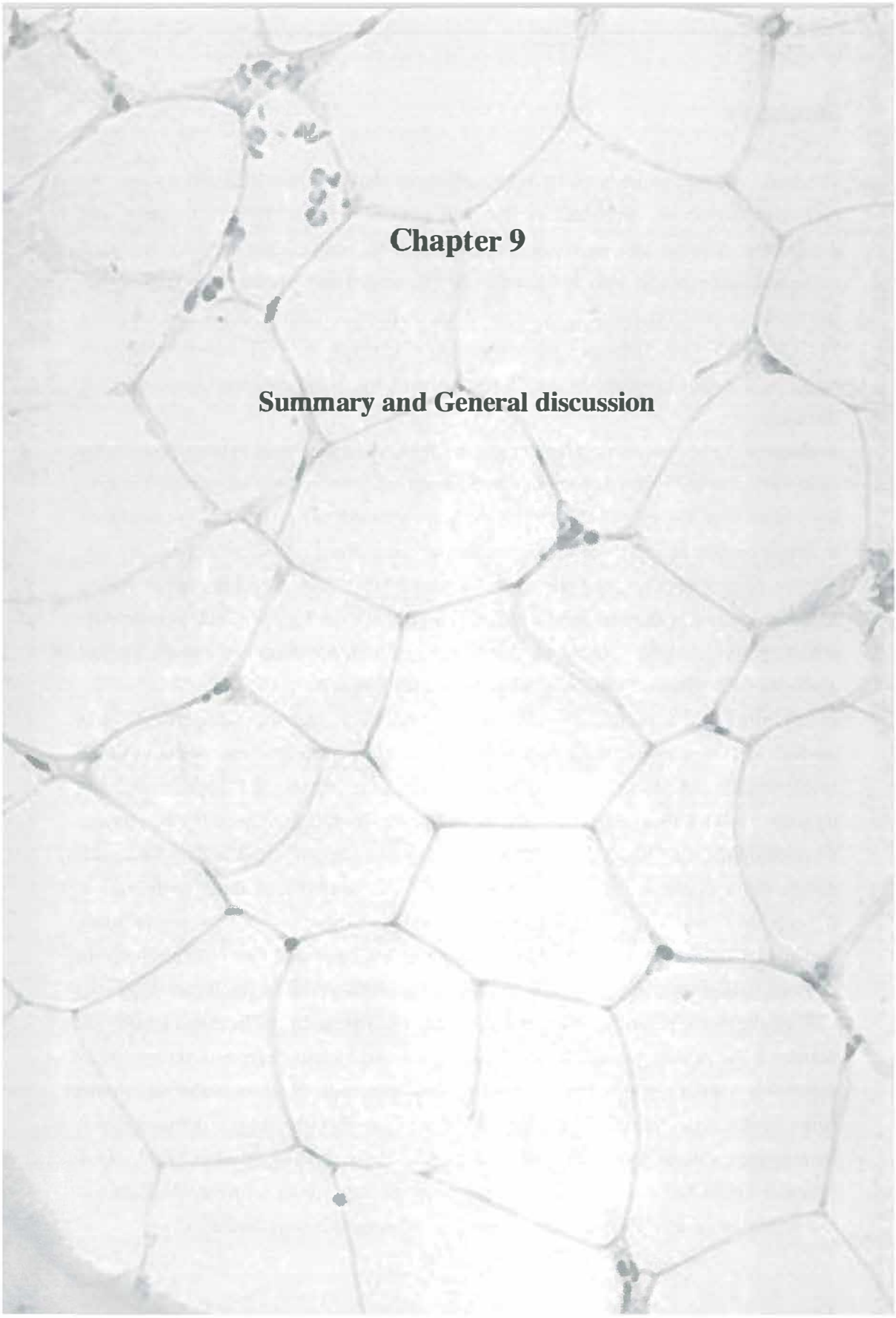

Chapter 9

Summary and General discussion

Summary

The bone marrow consists of different cell types that can be visualized by specific radiopharmaceuticals dependent on the cell type of interest. Different uptake and distribution patterns can be recognized which is not only determined by the used radiopharmacon but is also a reflection of the underlying disease. Imaging of the metabolic or proliferative activity of the bone marrow is recently developed by using ^{18}F-FDG or ^{18}F-FLT. Therefore, the application of gamma- and PET camera techniques might be a useful approach in the diagnostic work up of patients with hematological disorders.

In **chapter 2** an overview is given of the current knowledge of bone marrow imaging by using different radiolabeled compounds. Radioisotopes for the use on gamma cameras have been used for several decades in nuclear medicine; however, they are restricted to image certain cell types of the bone marrow compartment. PET tracers can provide a more comprehensive assessment of the whole bone marrow compartment with a higher resolution with restricted image of a specific cellular function such as metabolic activity or proliferative activity. Distinct uptake patterns are described and the clinical applications in various hematological diseases are discussed.

In **chapter 3** the proliferative activity of the bone marrow compartment was studied in patients with various hematological disorders including myelodysplasia, myeloproliferative disease, myelofibrosis, multiple myeloma and aplastic anaemia by using ^{18}F-FLT PET scan. This pyrimidine analog is phosphorylated by the enzyme thymidine kinase 1 (TK1), which leads to intracellular trapping. TK1 activity increases during DNA synthesis; therefore, ^{18}F-FLT uptake is related to cellular proliferation. Patients with myelodysplasia and myeloproliferative disorders showed significantly higher FLT uptake by the bone marrow compartment compared to a control group. In contrast, patients with myelofibrosis and aplastic anaemia showed a significant decreased FLT uptake by the pelvis while a significant increased uptake by the liver and spleen was noticed in the case of myelofibrosis. FLT scans showed various degrees of bone marrow expansion with exception of patients with aplastic anaemia. No correlation was shown between FLT activities reflected by the SUV at the iliac crest with the proliferation rate of bone marrow cells as defined by the Ki-67 staining. Based on these findings ^{18}F-FLT-PET provides visual and quantitative information on the entire bone marrow compartment and it may be beneficial in distinguishing various haematological disorders.

In **Chapter 4** the long term effects of the autologous stem cell transplantation (ASCT) was studied on the hematopoietic stem cell compartment by analyzing $CD34^+$ bone marrow cells in detail 6-9 months following ASCT. This study included patients with relapsing lymphoma and myeloma treated with intensive chemotherapy and ASCT. A significantly increased percentage of phenotypically defined GMP was demonstrated of bone marrow $CD34^+$ cells 6-9 months post-ASCT in conjunction with a reduction in the phenotypically defined CMP fraction. In vitro cell cycle analysis revealed a significantly higher fraction of $CD34^+$ cells in G2/S phase and a reduced percentage of cells in G1 phase compared to normal $CD34^+$ cells. ^{18}F-FLT-PET demonstrated a significant increase in SUV measured at different points of the bone marrow compartment in the post-transplantation patients. In addition, a significant expansion of the bone marrow compartment was noticed. These data demonstrate an enhanced proliferation rate of bone marrow cells defined with in vitro and in vivo assays following ASCT even when the peripheral blood cells have been normalized to great extent.

Chapter 5 deals with bone marrow visualization in patients with aplastic anemia by using ^{18}F-FLT-PET. Patients (n=17) were studied at presentation or at relapse or after having achieved a partial of complete normalization of peripheral blood cells following immunotherapy or allogeneic stem cell transplantation. The findings were compared with the findings of the bone marrow biopsy. A significant reduced uptake of ^{18}F-FLT by the pelvis was noted in untreated or relapsed patients. Patients in complete remission following allogeneic stem cell transplantation demonstrated a homogenous uptake throughout the skeleton while patients in partial remission following immunotherapy showed variable areas of increased uptake (hot spots) including the peripheral skeleton. In almost all the patients a normal uptake of the spleen was shown. These data demonstrate that ^{18}F-FLT-PET provides a highly distinctive picture that might be helpful to distinguish aplastic anemia patients from other hematological bone marrow disorders. In addition, it might be helpful to monitor the treatment response.

Chapter 6 describes the effect of radiotherapy and chemotherapy on the bone marrow function in patients with laryngeal carcinoma and non-seminomatous testicular germ cell tumors. Patients with laryngeal carcinoma receiving local radiotherapy (70 Gy) were studied by ^{18}F-FLT-PET before and after radiotherapy with special focus on the cervical region. Whole body ^{18}F-FLT-PET images were also assessed in patients with non seminomatous testicular germ cell tumors before and 4 months after the final chemotherapy consisting of 4 courses of bleomycin, cisplatin, and etoposide. A

significant decrease in ^{18}F-FLT uptake was observed in the cervical region of the adjacent bone marrow compartment after radiotherapy in all laryngeal carcinoma patients. The radiotherapy field was inversely related to the ^{18}F-FLT uptake (SUVmax 3.0 ± 1.28 and after radiotherapy 1.81 ± 0.72 (p= 0.0017). This study shows that the ^{18}F-FLT-PET can be used to visualize the effect of therapy-related bone marrow toxicity in patients being treated for malignancy, and might be a tool to define the residual hematopoietic activity.

Chapter 7 shows the utility of ^{18}F-FLT-PET to detect extramedullary hematopoiesis in a patient presenting with a history of hemoglobin-E and β-thalassemia. Extramedullary hematopoiesis (EMH) is a rare disorder defined as the localization and probably production of myeloid and erythroid cells outside of the bone-marrow cavity. In this patient a large mass was identified. The MRI could not differentiate between lymphoma and EMH. Therefore an ^{18}F-FLT PET was performed and demonstrated a large mass bilateral and paravertebral in the thorax with an elevated SUV suspect of EMH. These findings demonstrated that ^{18}F-FLT PET is an additional, non-invasive technique for the diagnosis of EMH.

Chapter 8 demonstrates the additional value of somatostatin receptor scintigraphy (SRS) in patients with multiple myeloma (MM). In 60%-70% of the patients with MM osteolytic defects are identified by X-ray examination. These defects persist following treatment and no clear distinction can be made whether vital tumor cells are present in these lesions. Several small studies have demonstrated that FDG-PET might identify the metabolic activity of the malignant plasma cells. ^{99m}Tc sestamibi scanning can show increased uptake in the MM lesions. *In vitro* studies with plasma cell lines have shown that the somatostatin receptor is expressed on malignant plasma cells. We explored this feature with imaging of MM using SRS. SRS was performed in newly diagnosed and relapsing MM, and plasmacytoma. In addition in five patients SRS scans were repeated after 3-5 months of treatment. A positive SRS was found in 44% of newly diagnosed MM patients. Patients with solitary plasmacytoma showed in all cases a positive SRS. The relapsing group showed a positive SRS in 83% of these patients. 60% of the positive SRS with an enhanced SRS activity was not accompanied by new abnormalities on the whole body radiography. The follow up SRS scans revealed a complete disappearance of lesions in three patients and a partial response in two. These changes corresponded with reduced disease activity. In conclusion these data demonstrate that SRS can be used as an alternative method to detect disease activity in malignant plasma cell disorders.

General discussion and Future perspective

Gamma camera radiopharmaceuticals evaluates bone marrow compartment based on the target cell system (reticulo-endothelial system, the erythroid and myeloid bone marrow compartment). Limitations in resolution are a common draw back of gamma camera systems. In contrast PET permits the evaluation of the whole bone marrow compartment which might include cellularity and metabolic activity. Better resolution and more accurate quantification of PET systems results in better image quality and more accurate quantification of bone marrow activity that may be important for monitoring treatment response. In this thesis we demonstrate that ^{18}F-FLT uptake reflects in a certain degree the proliferative activity of the bone marrow compartment which provides a better tool for monitoring therapy response. Several patterns of bone marrow uptake can be identified depending on the hematopoietic activity and the underlying disorder. Also discordance between bone marrow biopsy and peripheral blood findings might be seen as in the case of aplastic anemia due to patchy areas of aberrant hematopoiesis in the bone marrow compartment.

In patients following ASCT, high uptake of ^{18}F-FLT by the bone marrow compartment was demonstrated which reflected a higher proliferative activity. In vitro cell cycle analysis of $CD34^+$ cells confirmed these results. These findings were noticed even when the peripheral blood cell counts have been normalized in great extent. It is conceivable that these findings correlate with a replicative stress response related to the transplantation procedure whereby a limited number of stem cells have been infused that have to replenish the total stem and progenitor compartment. In addition, an enhanced shortening of the telomeres and an enhanced aging process might be contributing and resulting in a shift to more committed cells that have the intrinsic property of a higher proliferative activity [1].

In the future new techniques might be developed and used to visualize cell death. Annexin V is expressed by dying (apoptosis or necrotic) cells [2]. In the early phases of apoptosis, cells can be directly engulfed by phagocytes. Phagocytes identify their targets by the prolonged extensive exposure of the anionic membrane phospholipid phosphatidylserine (PS) on the surface of unwanted cells. There is evidence that annexin V binds to PS exposed on the cell surface and forms a protein crystal followed by rapid internalization via a unique pathway of pinocytosis. ^{99m}Tc-labeled annexin V was proposed as a method to study tumor behavior and therapy response [3]. Since PET has

major advantages for quantitative imaging, several approaches have been developed to label annexin V with ^{18}F [4,5]. ^{18}F-annexin V PET may be of use to study the effectiveness of the applied therapy in leukemia, myeloma or myeloproliferative disorders. A major challenge will be to define the optimal time point of imaging in particular in the setting of defining tumor response following chemotherapy or radiotherapy. Blankenberg et al. reported an increased annexin V uptake by bone marrow cells as early as 8 hours after cyclophosphamide treatment and lasted approximately 2 days [6]. Animal models might be of great help to perform these preclinical studies. For studies of steady state hematopoiesis a different approach might be used.

CD66 antigen is expressed at the cell surface of mature myeloid cells. Anti-CD66 monoclonal antibodies (mAbs) labelled with beta-emitting nuclides (^{188}Re and ^{90}Y) has already been introduced and is suited as myelo-ablative radioimmunotherapy prior to stem cell transplantation in acute leukemia [7]. Therefore, it is of interest to determine the CD66 distribution in the bone marrow compartment to assess therapy response following treatment. ^{18}F-Immuno-PET may, therefore, be a useful tool in the future.

New imaging tools with ^{89}Zr-bevacizumab have become available in solid tumors for visualization the neovascularisation of the affected organ [8]. Vascular endothelial growth factor (VEGF) has a prominent position in triggering neoangiogenesis [9]. ^{89}Zr-bevacizumab PET provides a noninvasive tool to monitor the expression of tumor VEGF as well as response on treatment [10]. Also in haematological disorders this approach might be an attractive option to visualize the enhanced bone marrow microvessel density for example in myeloma and leukemia and monitor the response on anti-VEGF treatment[11].

To date, somatostatin receptor scintigraphy (SRS) using ^{111}In-pentetreotide a radiolabelled analogues of somatostatin have been used for imaging and treatment in neuroendocrine tumors (NETs). Recently ^{68}Ga- labelled octreotide analogues are introduced to image somatostatin receptors (sstr) in NETs [12,13]. Peptide receptor radionuclide therapy (PRRT) with somatostatin analogues ^{90}Y-DOTATOC and ^{177}Lu-DOTATATE has been used in NETs [14]. SSTR has also been reported to be highly expressed in other malignancy, including lymphomas [15]. We noted sstr overexpression in MM; however, only subtypes 3 and 5 are studied in these patients. Therefore, it is interesting in the future to study all sstr subtypes especially sstr2 in more patients and possible applying of PRRT with somatostatin analogues ^{90}Y-DOTATOC and ^{177}Lu-DOTATATE. In addition,

^{68}Ga PET is a possible future technique in the diagnosis of MM as it provides a better resolution and more accurate quantification thereby increasing diagnostic accuracy.
Cancer cells frequently exhibit increased glycolysis [16]. Mitochondrial malfunction and hypoxia in the tumor microenvironment are considered two major contributing factors [17]. However, whether the increase of glycolytic activity in cancer cells is mainly due to inherent metabolic alterations or due to anaerobic micro environment in the tumor tissues remains controversial [18]. Insufficient blood supply can occur due to the rapid expansion of the tumor mass. Limitation of the availability of oxygen for use in mitochondrial respiration up-regulates the glycolytic pathway which is mediated by increased expression of various kinases required for glycolysis. The metabolic consequence of the mitochondrial malfunction and hypoxia is increased glycolysis to provide energy supply and thus renders cancer cells highly dependent on this metabolic pathway for survival [19]. A number of PET radiopharmaceuticals are recently developed to image hypoxia. Intercellular trapping by reductive mechanisms occurs due to low oxygen tension in hypoxic tissue. [^{18}F]Fluoromisonidazole-3-fluoro-1-(2 □-nitro-1 □-imidazolyl)-2-propanol (^{18}F-MISO) and ^{64}Cu-diacetyl-bis(N^4-methylthiosemicarbazone (^{64}Cu-ATSM), and the recently introduced [^{18}F]fluoroazomycinarabinoside (^{18}F-FAZA) can potentially be used to image bone marrow hypoxia as non-invasive method [20,21]. Bone marrow uptake of ^{18}F-FAZA may potentially increase during hypoxic circumstances. This might be attractive approach to define whether the increased uptake of FDG-PET by myeloma cells is a reflection of enhanced glycolysis in association with hypoxia. Furthermore, bone marrow biopsy material might be of importance to demonstrate whether the enhanced glucose uptake by the myeloma cells is associated with an enhanced expression of glut -1 and glut-3 [22].
In summary these data show that different aspects of the bone marrow can be non-invasively imaged by using a variety of radiopharmaceuticals. Selective bone marrow biopsy can be achieved after bone marrow land marking using nuclear medicine imaging. In addition the imaging techniques might be used during and following specific therapies dependent on the underlying haematological disorder.

Reference List

1. *Ju Z, Jiang H, Jaworski M, Rathinam C, Gompf A ,et al. Telomere dysfunction induces environmental alterations limiting hematopoietic stem cell function and engraftment. Nat Med. 2007;13:742-747.*

2. *Blankenberg FG. In vivo detection of apoptosis. J Nucl Med. 2008 49 Suppl 2:81S-95S. Review.*

3. *Belhocine T, Steinmetz N, Hustinx R, Bartsch P, Jerusalem G,et al. Increased uptake of the apoptosis-imaging agent (99m)Tc recombinant human Annexin V in human tumors after one course of chemotherapy as a predictor of tumor response and patient prognosis. Clin Cancer Res. 2002;8:2766-74.*

4. *Yagle KJ, Eary JF, Tait JF, Grierson JR, Link JM, Et al. Evaluation of 18F-annexin V as a PET imaging agent in an animal model of apoptosis. J Nucl Med. 2005 ;46:658-66.*

5. *Murakami Y, Takamatsu H, Taki J, Tatsumi M, Noda A, et al. 18F-labelled annexin V: a PET tracer for apoptosis imaging. Eur J Nucl Med Mol Imaging. 2004;31:469-74.*

6. *Blankenberg FG, Naumovski L, Tait JF, Post AM, Strauss HW. Imaging cyclophosphamide-induced intramedullary apoptosis in rats using 99mTc-radiolabeled annexin V. J Nucl Med. 2001;42:309-16.*

7. *Ringhoffer M, Blumstein N, Neumaier B, Glatting G, von Harsdorf S, et al. 188Re or 90Y-labelled anti-CD66 antibody as part of a dose-reduced conditioning regimen for patients with acute leukaemia or myelodysplastic syndrome over the age of 55: results of a phase I-II study. Br J Haematol 2005;130:604–13.*

8. *Nagengast WB, de Vries EG, Hospers GA, Mulder NH, de Jong JR, et al. In vivo VEGF imaging with radiolabeled bevacizumab in a human ovarian tumor xenograft. J Nucl Med. 2007;48:1313-9.*

9. *Dvorak HF, Brown LF, Detmar M, Dvorak AM. Vascular permeability factor/vascular endothelial growth factor, microvascular hyperpermeability, and angiogenesis. Am J Pathol. 1995;146:1029-39. Review.*

10. *Nagengast WB, de Korte MA, Oude Munnink TH, Timmer-Bosscha H, den Dunnen WF, et al. 89Zr-bevacizumab PET of early antiangiogenic tumor response to treatment with HSP90 inhibitor NVP-AUY922. J Nucl Med. 2010 ;51:761-7.*

11. *Li WW, Hutnik M, Gehr G. Antiangiogenesis in haematological malignancies. Br J Haematol. 2008;143:622-31. Review.*

12. *Campana D, Ambrosini V, Pezzilli R, Fanti S, Labate AM, et al. Standardized uptake values of (68)Ga-DOTANOC PET: a promising prognostic tool in neuroendocrine tumors. J Nucl Med. 2010;51:353-9.*

13. *Prasad V, Baum RP. Biodistribution of the Ga-68 labeled somatostatin analogue DOTA-NOC in patients with neuroendocrine tumors: characterization of uptake in normal organs and tumor lesions. Q J Nucl Med Mol Imaging. 2010;54:61-7.*

14. *Kwekkeboom DJ, Mueller-Brand J, Paganelli G, Anthony LB, Pauwels S, et al. Overview of results of peptide receptor radionuclide therapy with 3 radiolabeled somatostatin analogs. J Nucl Med. 2005;46 Suppl 1:62S-6S. Review.*

15. *Raderer M, Traub T, Formanek M, Virgolini I, Osterreicher C, et al. Somatostatin-receptor scintigraphy for staging and follow-up of patients with extraintestinal marginal zone B-cell lymphoma of the mucosa associated lymphoid tissue (MALT)-type. Br J Cancer. 2001;85:1462-6.*

16. *Vander Heiden MG, Cantley LC, Thompson CB. Understanding the Warburg effect: the metabolic requirements of cell proliferation. Science. 2009;324:1029-33. Review.*

17. *Young CD, Anderson SM. Sugar and fat - that's where it's at: metabolic changes in tumors. Breast Cancer Res. 2008;10:202. Review.*

18. *Zu XL, Guppy M. Cancer metabolism: facts, fantasy, and fiction. Biochem Biophys Res Commun. 2004;313:459-65.*

19. *Xu RH, Pelicano H, Zhou Y, Carew JS, Feng L, et al. Inhibition of glycolysis in cancer cells: a novel strategy to overcome drug resistance associated with mitochondrial respiratory defect and hypoxia. Cancer Res. 2005;65:613-21.*

20. *Souvatzoglou M, Grosu AL, Roper B, Krause BJ, Beck R, et al. Tumour hypoxia imaging with [18F]FAZA PET in head and neck cancer patients: a pilot study. Eur J Nucl Med Mol Imaging. 2007;34:1566-75.*

21. Padhani A. PET imaging of tumour hypoxia. Cancer Imaging. 2006;6:S117-S121.

22. Tian M, Zhang H, Nakasone Y, Mogi K, Endo K. Expression of Glut-1 and Glut-3 in untreated oral squamous cell carcinoma compared with FDG accumulation in a PET study. Eur J Nucl Med Mol Imaging. 2004;31:5-12.

Chapter 10

Nederlandse samenvatting

Nederlandse samenvatting

Het beenmergcompartiment kan gevisualiseerd worden door gebruik te maken van specifieke radiofarmaca die verschillende celtypen binnen dit geheel kunnen herkennen. De afbeelding ervan vindt plaats met gammacamera's en PET-technieken. Verschillende distributiepatronen en intensiteiten kunnen worden gezien, afhankelijk van het onderliggend ziektebeeld van het beenmerg. De toepassing van deze technieken kan van belang en aanvullend zijn in het diagnostische proces van patiënten met hematologische aandoeningen. Dit wordt nader toegelicht in hoofdstuk 2.

In **hoofdstuk 2** wordt een overzicht gegeven van de huidige kennis over beenmerg beeldvorming met verschillende gelabelde radioisotopen. Radioistopen voor de gammacamera's zijn al enkele decennia in gebruik in de nucleaire geneeskunde en worden ingezet om bepaalde functies van het beenmerg te onderzoeken. PET-camera's geven in vergelijking met de gammacamera een nauwkeuriger beeld van het hele beenmerg compartiment met een hogere resolutie waarbij ook een meer specifieke cellulaire functie kan worden onderzocht afhankelijk van de gebruikte PET radiofarmacon. Verschillende opnamepatronen zijn zichtbaar gemaakt en de klinische toepassingen bij diverse hematologische ziekten worden besproken.

In **hoofdstuk 3** is de in vivo proliferatieve activiteit van het beenmerg compartiment bestudeerd met behulp van de ^{18}F-FLT-PET scan bij patiënten met verschillende hematologische aandoeningen, zoals myelodysplasie, myeloproliferatieve ziekten inclusief myelofibrose, multipel myeloom en aplastische anemie. Patiënten met myelodysplasie en myeloproliferatieve ziekten toonden een significant hogere ^{18}F-FLT opname in het beenmerg in vergelijking met de controle groep. Dit in tegenstelling tot patiënten met myelofibrose en aplastische anemie die een significante lagere ^{18}F-FLT opname vertoonden in het beenmerg maar een aanzienlijk hogere opname in de lever en de milt in het geval van myelofibrose. Er bleek geen correlatie te bestaan tussen de ^{18}F-FLT activiteit in het bekken en de Ki-67 activiteit (proliferatie marker) in het beenmergaspiraat. Gebaseerd op deze bevindingen kan ^{18}F-FLT-PET behulpzaam zijn in het onderscheiden van verschillende hematologische aandoeningen en daardoor van waarde zijn in het diagnostisch proces.

In **hoofdstuk 4** zijn de lange termijn effecten van autologe stamceltransplantatie (ASCT) onderzocht op het hematopoietische stamcel compartiment door de beenmergcellen zowel in-vitro als in-vivo te onderzoeken. De studie omvatte patiënten die behandeld waren voor een recidief lymfoom of multipel myeloom met intensieve chemotherapie

en autologe stamcel reïnfusie. 6-9 maanden na de transplantatie zijn de onderzoekingen verricht. Facs analyse van de beenmergcellen liet een verschuiving in het progenitor compartiment zien. Dit ging samen met een significante hogere delingsfractie in de $CD34^+$ celfractie. In vivo experimenten met ^{18}F-FLT-PET beeldvorming bevestigden deze gegevens.

Hoofdstuk 5 is ^{18}F-FLT-PET gebruikt om het beenmerg compartiment te onderzoeken bij patiënten met een aplastische anemie (AA). Recent gediagnosticeerde AA patiënten, patiënten met een recidief AA en patiënten na behandeling zijn onderzocht. De bevindingen zijn vergeleken met de gegevens van het beenmergbiopt. Een aanzienlijk verminderde opname van ^{18}F-FLT in het bekken werd waargenomen bij patiënten met actieve AA ziekte. Patiënten in volledige remissie na allogene stamceltransplantatie toonden een homogene opname in het skelet terwijl patiënten in gedeeltelijke remissie na immunotherapie een sterke variabele opname (hot spots) vertoonden, inclusief opname in het perifere skelet. Deze gegevens tonen aan dat AA middels ^{18}F-FLT-PET van andere hematologische beenmergaandoeningen kan worden onderscheiden. Bovendien zou het van waarde kunnen zijn om de respons op de behandeling te vervolgen.

Hoofdstuk 6 beschrijft het effect van radiotherapie en chemotherapie op de ^{18}F-FLT opname van het beenmerg compartiment. De hals regio bij patiënten met een larynxcarcinoom die behandeld zijn met 70 Gy radiotherapie toonde geen ^{18}F-FLT opname meer 6 maanden na de behandeling. Dit in tegenstelling tot patiënten die behandeld zijn met chemotherapie voor non-seminomateuze testiculaire kiemceltumoren. Vier maanden na de laatste chemotherapie was er geen verschil met de controle groep suggererend dat deze vorm van chemotherapie geen blijvend effect heeft op de cyclische activiteit van het hematopoietisch beenmerg compartiment.

Hoofdstuk 7 toont de waarde van ^{18}F-FLT-PET aan om lokalisaties van extramedullaire hematopoiese (EMH) op te sporen. Een patiënt bekend met hemoglobine-E β-thalassemie wordt gepresenteerd met een grote massa bilateraal en paravertebraal in de borstholte. De MRI kon geen duidelijk onderscheid maken tussen lymfoom of EMH. De vervolgens uitgevoerde ^{18}F-FLT-PET toonde verhoogde opname van ^{18}F-FLT aan in het proces bilateraal en paravertebraal in de thorax dat qua intensiteit vergelijkbaar was met de opname in beenmerg en milt hetgeen verdacht is voor EMH.

Hoofdstuk 8 beschrijft de waarde van somatostatine receptor scintigrafie (SRS) bij patiënten met een multipel myeloom (MM). In 60% -70% van de patiënten met MM worden osteolytische afwijkingen geïdentificeerd door het verrichten van röntgen on-

derzoek van het skelet. Deze afwijkingen blijven bestaan na de behandeling waardoor er geen goed onderscheid gemaakt kan worden tussen vitale tumorcellen versus oude restafwijkingen in het skelet. Somatostatine receptoren zijn in het verleden al aangetoond op maligne plasmacellen door middel van immunohistochemische technieken. De resultaten van het huidige onderzoek tonen aan dat SRS goed gebruikt kan worden om ziekteactiviteit bij patiënten met een recidief MM aan te tonen. Een positieve SRS werd gevonden in 44% van de nieuw gediagnosticeerde MM patiënten, bij alle patiënten met een solitair plasmacytoom en in 83% van de patiënten met hernieuwde ziekteactiviteit. De follow-up SRS-scans bij vijf patiënten liet een volledige verdwijning zien van de laesies bij drie patiënten en een gedeeltelijke respons bij twee patiënten. Deze wijzigingen correspondeerden met een verminderde ziekteactiviteit. Deze gegevens duiden erop dat SRS kan worden gebruikt als een alternatieve methode om ziekteactiviteit bij maligne plasmacel aandoeningen te detecteren.

Samenvattend lijkt het dat ^{18}F-FLT-PET een waardevolle techniek is om verschillende hematologische aandoeningen van het beenmerg compartiment te diagnosticeren en mogelijk naar de toekomst te gebruiken als follow-up parameter tijdens of na de behandelingsfase. Toekomstige ontwikkelingen zijn het afbeelden van nieuwe targets bij hematologische ziektebeelden, zoals specifieke receptoren en celprocessen. Te denken valt aan angiogenese, waarbij de vaso-endotheliale groei factor (VEGF) een belangrijke rol speelt. Dit kan bijvoorbeeld met ^{89}Zr-bevacizumab PET afgebeeld worden. Een ander belangrijk proces is apoptosis (geprogrammeerde celdood). Dit kan met radioactief gelabelde annexine-V worden afgebeeld. Bepaalde hematologische aandoeningen zoals leukemie, multipel myeloom, en myeloproliferatieve aandoeningen, gaan na behandeling in apoptose. ^{99m}Tc-annexine SPECT zou hierin een rol kunnen spelen voor het monitoren van de behandeling. Een aantal PET radiofarmaca zijn ook ontwikkeld om hypoxie af te kunnen beelden in maligne tumoren. Weinig hierover is bekend bij de verschillende bestudeerde aandoeningen.
Somatostatine receptor scintigrafie kan gebruikt worden als een alternatieve methode om ziekteactiviteit te detecteren met name bij patiënten met hernieuwde ziekte activiteit van het multipel myeloom. ^{68}Ga-gelabelde somatostatine PET is mogelijk een nog nauwkeuriger techniek om multipele myeloom activiteit aan te tonen, vanwege de hogere resolutie in vergelijking tot een gammacamera.

ABBREVIATIONS

^{18}F-MISO	[^{18}F]Fluoromisonidazole-3-fluoro-1-(2′-nitro-1′-imidazolyl)-2-propanol
^{18}F-FAZA	[^{18}F]fluoroazomycinarabinoside
^{64}Cu-ATSM	^{64}Cu-diacetyl-bis(N^4-methylthiosemicarbazone
^{99m}Tc-AGAb	^{99m}Tc-labelled antigranulocyte antibodies
^{111}In-CL_3	^{111}Indium-chloride
^{64}Cu-ATSM	^{64}Cu-diacetyl-bis(N^4-methylthiosemicarbazone
AA	Aplastic anemia
ALL	acute lymphoblastic leukemia
AML	acute myeloid leukemia
ASCT	autologous stem cell transplantation
BFU-E	burst forming unit erythroid
BM	bone marrow
CFC	colony forming cell
CFU-GM	Colony forming unit –granulocyte macrophage
CI	confidence interval
CML	chronic myeloid leukemia
CMP	common-myeloid progenitor
CR	complete response
CT	computed tomography
DLBCL	diffuse large B-cell lymphoma
DNA	deoxyribonucleic acid
EHM	Extramedullary hematopoiesis
FDG	Fluorodeoxyglucose
FLC	free light chain

FLT	3-fluoro-3-deoxy-L-thymidine
G-CSF	granulocyte colony-stimulating factor
GMP	granulocyte-macrophage progenitor
GM-CSF	granulocyte-macrophage colony-stimulating factor
HA	Hemolytic anemia
HGF	hematopoietic grow factor
HL	Hodgkin Lymphoma
HSCs	hematopoietic stem cells
mAbs	monoclonal antibodies
MBq	megabecquerel
MDS	Myelodysplastic syndromes
MEP	megakaryocytic-erythroid progenitor
MeV	mega electron volt
MF	myelofibrosis
MM	Multiple myeloma
MPDs	Myeloproliferative diseases
MRI	magnetic resonance imaging
NCA-95	non-specific cross reacting antigen 95
NETs	neuro-endocrine tumors
NSCLC	non-small cell lung cancer
PET	Positron Emitting Tomography
PR	partial response
PSA	prostate specific antigen
PV	Polycythemia vera
RES	reticulo-endothelial system
ROI	region of interest
RT	radiotherapy
SPECT	Single Photon Emission Computed Tomography
SRS	Somatostatin receptor scintigraphy
sstr	somatostin receptor
SUV	standardized uptake value
TK1	thymidine kinase 1
VEGF	vascular endothelial growth factor
WBC	white blood cells

Dankwoord

Dankbaarheid is het geheugen van het hart *(Gospel Doctrine)*

Allereerst wil ik mijn promotie team bedanken.
Mijn promotor Prof. dr. E. Vellenga. Beste Edo, bedankt voor de mogelijkheid om het promotieonderzoek te mogen verrichten. Ik heb grote bewondering voor de manier waarop jij de zaken regelt. Bedankt voor je continue, nauwkeurige en wetenschappelijke begeleiding in de afgelopen jaren. Ik wil je daarnaast nog bedanken voor jouw zeer gedetailleerde commentaar op mijn stukken en voor jouw advies, steun, vertrouwen en positieve feedback.

Mijn copromotor dr. R.H.J.A. Slart. Beste Riemer, jouw enorme enthousiasme en positieve instelling heeft me menig keer geholpen om door te zetten. Je hebt altijd een grote rol gespeeld in mijn begeleiding. Je hebt mij echt door de laatste loodjes heen gesleept en mijn stukken ongekend snel van commentaar en correcties voorzien.

Mijn tweede promotor Prof. dr. R. Dierckx, beste Rudi, bij dezen wil ik je bedanken voor het bieden van de mogelijkheid om te promoveren binnen de afdeling Nucleaire Geneeskunde. Bedankt voor het vertrouwen en de stimulerende gesprekken die we de afgelopen jaren gevoerd hebben.

Daarnaast wil ik Prof. dr. P.L. Jager bedanken voor de begeleiding tijdens mijn opleiding en alle hulp bij het opzetten van het eerste onderzoek van dit proefschrift. Ik kijk met veel plezier terug op deze periode.

De leden van de leescommissie, Prof. dr. P.M. Kluin, Prof. dr. P.H. Elsinga en Prof. dr. C. van de Wiele wil ik bedanken voor de tijd en moeite die ze hebben genomen om mijn proefschrift te beoordelen.

De stafleden van de afdeling NGMB wil ik bedanken. Jan Pruim en Adrienne Brouwers, beste Jan en Adrienne, bedankt voor jullie supervisie tijdens mijn opleiding en de vele fijne gespreken. Jan, bedankt voor jouw technische ondersteuning bij het afronden van het review artikel. Andor Glaudemans, Andor de samenwerking met jou was prettig en vlot hetgeen erg heeft bijgedragen aan het vlotte afronden van het schrijven en publiceren van het review artikel.

Veel dank ben ik verschuldigd aan de MNW-ers van het PET centrum in het bijzonder Johan, Remko en Paul. Beste Paul, je bent altijd enthousiast, bedankt voor de moeite en de tijd om de PET scans keurig en op tijd naar mijn toe te zenden. Ook de overige MNW-ers van de afdeling NGMB wil ik bedanken voor de prettige samenwerking.

Sylvia Koster en Ineke ten Have, bedankt voor jullie ondersteunende hulp en het regelen van alle zaken o.a. gesprekken met mijn promotie team.

Mijn dank gaat ook uit naar mijn collega's bij het Ziekenhuisgroep Twente, Clemens Ticheler, Marc Zuijdwijk en Nils Wagenaar. Bedankt voor de vriendelijke en uitstekende werksfeer, en de goede organisatie zodat ik nog aan mijn proefschrift heb kunnen werken. Tevens wil ik de MNW-ers en de secretaresses van afdeling nucleaire geneeskunde Ziekenhuisgroep Twente bedanken voor de gezellige sfeer.

Bart Schot, internist. Beste Bart, we hebben het eerste artikel van dit proefschrift samen afgerond onder begeleiding van Prof. Dr. E. Vellenga en Prof. dr. P.L. Jager. Dit was een mooi begin van mijn promotietraject. Gelukkig werken we allebei nog steeds in Twente.

Mijn paranimfen, Ha Phan en Klaas Pieter Koopmans, ik waardeer jullie hulp en steun. Ik ben blij dat jullie mijn paranimfen willen zijn. Ik vergeet nooit de prachtige opleidingsperiode. Ik hoop dat we contact blijven houden en elkaar regelmatig zien.
Beste Ha, nog bedankt voor het nalezen van mijn proefschrift.
Bv. Beste Klaas Pieter, ik vond het een eer dat ik toen jouw paranimf mocht zijn. Bedankt dat je nu mijn paranimf wilt zijn.

Mijn fijne collega's tijdens mijn opleiding in het UMCG, Mohammed Dal, Silvia Eshuis en later Niels Veltman wil ik tevens bedanken. Ik kijk met veel plezier terug op deze periode.

De grootste bron van inspiratie waar ik mijn kracht uitput is mijn familie en gezin. Lieve familie, ik weet dat jullie erg blij zijn, echter door de moeilijke omstandigheden in Irak krijg ik een pijnlijk gevoel dat niemand van jullie mijn promotie kan meemaken. Ik kan het goed voelen hoe mijn moeder elke dag voor mij bidt. Broers en zusters bedankt voor jullie steun vooral emotioneel. Daarnaast wil ik mijn gezin bedanken, Hind en mijn vrolijke schatjes, Tasnim en Muhammed. Bedankt voor jullie begrip en steun.

Mijn grootste angst is dat als het boekje klaar is, ik er pas achter kom dat ik iemand vergeten heb te bedanken. Bij dezen, alsnog bedankt!

Curriculum Vitae

Ali Agool werd op 14 juli 1967 geboren te Bagdad. Het VWO diploma werd behaald in 1985.

In hetzelfde jaar werd begonnen met de studie geneeskunde aan de Al-Mustansiriya Universiteit te Bagdad. Het artsexamen werd behaald in 1991. In 1992 begon hij als arts-assistent in Ibn Alnafis ziekenhuis te Bagdad. Na zijn komst naar Nederland in 1994 studeerde hij Nederlands en heeft hij zijn co-schappen gevolgd in het UMCG te Groningen. In november 1999 behaalde hij zijn vereiste tweede artsdiploma. Hij heeft in 2002 gewerkt als arts -assistent op de afdeling Chirurgie van het TweeSteden ziekenhuis in Tilburg. Vervolgens als arts-assistent op de afdeling Interne Geneeskunde van het Groene Hart Ziekenhuis te Gouda. Van september 2002 tot september 2006 volgde hij de opleiding tot nucleair geneeskundige op de afdeling Nucleaire Geneeskunde in het UMCG met als opleider Prof. dr. P.L. Jager. Vanaf oktober 2006 tot heden werkt hij als nucleair geneeskundige in het Ziekenhuisgroep Twente. Hij kreeg in 2006 een promotie-aanstelling als onderzoeker bij afdelingen Nucleaire Geneeskunde en Hematologie van het UMCG. Ali Agool is getrouwd met Hind R. Karim en heeft 2 kinderen.